



**COALTECH 2020**

## **Task 1.4**

# **Geotechnical factors affecting high- and low-wall stability in opencast coal mines**

by

**Grant van Heerden, Pr.Sci.Nat.**

**May 2004**

## EXECUTIVE SUMMARY

In the study presented in this report the geotechnical factors affecting the stability of coal opencast highwalls were investigated and a methodology to predict unstable slopes was proposed.

The four principal failure mechanisms were briefly reviewed in order to develop an understanding of what geometrical conditions must be met before a slope will fail in a prescribed manner. The four mechanisms are: circular; plane; toppling; and wedge failure. Plane and wedge failure are more commonly observed in local opencast coal mines than circular or toppling failure. Circular failure, however, is important with regard to soft and highly weathered overburden and low-wall spoil piles.

Geological and geotechnical field investigations were conducted at two operating opencast coal mines - *New Vaal Colliery* and *Wonderwater Strip Mine*. The two mines are situated in differing geological and geotechnical environments, yet the controls on highwall stability are the same at both sites. These controls are primarily based on the interactions between the highwall and the geological discontinuities present in the rock mass.

One mine was the site for a geophysical wireline logging exercise. A series of boreholes was drilled along a future highwall crest. The boreholes were geophysically wireline logged while the cores were both geologically and geotechnically logged. The use of geophysical wireline logging was shown to assist with the identification of geological discontinuities ahead of mining.

Interpretation of geophysical wireline data by stereography allows for an understanding of the relationships and potential interactions between the discontinuities and the future highwall to be developed. This in turn allows for slope stability hazard plans to be generated to assist with mine planning and production scheduling.

Knowledge of potential hazards relating to opencast coal highwalls will allow for safer and more productive operations to be conducted.

## CONTENTS

	<b>Page</b>
EXECUTIVE SUMMARY	2
LIST OF FIGURES	4
LIST OF TABLES	5
1. INTRODUCTION	6
2. A REVIEW OF FAILURE MECHANISMS	9
2.1 Introduction	9
2.2 Circular Failure	9
2.3 Plane Failure	10
2.4 Toppling Failure	10
2.5 Wedge Failure	13
2.6 Summary	14
3. GEOTECHNICAL FIELD INVESTIGATIONS AND GEOLOGICAL MODELLING	14
3.1 New Vaal Colliery	14
3.2 Wonderwater Strip Mine	19
3.3 Summary	22
3.4 Geophysical Wireline Logging	22
3.5 Conclusion	23
4. PREDICTIVE METHODOLOGY FOR SLOPE STABILITY HAZARD RATING	23
4.1 Introduction	23
4.2 Methodology	23
4.2.1 Analysis of the geological model	23
4.2.2 Analysis of geophysical data: Stereography	32
4.3 Application of the Methodology in a Real Case Scenario	39
4.3.1 Hazard rating for highwall sectors 119/93 and 119/94	40
4.3.2 Hazard rating for highwall sector 119/95	46
4.3.3 Overall test site highwall slope stability	55
4.4 Conclusion	55
5. RECOMMENDATIONS	55
6. REFERENCES	56

## LIST OF FIGURES

		Page
1.1	Simplified locality plan of New Vaal Colliery and Wonderwater Strip Mine	6
1.2	Highwall failure at New Vaal Colliery	7
2.2.1	Basic geometry of circular failure	10
2.3.1.a	Section view of plane failure	11
2.3.1.b	3D view of plane failure	11
2.3.1.c	Plane failure through a narrow slope	11
2.3.2.a	Plane failure with tension crack on surface	12
2.3.2.b	Plane failure with tension crack in slope face	12
2.4.1	An example of toppling failure induced by soft overburden sloughing over vertically jointed hard overburden	12
2.4.2	An example of toppling failure in highly fractured (blocky) rock mass overlying a steeply dipping floor	13
2.5.1	The basic geometry of wedge failure	13
3.1.1	Topographic zoning based on bottom seam coal floor elevation contours	14
3.1.2	Known dyke distribution at New Vaal Colliery	15
3.1.3	Extensional fracturing resulting from W-E principal horizontal stress	16
3.1.4	Known fault distribution at New Vaal Colliery	17
3.1.5	Dominant joint set orientations	17
3.1.6	Wedge failure in hard overburden	18
3.1.7	Highwall orientations in the pit indicating direction of advance	18
3.2.1.a	No. 2B Seam floor elevation	19
3.2.1.b	No. 2B Seam thickness isopach	19
3.2.2.a	Wonderwater dyke distribution	20
3.2.2.b	Wonderwater fault distribution	20
3.2.3	A failed highwall where the mode of failure was planar	21
3.2.4	Interburden wedge failure	21
4.2.1.1	West Pit test site, New Vaal Colliery	25
4.2.1.2	Generalised stratigraphic column for New Vaal Colliery	26
4.2.1.3	Surface elevation contours in metres above mean sea level (m.a.m.s.l)	27
4.2.1.4	Top Seam Coal floor elevation contours (m.a.m.s.l)	28
4.2.1.5	Middle Seam Coal floor elevation contours (m.a.m.s.l)	29
4.2.1.6	Bottom Seam Coal floor elevation contours (m.a.m.s.l)	30
4.2.1.7	A 3-dimensional profile view of the top seam floor topography	31
4.2.2.1	Positions of geophysically logged boreholes (A to F) relative to highwall	32
4.2.2.2	Stereoplot of planar fractures in overburden	35
4.2.2.3	Stereoplot of open fractures in overburden	36
4.2.2.4	Stereoplot of open fractures in top seam coal	38
4.2.2.5	Stereoplot of bedding planes in top seam coal	39
4.3.1.1	Potential discontinuity pattern (faults and joints) in overburden and top seam coal units inferred from contour data	40
4.3.1.2	Stereoplot of discontinuities identified in Borehole A for overburden, top seam coal and interburden	41
4.3.1.3	Slope stability hazard rating matrix for Borehole A	42
4.3.1.4	Stereoplot of discontinuities identified in Borehole C for overburden, top seam coal and interburden	43
4.3.1.5.a	Great Circles for discontinuities D1 to D6	44
4.3.1.5.b	Intersections (circled) between conjugate pairs forming wedges	44
4.3.1.5.c	Lines drawn through intersections indicating direction of potential sliding	44
4.3.1.5.d	Danger zones (red hatched) where a conjugate pair's line of intersection is greater than 30°	44
4.3.1.6	Hazard matrix for Borehole C – modified for wedge failure hazards only	45

4.3.2.1	Stereoplot of discontinuities identified in Borehole D for middle and bottom seam coal units	47
4.3.2.2.a	Great Circles for discontinuities D1 to D6	48
4.3.2.2.b	Intersections (circled) between conjugate pairs forming wedges	48
4.3.2.2.c	Lines drawn through intersections indicating direction of potential sliding	48
4.3.2.2.d	Danger zones (red hatched) where a conjugate pair's line of intersection is greater than 30°	48
4.3.2.3	Hazard matrix for Borehole D – modified for wedge failure hazards only	49
4.3.2.4	Stereoplot of discontinuities identified in Borehole E for middle and bottom seam coal units	50
4.3.2.5	Great Circles for discontinuities that may result in plane failure. Also indicated are the individual directions of potential sliding for each discontinuity	51
4.3.2.6.a	Great Circles for discontinuities D1 to D7	52
4.3.2.6.b	Intersections (circled) between conjugate pairs forming wedges	52
4.3.2.6.c	Lines drawn through intersections indicating direction of potential sliding	52
4.3.2.6.d	Danger zones (red hatched) where a conjugate pair's line of intersection is greater than 30°	52
4.3.2.7	Hazard matrix for Borehole E – modified for plane failure hazards only	53
4.3.2.8	Hazard matrix for Borehole E – modified for wedge failure hazards only	54

## LIST OF TABLES

	<b>Page</b>	
4.2.2.1	Combined geotechnical / lithological log	33
4.2.2.2	Geotechnical orientation data for overburden and top seam coal units	34

## 1. INTRODUCTION

During 2002, several high- and low-wall collapses occurred at New Vaal Colliery, an Anglo Coal opencast mine situated in the northern Free State on the southern banks of the Vaal River, south of Vereeniging (Figure 1.1).

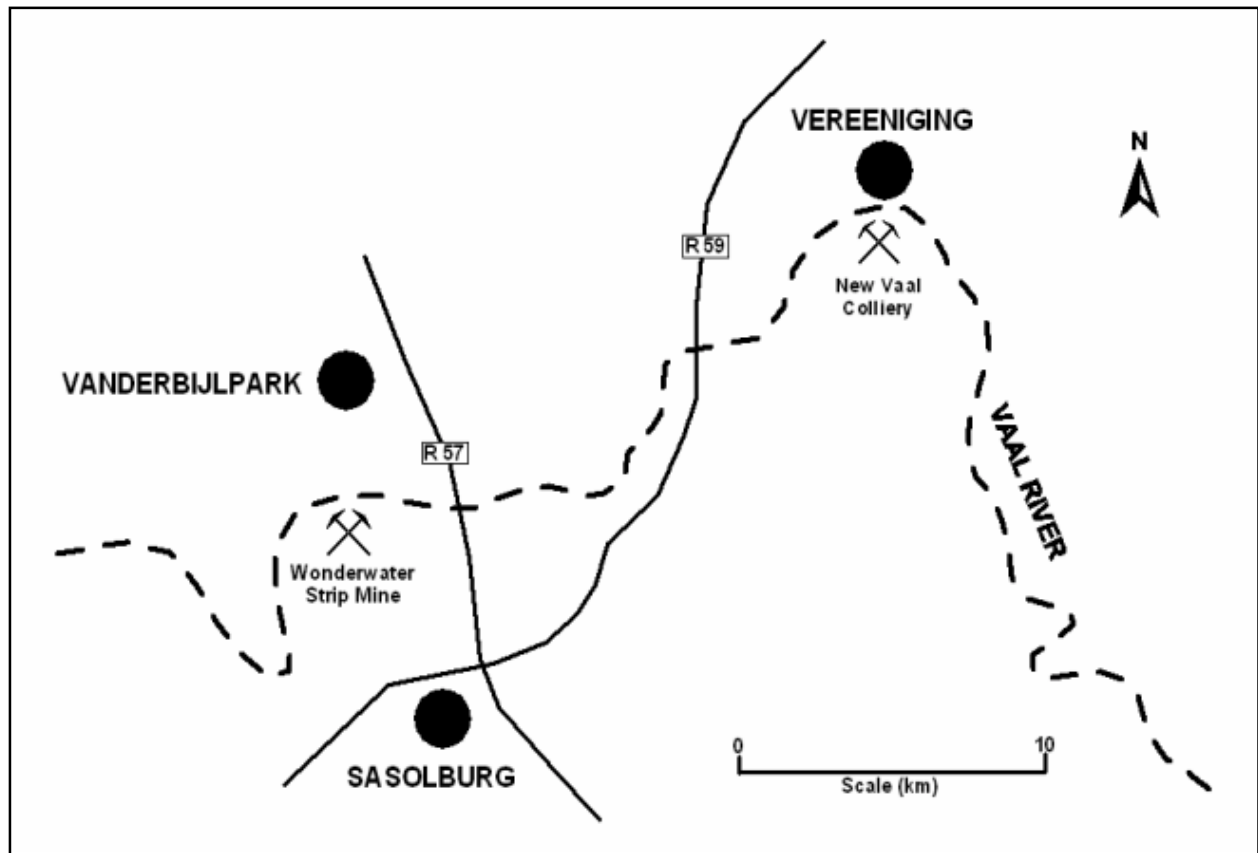


**Figure 1.1:** Simplified locality plan of New Vaal Colliery and Wonderwater Strip Mine

These events prompted a COALTECH 2020 research project to investigate geotechnical factors affecting high- and low-wall stability in opencast coal mines. A key outcome of this investigation was the development of a predictive methodology for slope stability hazard rating. Figure 1.2 is a photograph of a highwall failure that occurred at New Vaal Colliery in March 2002. Although neither injuries to personnel nor damage to equipment resulted from this incident, significant coal production delays occurred. All these factors add to the total operational cost of any mine, and must therefore be minimised, and preferably eliminated.

In most instances, however, it is not always possible to eliminate counter-productive and hazardous situations resulting from adverse geological conditions, yet it is possible to minimise their impacts. In the underground mining situation, this approach has been successful in minimising falls of ground by the use of various roof support systems, e.g. roof bolts, packs and hydraulic props. However, no mechanical support systems are appropriate for an advancing coal opencast highwall.

In fact, as late as 2001, no rationale existed for the safe cleaning and, more significantly, for the making safe of coal opencast highwalls (Butcher *et al.*, 2001). Much work has been devoted to *open pit* slope stability, both locally and internationally, however, little research has been conducted regarding *opencast* (strip mining) highwall design (Butcher *et al.*, 2001). This implies that opencast mine design has traditionally been a function of optimising resource exploitation, i.e. maximising reserve extraction, minimising waste rehandle, and trial and error.



**Figure 1.2:** Highwall failure at New Vaal Colliery (photograph courtesy of New Vaal Colliery)

Opencast coal mining in South Africa has typically been practiced under favourable geotechnical conditions and highwall stability issues have, therefore, never been a major factor in opencast mine design (Butcher *et al.*, 2001). However, as shallow (<35m) opencastable, good quality virgin resources become depleted, opencast mining is progressing into deeper areas and into areas where coal seams have already been mined by underground methods (pillar extraction by opencast methods). This has introduced geotechnical factors never before considered.

Underground mining has always required that more attention is paid to rock mass behaviour and, consequently, rock mass classification systems have developed out of a need to characterise the various types of underground excavations (Hack, 2002). These systems have assisted engineers and engineering geologists to design underground excavations and tunnels appropriate to the surrounding rock masses in which they occur. These systems also take into account various support mechanisms, desired stand-up times, mining methods and other relevant factors.

The success of these systems in underground situations has led to their being applied to rock slopes. Initial results were unsatisfactory and these systems thus needed adjustments and recalibration before they could be successfully applied to slope stability problems (Hack, 2002).

A number of classification systems have been developed, such as the systems developed by Bieniawski (1989), Romana (1991) and Haines and Terbrugge (1991) to name a few. The systems do not use the same set of parameters and, where the same parameters are used, each system applies a different weighting to them. This implies that, for the same slope, the individual systems could indicate a different level of slope stability.

The Salamon pillar design formula is used almost exclusively in underground coal mine design and provides a factor of safety for the various types of excavation. This formula is applicable to all underground coal mines and therefore provides consistency in the design of underground coal mines, whereas this is not the case for opencast coal mines.

The use of a slope stability classification system will primarily be driven by the types and amount of data available. The various input parameters are given below, some of which will be discussed in more detail later in this report:

- Intact rock strength (represented by uniaxial compressive strength, UCS, determined typically from laboratory tests);
- Rock quality designation, RQD;
- Spacing of discontinuities;
- Persistence of discontinuities (along strike and along dip);
- Condition of discontinuities;
- Anisotropic discontinuity roughness;
- Susceptibility to weathering;
- Relative orientation of slope and discontinuities;
- Slope height;
- Water / water pressure in discontinuities;
- Ice and snow influence;
- Dynamic loading (earthquakes and possibly effects of nearby blasting operations);
- Method of excavation.

The following are some of the factors not taken into account for various reasons (not discussed):

- Deformation of intact rock and rock mass, stress relief, and external stresses;
- Uncertainty in any parameter measurements;
- Assumed homogeneity of geotechnical units;
- Subjectivity of assigning values to certain parameters.

The slope stability probability classification (SSPC) system developed by Hack (1998) attempts to consider the shortcomings of previous systems and is currently being applied (with minor modifications) at opencast coal mines internationally (Lindsay *et al.*, 2000). The SSPC system is a detailed and somewhat complex classification system requiring significant, yet easily obtainable, input data. For more discussion and detail regarding the SSPC system, the reader is referred to Hack (2002) and Lindsay *et al.* (2000).

What is evident from these classification systems, and from rock slope engineering studies (Hoek and Bray, 1981), is the significant role that geological discontinuities play in the overall stability of rock slopes. The stability of coal opencast highwalls is strongly influenced by geotechnical factors. Geotechnical factors, in the present context, are considered to be geological discontinuities such as faults and joints and, to a lesser degree, bedding planes and dolerite dykes. More than the presence of discontinuities, it is specifically the relationship between the attitudes of the discontinuities with the exposed highwall face. In other words, the stability of a highwall is, to a large extent, controlled by the interaction between geological discontinuities and the exposed highwall.

It is therefore necessary to develop an understanding of what particular relationships between discontinuities and slope faces would result in potentially unstable highwalls. Only then would it be possible to consider the development of a methodology to predict the behaviour of highwalls in a given geological setting. The literature reviewed in this study allowed for an understanding of the particular relationships that would result in highwall instability and introduced additional factors that need to be considered for assisting and guiding the fieldwork.

Although this study was scoped to encompass low-wall stability issues as well, in most instances, low-walls of coal opencast mines are waste rock piles (spoils) and their stability is a function of soil mechanics, not geotechnical factors. The low-wall failure at New Vaal, referred to at the beginning of this section, actually occurred in the low-wall side of a box-cut, and is therefore treated as a highwall failure. No further investigations were conducted into low-wall stability.

The fieldwork and geological modelling, conducted during this study, were not restricted to one mine site. Field investigations were carried out at SASOL Mining's Wonderwater Strip Mine as well as at New Vaal Colliery. The main reason for this was to ensure that the predictive methodology being developed (Section 4) is applicable to opencast operations in differing geological settings. The geological setting at each site is described in more detail in Section 3. The reader will thus far appreciate that it is the prediction and the description of the geological discontinuities (geotechnical factors) that impact on and therefore control the stability of coal opencast highwalls. The methodology therefore focuses on these aspects, thereby making it applicable in a variety of geological settings.

## **2. A REVIEW OF FAILURE MECHANISMS**

### **2.1 Introduction**

It is necessary to develop an understanding of the various modes of rock slope failure before field observations can be clarified with any certainty. In other words, before a predictive methodology can be considered, it is necessary first to understand what conditions must be met before a slope will fail in a prescribed manner.

The reader is referred to Hoek and Bray (1981) for detailed discussions and worked examples regarding the mathematical approaches to failure analysis. This is not within the scope of this project and is presented in this section merely as an overview of the basic geometrical conditions needed for the various modes of failure to occur. This allows for coarse back analysis of failed slopes and the identification, based on field observations, of potential failure mechanisms in highwall slopes.

### **2.2 Circular Failure**

Circular failure is considered to be particularly relevant to soils, highly weathered overburden material and crushed rock waste piles (Hoek and Bray, 1981). Since soil and weathered overburden typically form the upper zone of most South African coal opencast highwalls, this failure mechanism is considered. In addition, this mode of failure is relevant to the stability of low-wall spoil piles. The reader will also observe that the general shape of the failure plane seen in Figure 1.2 is circular. Although this failure occurred through soil as well as through competent rock and coal, it is considered to be unique to the geological setting of New Vaal, and is discussed further in Section 3.

Circular failure occurs in soil (or a rock mass) where the individual particles are very small when compared to the slope size (height) and where the particles, due to their shape, are not effectively interlocked (Hoek and Bray, 1981). Soils and unconsolidated waste rock piles contain no significant continuous geological discontinuities that can impact noticeably on their stability in slopes. Groundwater has a major impact on soil slope stability and the reader is referred to Hoek and Bray (1981) for more detailed discussions regarding circular failure. Figure 2.2.1 illustrates the basic conditions under which circular failure occurs. The phreatic surface is the equivalent of the water table, below which the material is saturated.

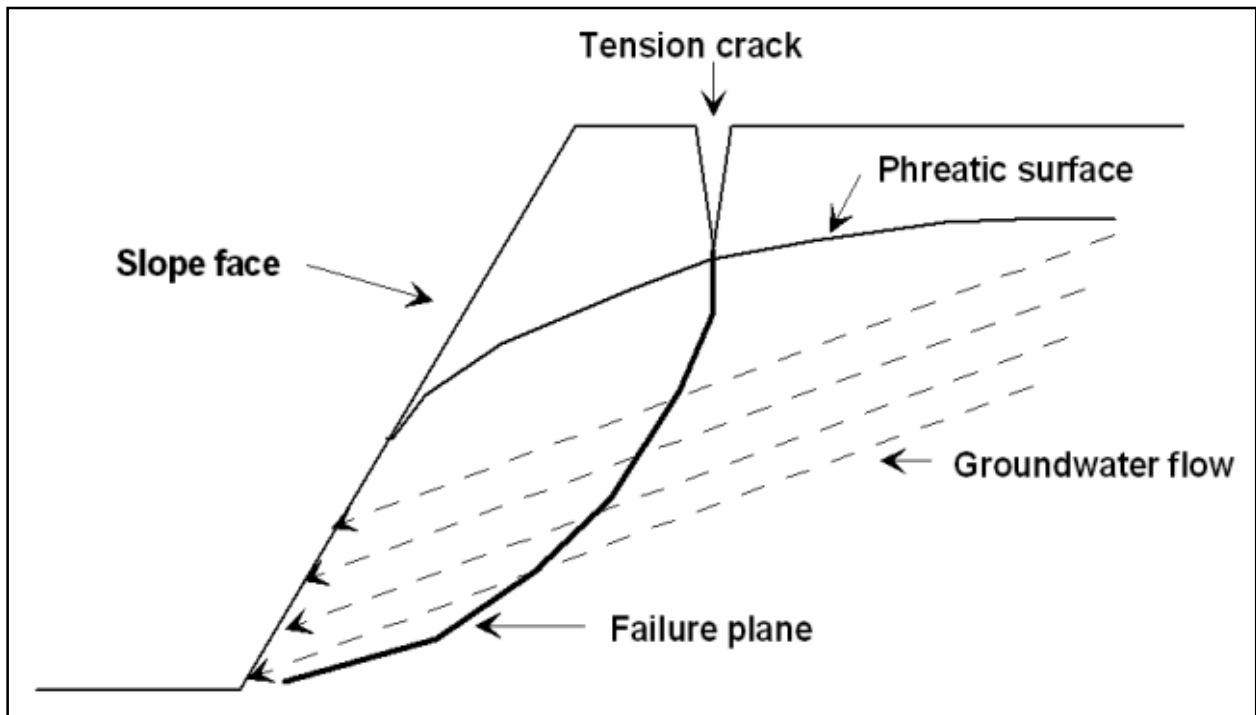


**Figure 2.2.1:** Basic geometry of circular failure

### 2.3 Plane Failure

Plane failure is considered by Hoek and Bray (1981) to be a relatively rare occurrence in rock slopes. This is because the geometrical conditions required for plane failure to occur are only rarely met in an actual slope. Plane failure is often seen as a special case of wedge failure (see Section 2.4) by many rock slope engineers (Hoek and Bray, 1981).

The geometrical conditions that need to be met, according to Hoek and Bray (1981) for failure or sliding to occur on a single plane are:

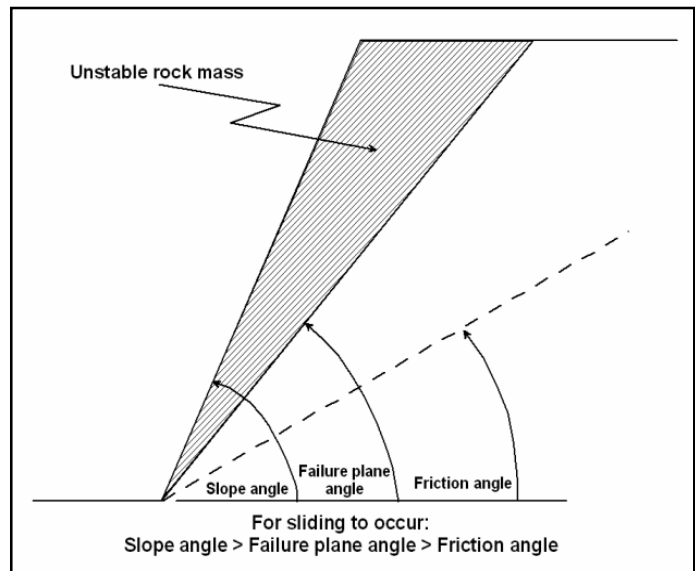
- i. The failure plane must strike parallel or sub-parallel ( $\leq 20^\circ$ ) to the slope face;
- ii. The failure plane must 'daylight' in the slope face, i.e. the failure plane dip must be less than the slope dip;
- iii. The failure plane dip must be greater than the friction angle of the plane (under normal loading conditions);
- iv. Release surfaces must be present in the rock mass to define the lateral extent (width) of the sliding block. These planes must have little resistance to sliding and be favourably oriented to allow the rock mass to move (alternatively, the failure can occur through the nose of a convex slope, or narrow slope, where the failure plane transects the entire slope).

These four geometrical conditions are illustrated in Figure 2.3.1. There are two additional cases where plane failure can occur and these involve the added influence of a tension crack, either present on the upper surface of the slope or in the slope face itself (Figure 2.3.2).

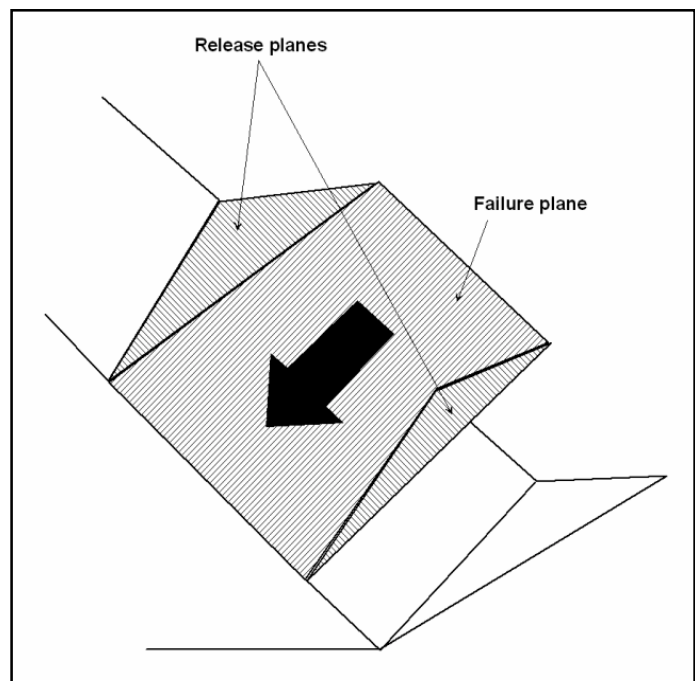
### 2.4 Toppling Failure

Toppling failure is unique in that it does not involve the sliding of soil or a rock mass on a plane (as with circular and plane failure) or a combination of planes (as with wedge failure - see next section). This mode of failure involves the rotation of blocks or columns of rock about a fixed base. Several types of toppling failure have been described (Hoek and Bray, 1981) although little detail will be given here, since this failure mechanism is not considered to be significant in local opencast coal mines.

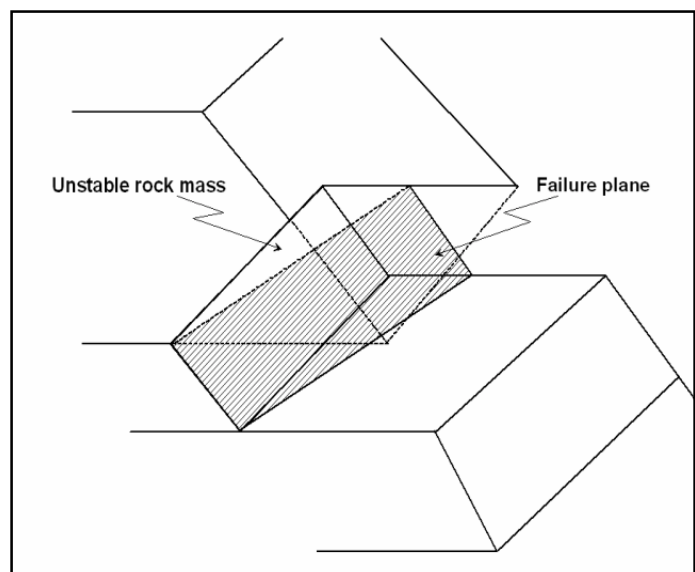
**Figure 2.3.1:** a) Section view of plane failure



**Figure 2.3.1:** b) 3D view of plane failure



**Figure 2.3.1:** c) Plane failure through a narrow slope



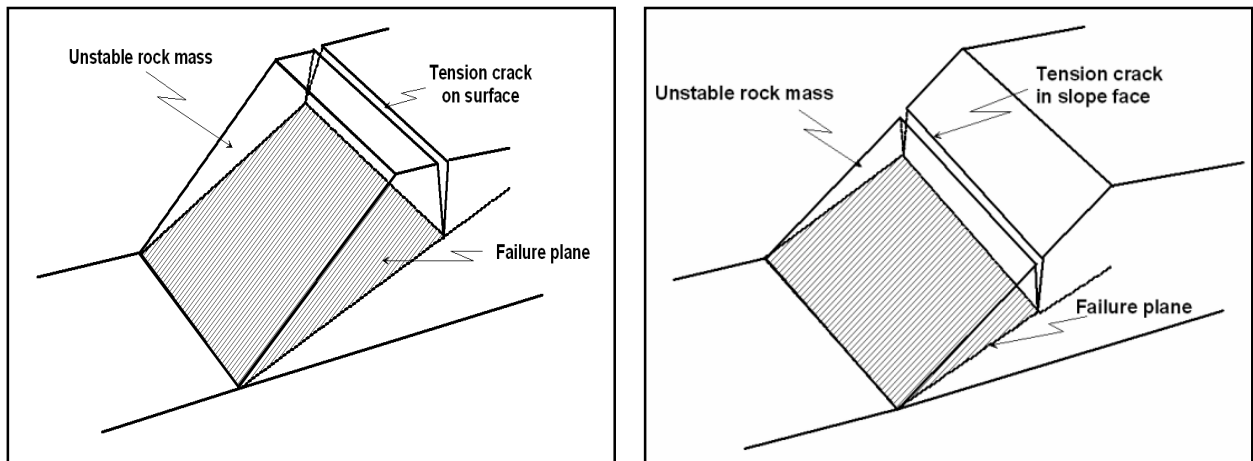


**Figure 2.3.2:** a) Plane failure with tension crack on surface; b) Plane failure with tension crack in slope face

A prerequisite for toppling failure to occur in a slope is that the rock mass forming the slope is characterised by extensive (along dip and strike) vertical or near vertical joints. Alternatively, the rock mass must be very blocky in nature due to geological discontinuities or a combination of geological discontinuities and blasting fractures. Figure 2.4.1 and Figure 2.4.2 illustrate two situations where toppling failure may occur in opencast coal mines.

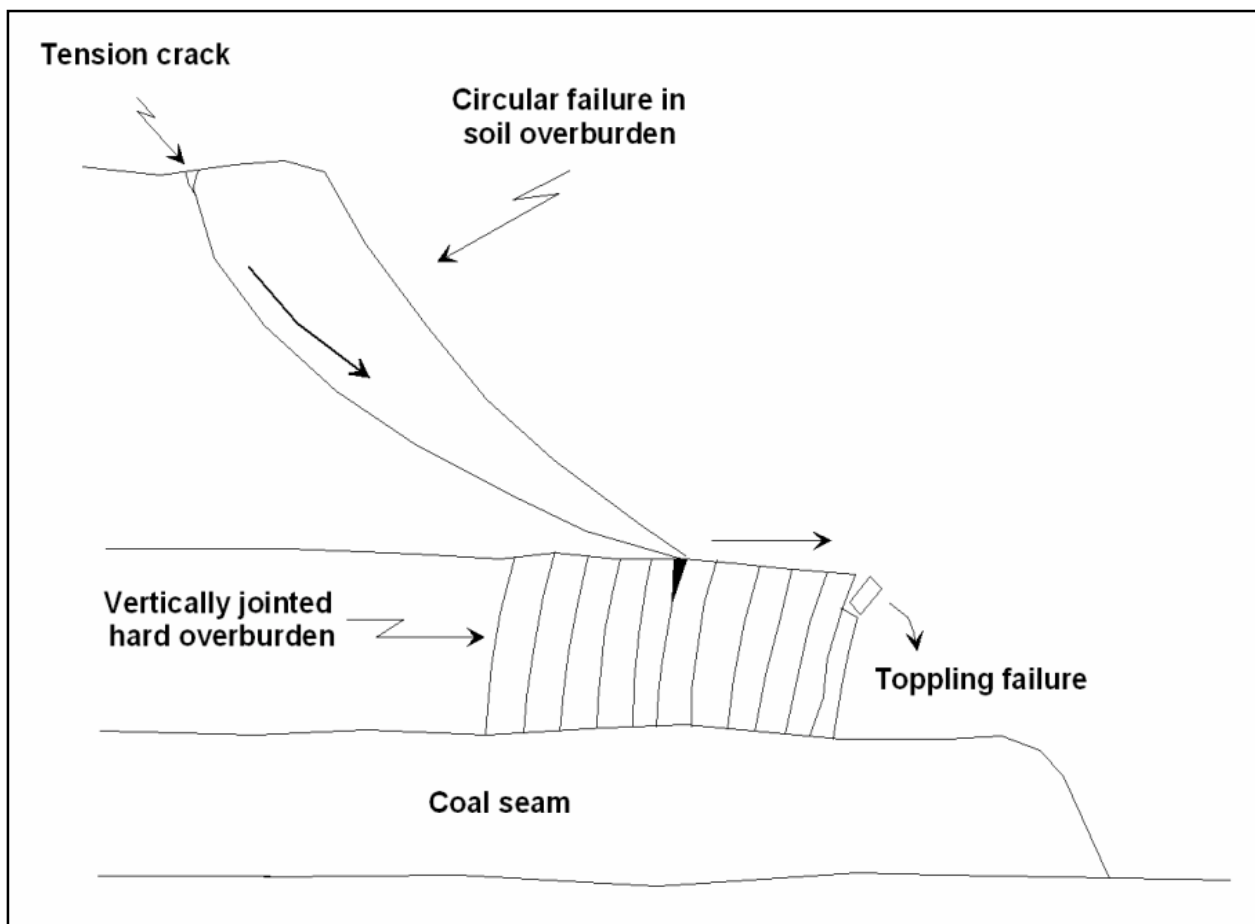


**Figure 2.4.1:** An example of toppling failure induced by soft overburden sloughing over vertically jointed hard overburden

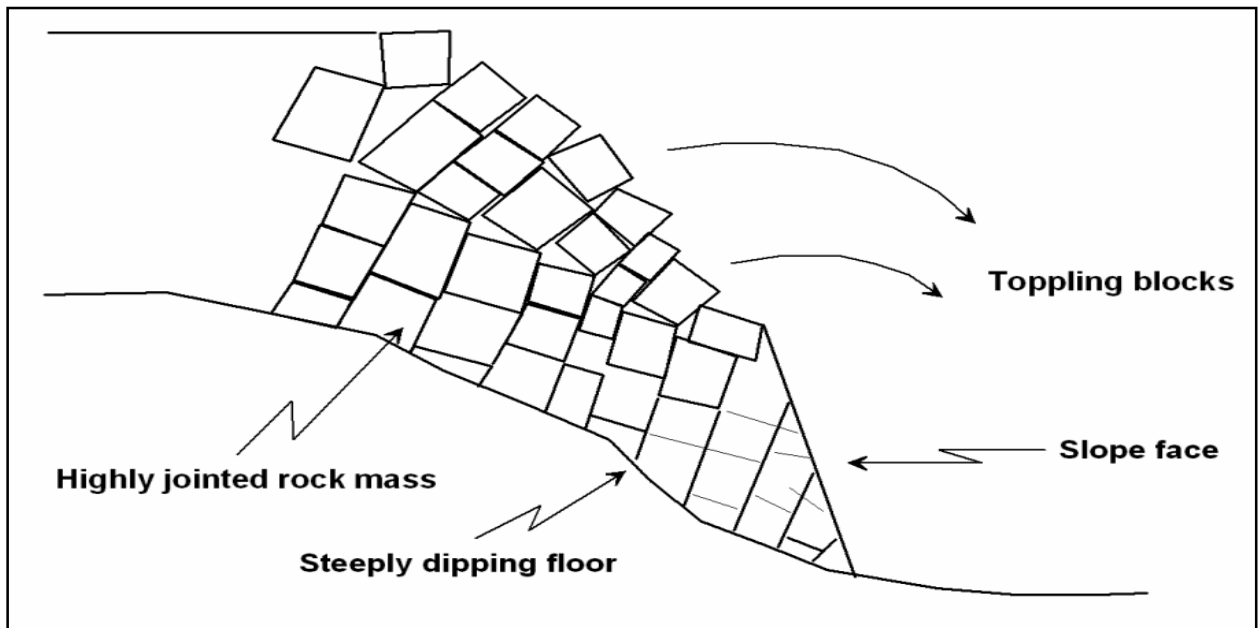


**Figure 2.4.2:** An example of toppling failure in highly fractured (blocky) rock mass overlying a steeply dipping floor

## 2.5 Wedge Failure

Wedge failure is probably the most commonly observed mode of highwall failure in local opencast coal mines. This is due to the fact that the geometrical conditions needed for this type of failure are very commonly met in typical highwall rock masses. Circular and plane failures both require a single geological discontinuity on which, given the right conditions, movement can occur. With wedge failure, however, at least two *intersecting* discontinuities are required, and the line of intersection of the two must produce an angle less than the angle of the slope face and greater than the average friction angle of the two discontinuities. The basic geometry of wedge failure is illustrated in Figure 2.5.1.

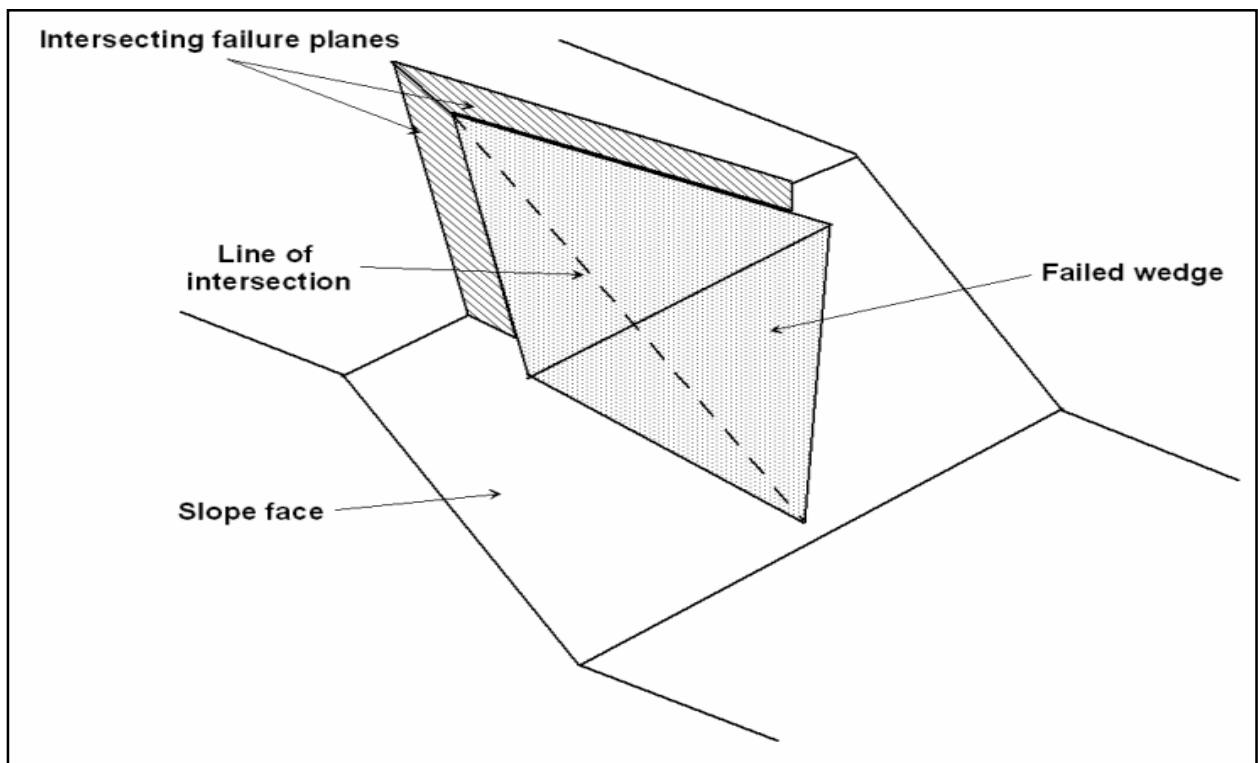


**Figure 2.5.1:** The basic geometry of wedge failure

## 2.6 Summary

Having considered the geometries of the various failure mechanisms, field observations can now be linked to a particular mode of failure or potential failure. Additional parameters that impact on stability, such as groundwater (pore pressure), discontinuity condition in terms of in-fill materials and discontinuity persistence, among others, are discussed in the following sections.

## 3. GEOTECHNICAL FIELD INVESTIGATIONS AND GEOLOGICAL MODELLING

### 3.1 New Vaal Colliery

New Vaal Colliery is underlain by dolomites of the Chuniespoort Group. The basement (or floor) topography in a sedimentary environment plays a significant role in the formation of the geotechnical environment of the overlying sediments. It can be anticipated that sediments deposited on a highly undulating floor will exhibit more geotechnical features (faults and jointing) than sediments deposited on a relatively flat floor.

Analysis of the mine-scale geological model identified three prominent N-S trending zones (Figure 3.1.1), representing regional variations in floor topography: gently undulating floor topography in the east to localised and highly variable floor topography in the west (Stewart and Letlotla, 2003). These topographic variations are due to the irregular weathering of the dolomites prior to the deposition of the Ecca Group. This irregular floor topography has significantly influenced the distribution, frequency and orientation of localised geological discontinuities, especially those occurring in the lower stratigraphic units.

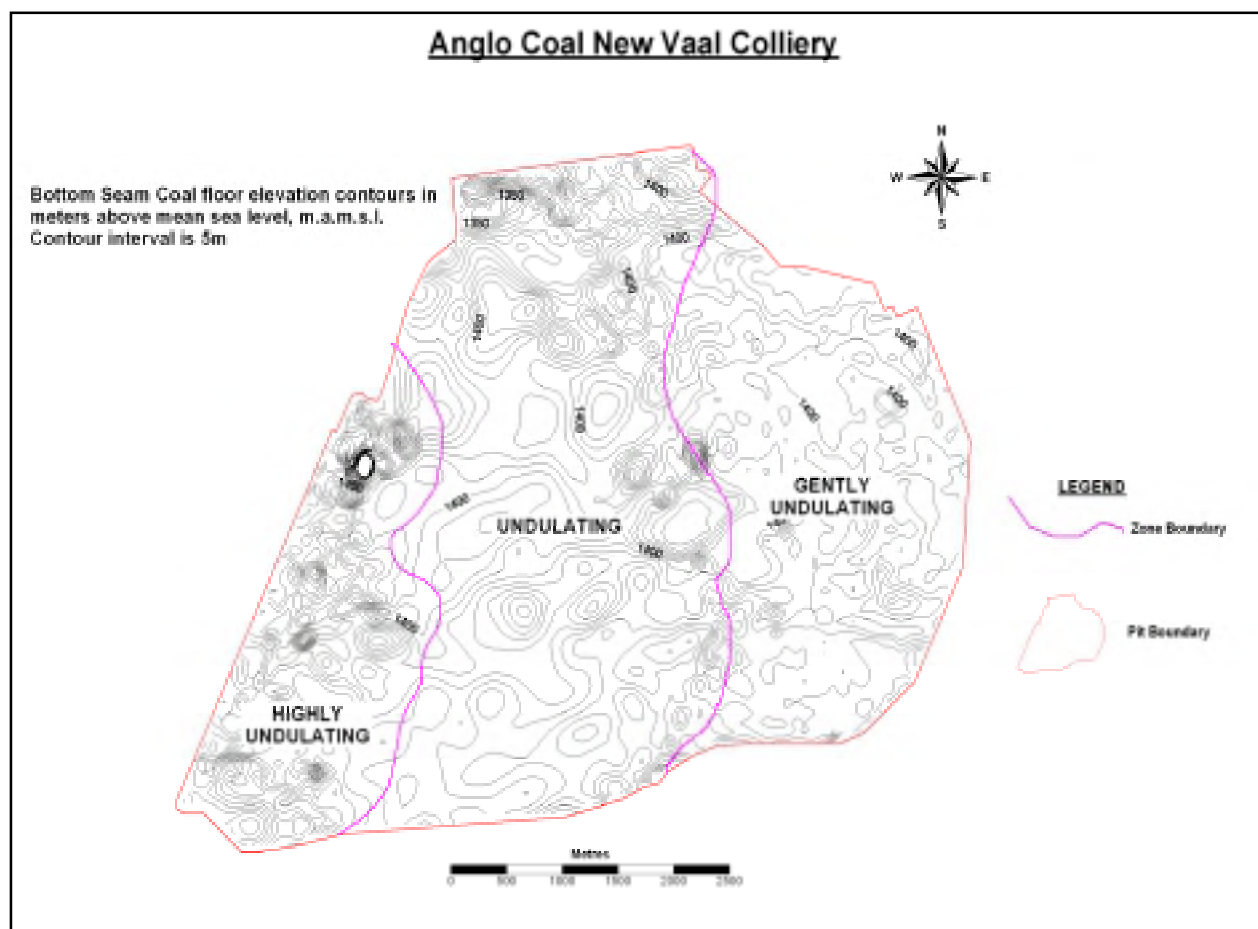


**Figure 3.1.1:** Topographic zoning based on Bottom Seam Coal floor elevation contours

Although the regional horizontal stresses (magnitudes and directions) were not investigated, the resultant regional structures have been identified. A number of dolerite dykes have been encountered in the mining area while airborne magnetic surveys have identified several others.

The prominent strike of these intrusions is W-E (Figure 3.1.2). This observation may indicate that the maximum principal horizontal stress is also W-E, resulting in W-E trending extensional fractures developing (Figure 3.1.3) that are susceptible to igneous intrusions in the form of dolerite dykes. The observed regional faulting pattern also displays predominant W-E strike trend (Figure 3.1.4). An in-pit joint survey (Sonneveldt and Enserink, 1997) identified two major joint sets, striking predominantly NE-SW and NW-SE (Figure 3.1.5). If the maximum principal horizontal stress is W-E, then these joints sets are considered to be conjugates resulting from this maximum principal horizontal stress.

A brief review of the highwall incident reports obtained from the mine indicates that the major factors contributing to the highwall instability were the presence and orientations of geological discontinuities relative to the highwall and floor topography.

In-pit geological and geotechnical mapping, conducted during this investigation, identified two predominant failure mechanisms, namely wedge failure and planar failure (Stewart and Letlotla, 2003). Wedge failure appears to occur more commonly in the Bottom and Middle Seam coal horizons, and overlying interburden, whilst planar failure appears more common in the Top Seam coal horizon and overlying hard overburden. A possible explanation for this observation is that the geotechnical conditions that need to be met for wedge failure are more often present in the lower stratigraphic units than in the upper units. The same is true for planar failure, in that the geotechnical conditions that result in this mode of failure are largely present in the uppermost stratigraphic units. This, however, does not mean that wedge failure cannot occur in the upper zone, as evidenced by the wedge failure that occurred in the hard overburden (Figure 3.1.6).

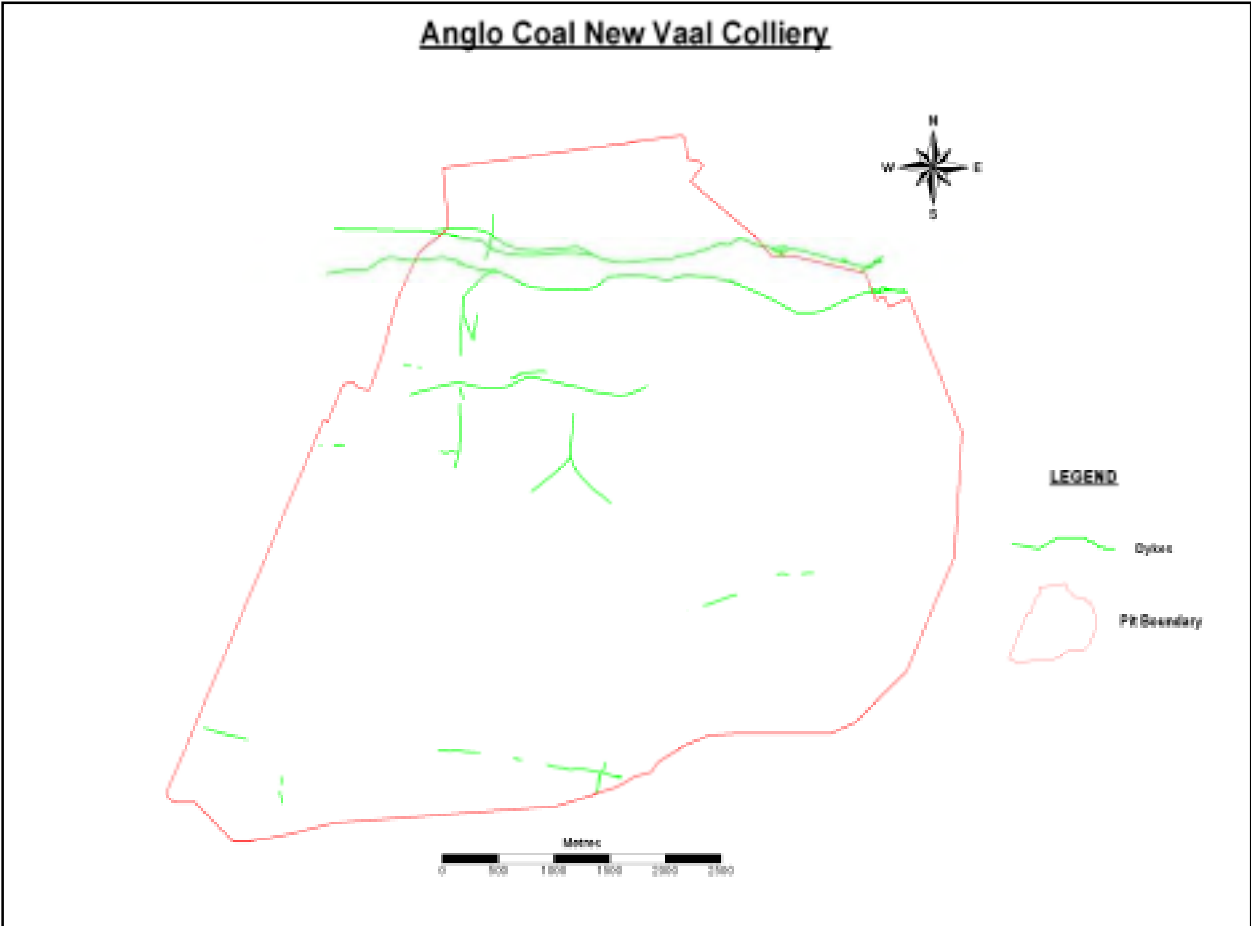


**Figure 3.1.2:** Known dyke distribution at New Vaal Colliery (notice dominant W-E strike)

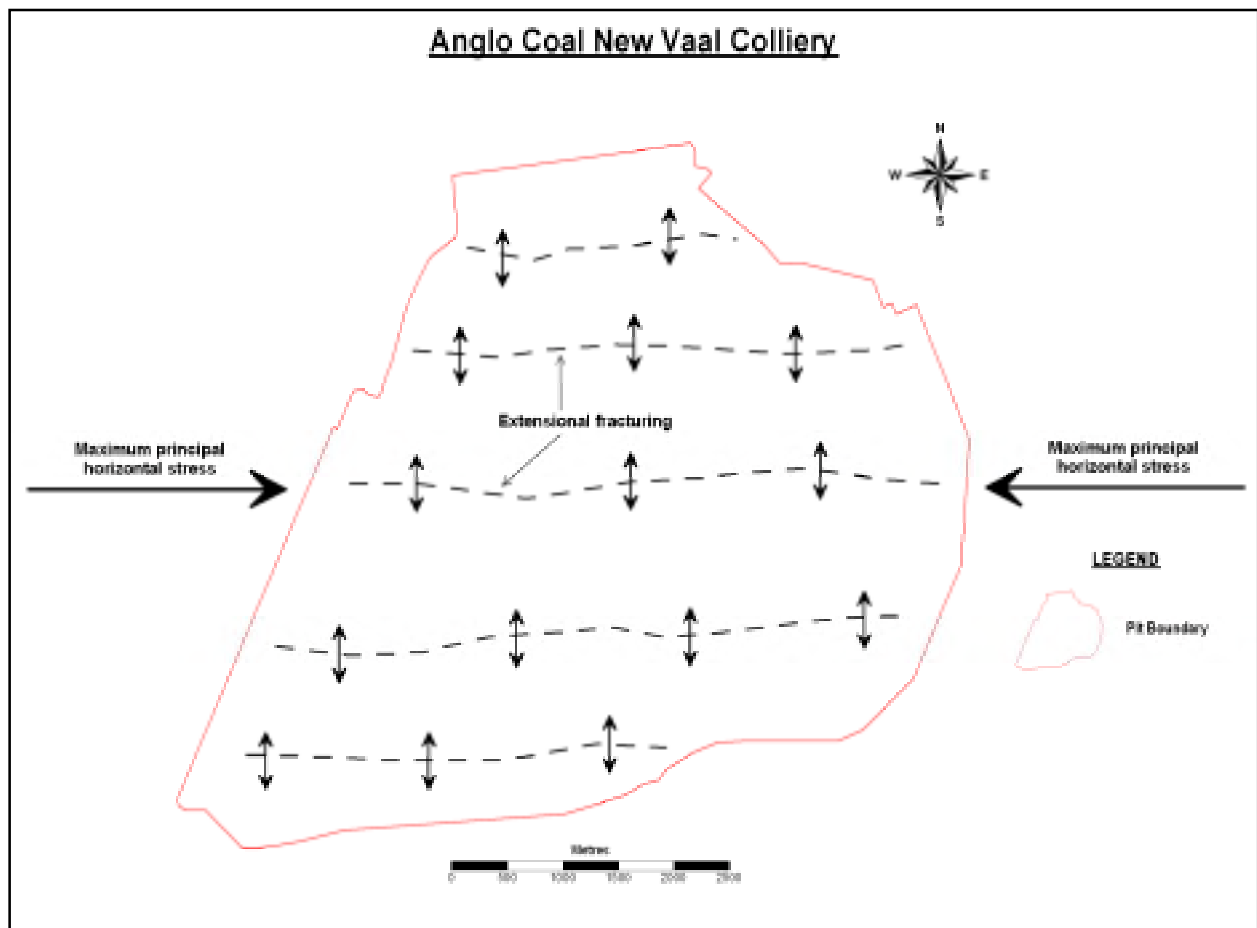


**Figure 3.1.3:** Extensional fracturing resulting from W-E principal horizontal stress

Additional geotechnical features observed that impact on slope stability are localised faults and joints. These discontinuities result mainly from differential compaction of coal and sediments during burial and are therefore greatly influenced by the palaeotopography. The faults are typically listric in nature and confined to single stratigraphic units. Antithetic jointing is also commonly observed. Since these localised features are significantly influenced by the palaeotopography, it follows that they will be more common in the lower stratigraphic units where topographic variations are more pronounced. Thus, there is a higher probability that the conditions needed for wedge failure will be met in the lower stratigraphic units thereby explaining the observed stratigraphic differentiation between modes of failure.

Actual highwall collapses and sloughs that occurred at New Vaal during the course of this work were investigated and back-analysed in order to determine the causes and modes of failure. Evidence indicates that several factors collectively contribute to the instability of the highwall. The factors listed below are not exhaustive but are considered to be the major controlling geological and geotechnical factors:

- Relative orientations of highwall and discontinuities (local and regional);
- Discontinuity spacing, frequency and persistence;
- Discontinuity dip and condition (including in-fill material);
- Bedding dip and direction (controlled by floor topography).

Since these factors are geological in nature, they are inherent and cannot be changed, with the exception of the orientation and dip of the highwall. However, the mine plan is based upon long-term production requirements and there exists little scope for the current layout to be altered. For this reason the highwall orientations as currently planned can be assumed to be fixed. Highwall orientations for the life of the mine can be seen in Figure 3.1.7.

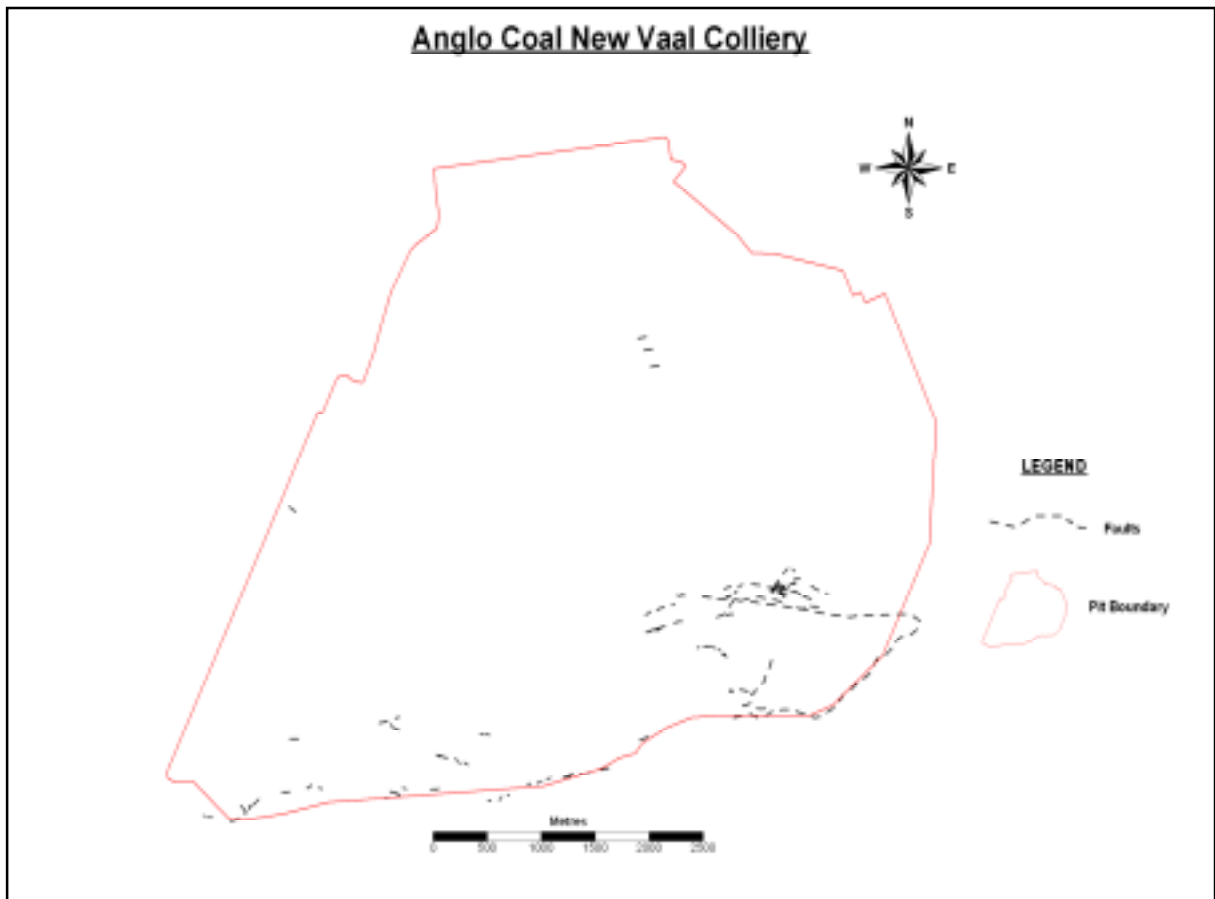


**Figure 3.1.4:** Known fault distribution at New Vaal Colliery (notice dominant W-E strike)

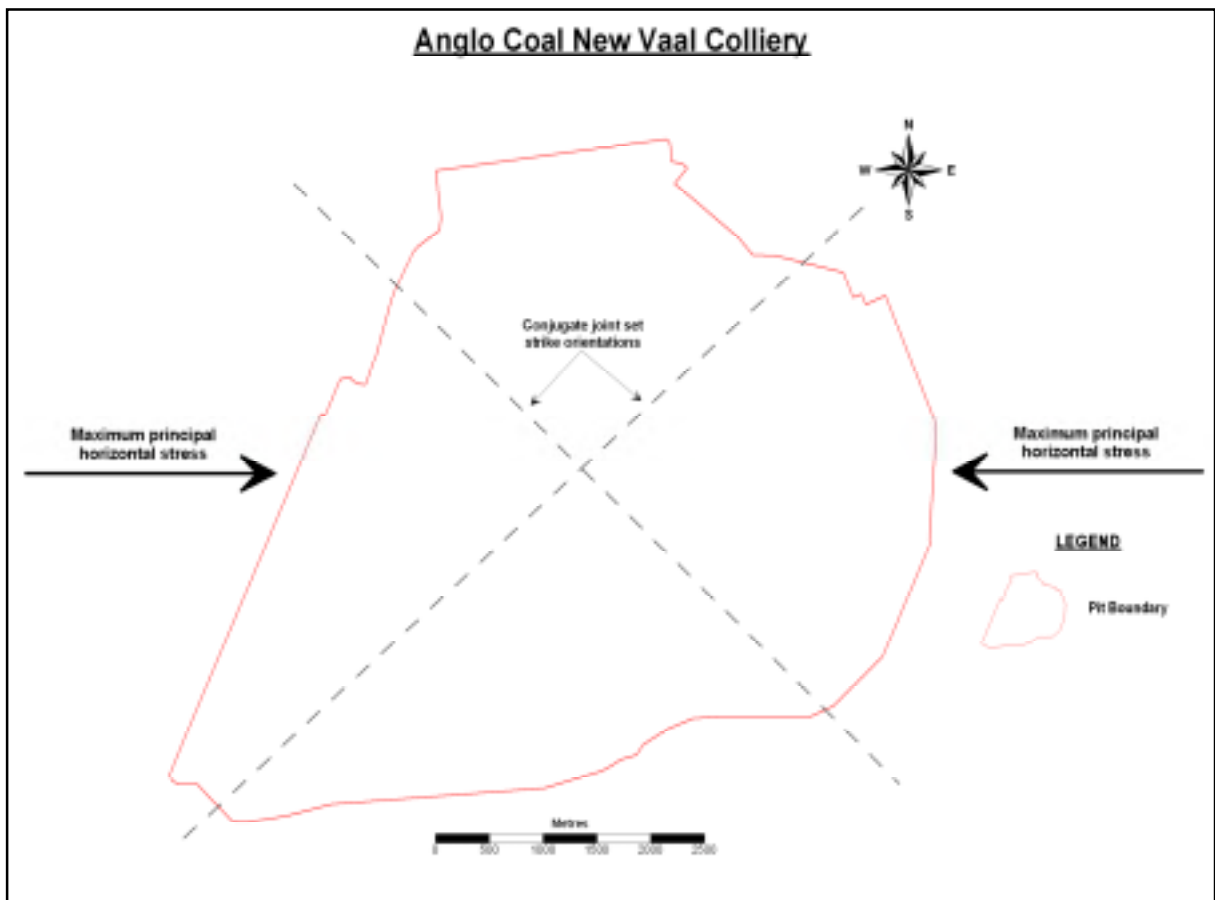


**Figure 3.1.5:** Dominant joint set orientations



**Figure 3.1.6:** Wedge failure in hard overburden (photograph courtesy of New Vaal Colliery)

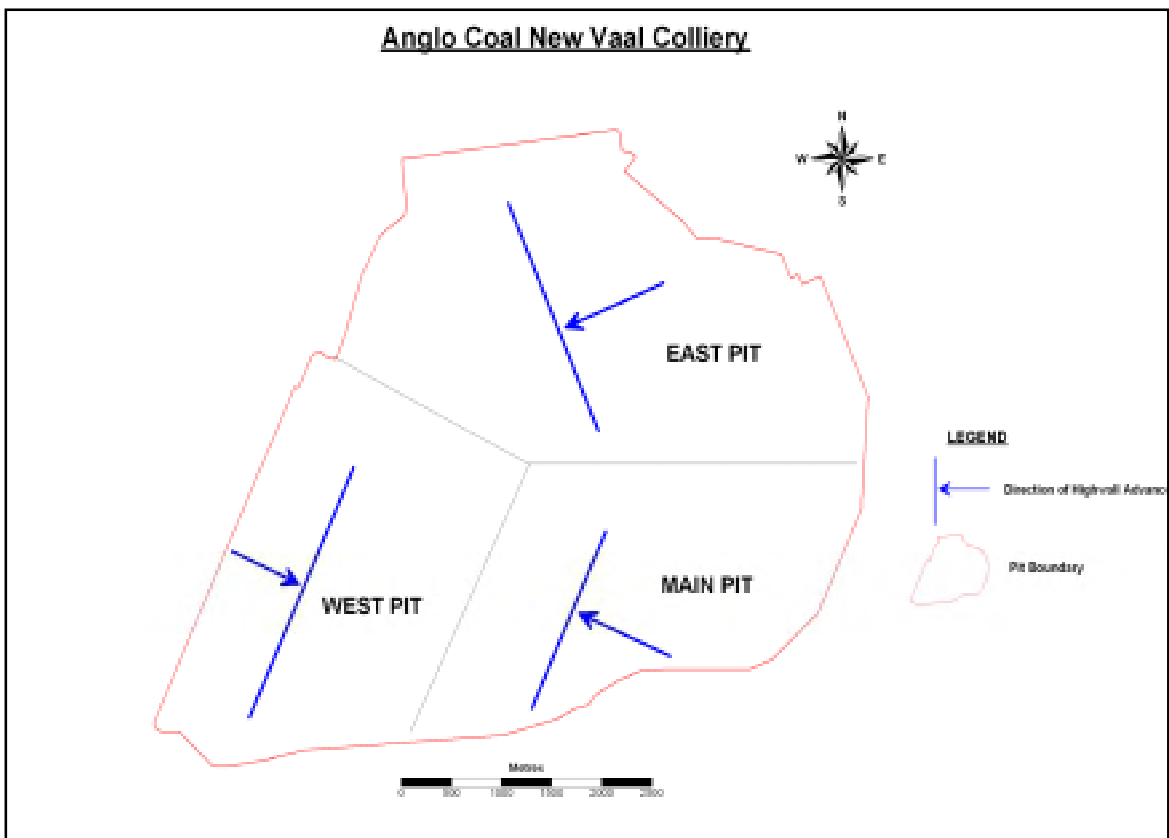


**Figure 3.1.7:** Highwall orientations in the pit indicating direction of advance

The effects of groundwater were not quantified during this investigation; however, observations indicate that water tends to have a lubricating and thus a destabilising effect on the rock mass. In-fill material was not observed in the majority of the discontinuities, and where in-fill material was present, it was mostly calcite (calcite lowers cohesion between joint surfaces). In-fill material either increases or lowers the cohesion between the contacts of a discontinuity, depending on the properties of the material.

### 3.2 Wonderwater Strip Mine

Wonderwater Strip Mine is located some 20km south-west of New Vaal Colliery (Figure 1.1). Although located in the same coalfield, the basement lithologies at each mine are different. Wonderwater is underlain by lavas of the Ventersdorp Supergroup as opposed to the dolomite basement at New Vaal, and it was considered possible that different causes would exist for highwall failure at Wonderwater (van Heerden, 2004a).

The palaeo-floor at Wonderwater, composed of lavas of the Ventersdorp Supergroup, provided a relatively flat and smooth surface onto which the Ecca Group sediments were deposited. Figure 3.2.1.a is a coloured contour plot of the floor of the No. 2B Seam, the lower of the two seams mined at Wonderwater. This plot indicates three prominent palaeo-highs in the western (1) and eastern (2) extremities of the central portion of the mine area. A significant fault, down-throwing the northern area, is also evident. Within the current pit boundaries, the plot shows that the strata are relatively flat lying and not as undulating as is the situation with the New Vaal strata. The seam thickness isopach plot for the No. 2B Seam (Figure 3.2.1.b) shows that the seam has a relatively constant thickness, except where it thins against the palaeo-highs. This is also indicative of sediment deposition on a relatively smooth topography.

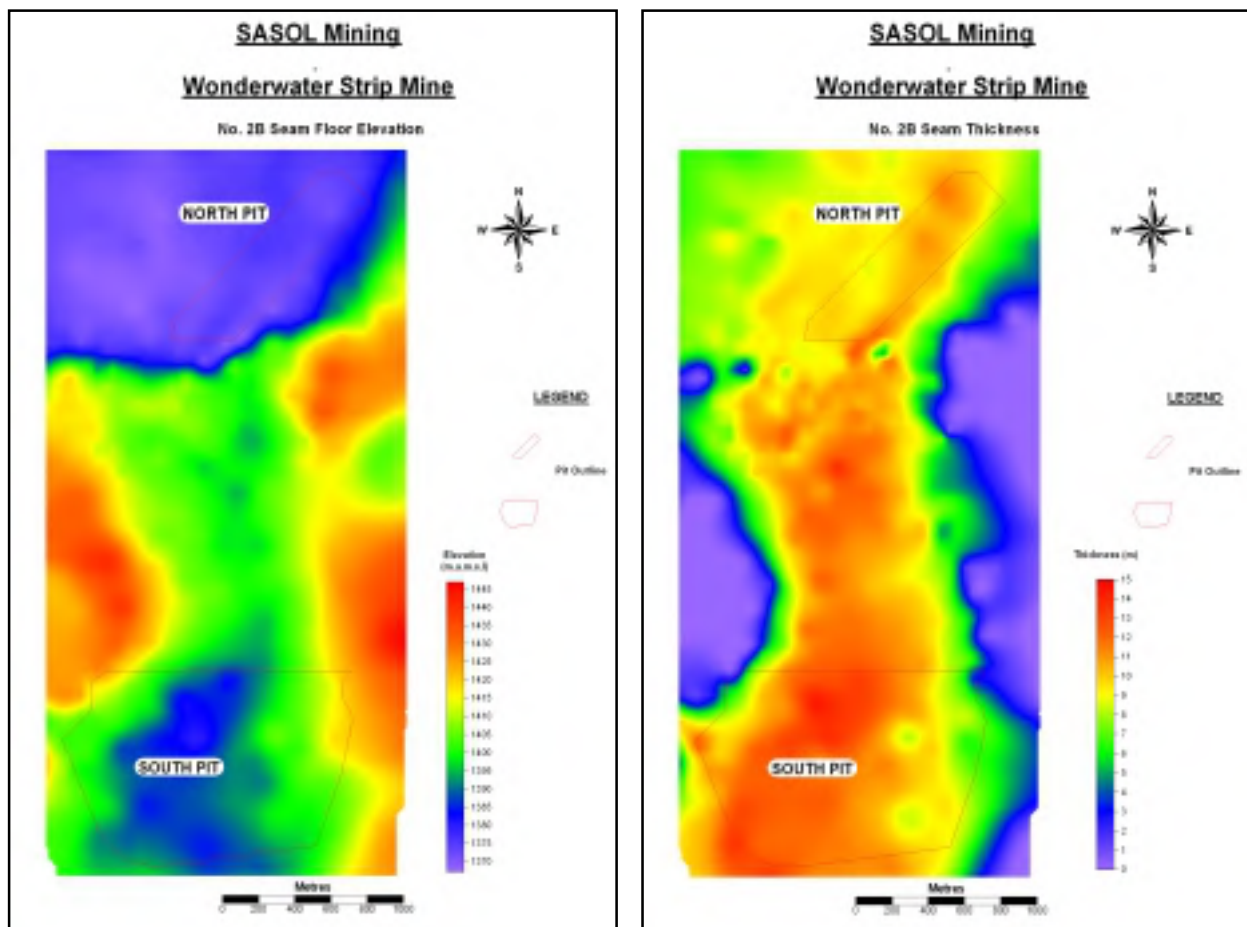
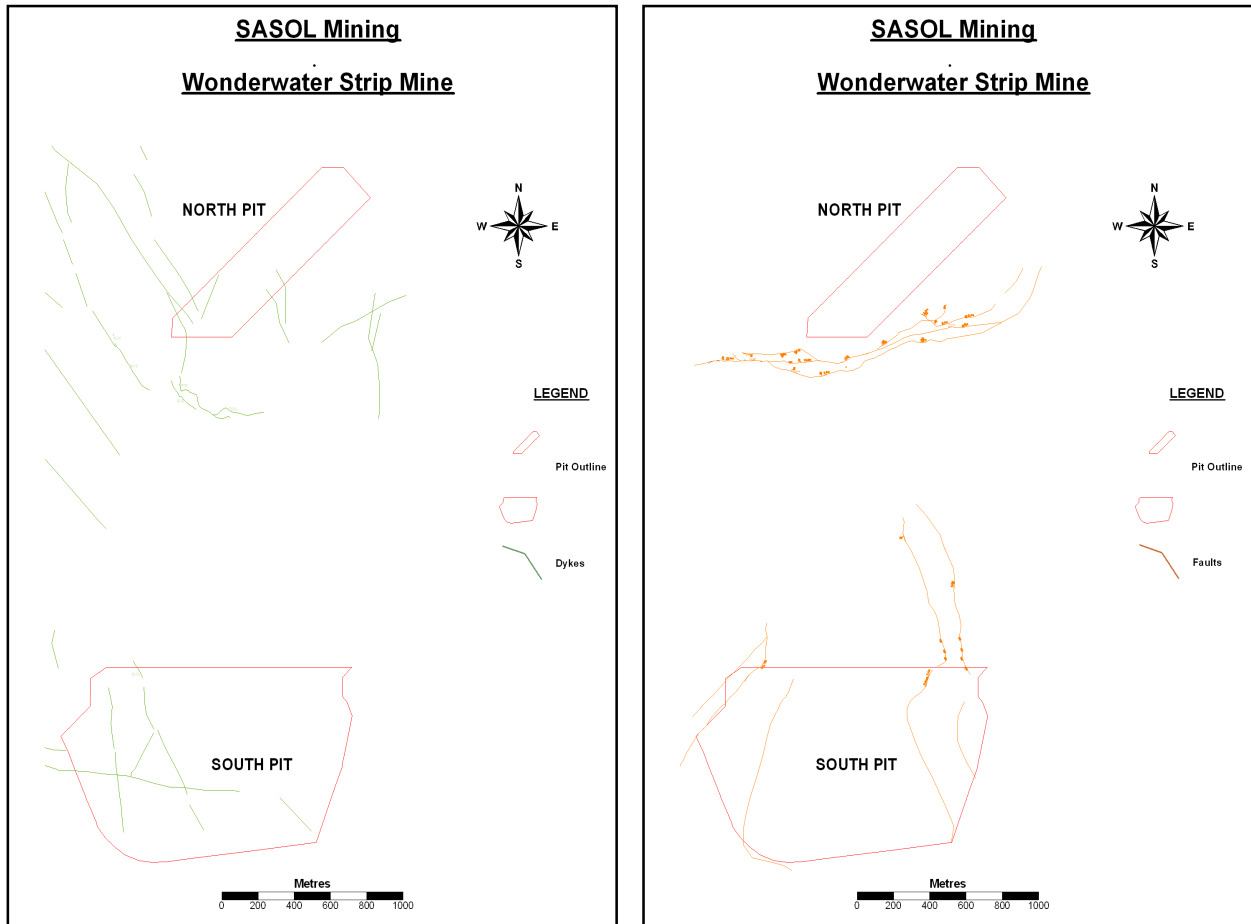


Figure 3.2.1: a) No. 2B Seam floor elevation; b) No. 2B Seam thickness isopach

Regional geological structures include dolerite dykes and normal faults. The predominant strike of the dykes is roughly NW-SE (Figure 3.2.2.a), while the fault orientations display an equal distribution between NNW-SSE and WSW-ENE strike trends (Figure 3.2.2.b). The roughly W-E striking faults on the southern boundary of the North Pit are associated with the major pre-Karoo fault in this area and are not considered to be associated with the maximum principal horizontal stress. Considering the orientations, therefore, of the dykes and southern faults, the maximum principal horizontal stress direction is likely to be NW-SE.



**Figure 3.2.2:** a) Wonderwater dyke distribution; b) Wonderwater fault distribution

Several post-failure highwall sites were visited in the Wonderwater pit, and the modes of failure were determined to be either planar or wedge. Figure 3.2.3 is a photograph of a failed highwall where the mode of failure was planar, and Figure 3.2.4 is a photographed example of wedge failure. Incident reports generated by the mine geologist regarding previous highwall collapses were also reviewed. In all these cases, the contributing factors to instability were the interactions between the highwall face and geological discontinuities. No physical measurements were taken on the failure surfaces due to strict mine regulations preventing personnel from approaching the highwall. However, Figure 3.2.3 clearly shows that the failure plane is striking nearly parallel to the highwall. Rock mass property investigations carried out by mine personnel indicate that the rock strengths are generally greater than the shear stress magnitudes and, therefore, failure should not typically occur through intact rock but rather on existing planes of weakness where their attitudes (orientation and dip) relative to the highwall allow movement to occur.

Highwall stability at Wonderwater Strip Mine is therefore primarily controlled by the relative orientations and interactions between the highwall and geological discontinuities.



**Figure 3.2.3:** A failed highwall where the mode of failure was planar (photograph courtesy of Wonderwater Strip Mine)

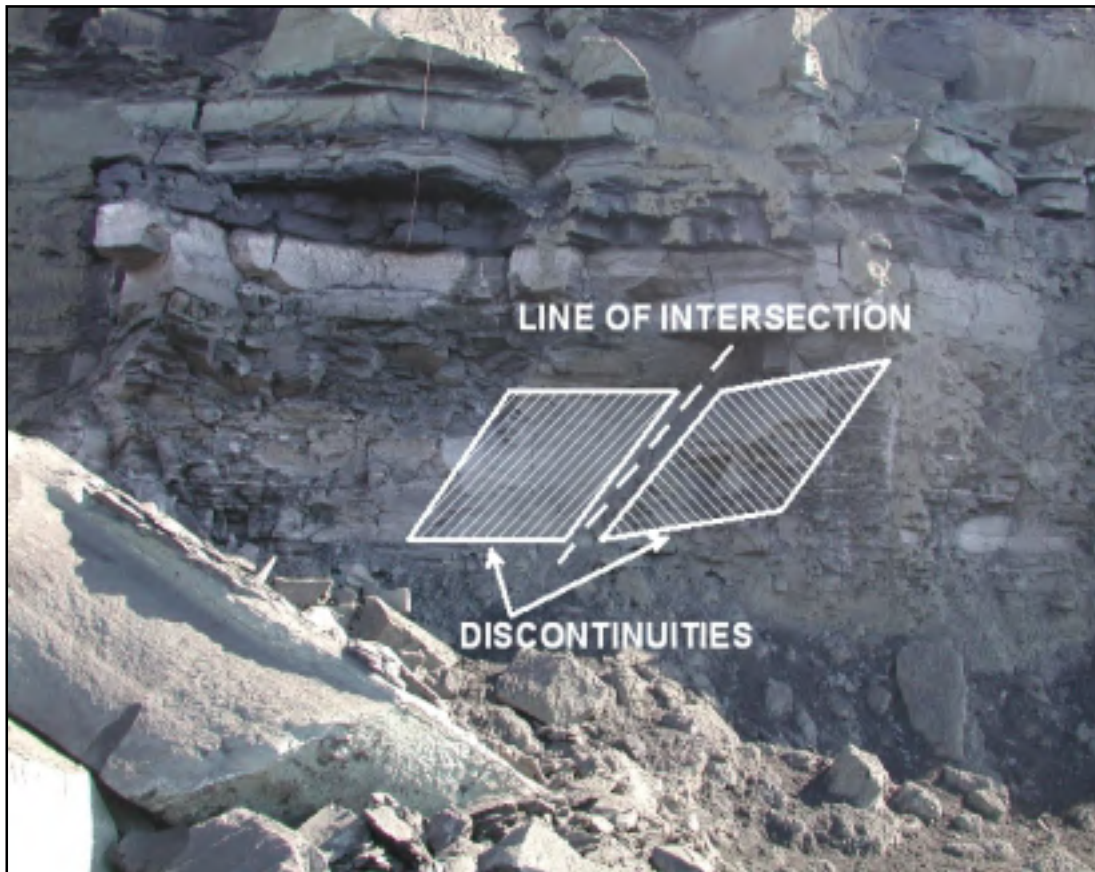


**Figure 3.2.4:** Interburden wedge failure (photograph courtesy of Wonderwater Strip Mine)

### **3.3 Summary**

Geological and geotechnical investigations were carried out at two operating opencast coal mines, namely New Vaal Colliery and Wonderwater Strip Mine. The two mines are situated in differing geological and geotechnical environments, yet the controls on highwall stability are the same at both sites. These controls are primarily the interactions between highwalls and the geological discontinuities present in the rock mass (van Heerden, 2004a).

The depositional and tectonic history of a coal deposit is considered to be the primary control on the present-day geotechnical environment. Regional joint sets and their relative orientations and dips are a function of regional horizontal stresses as well as the nature of the sedimentary pile, i.e. rock mass properties. The presence or absence of smaller scale geotechnical features is a function of both regional tectonics and the palaeodepositional environment. Regional post lithification tectonic activity, resulting in significant faulting, tends to introduce smaller scale features in the immediate vicinity of the major faults. Similarly, igneous intrusions, in the form of dolerite dykes, also cause the rock mass in the immediate vicinity of the dyke to be affected by an increase in the density of geotechnical features, such as joints and fractures.

Predicting the occurrence and nature of discontinuities, combined with knowledge of the floor topography, will enable the identification of hazardous areas in virgin ground ahead of mining. Geotechnical highwall mapping allows for the identification of geologically and mechanically induced discontinuities. This mapping, however, only allows for a short-term view of the highwall condition, since mapping can only be conducted once the highwall is exposed. In addition, blasting practices have a significant impact on the condition of the highwall and, therefore, on the applicability of the mapping procedure. Pre-split or smooth-wall blasting allows for reasonable mapping since the highwall produced is relatively undisturbed and the discontinuities observed can, more often than not, be differentiated according to geological or blasting origins. Buffer-blasting, on the other hand, tends to destroy the fabric of the rock mass to such an extent that mapping becomes almost irrelevant, although major discontinuities, such as faults with displacements of more than a few metres, will still be obvious.

Since the major controls on highwall stability are the orientations and interactions between discontinuities and the highwall face, it is imperative that geological discontinuities are identified and described to a fairly high degree of accuracy. In addition, it is preferable that these features are identified ahead of mining so that adverse conditions can be forecast prior to the highwall being exposed. This allows for appropriate mine planning in terms of safety, where measures can be put in place prior to the exposure of a hazardous highwall.

One method of identifying geotechnical features in virgin ground is through geotechnical logging of borehole core samples. For this method to be appropriate, core samples need to be obtained through the use of specialised drilling techniques. Typically, routine drilling on mines produces non-oriented and highly broken core samples, unsuitable for geotechnical core logging (van Heerden, 2004b). The application of geophysical wireline logging techniques has, therefore, been investigated in terms of identifying geotechnical features in virgin ground ahead of mining (van Heerden, 2004b).

### **3.4 Geophysical wireline logging**

A brief geophysical wireline logging exercise was conducted at New Vaal Colliery in order to determine if simple wireline techniques could be applied for the identification of geotechnical features in geological boreholes. This study showed that a minimum of three geophysical probes is necessary to adequately describe a sedimentary sequence in terms of macro-lithology and geotechnical features (van Heerden, 2004b). The three probes identified were:

- 1) the density (gamma-gamma) probe;
- 2) the optical televiewer, and;
- 3) the acoustic televiewer probes.

The density probe is used to differentiate between the two major lithotypes found in typical Ecca Group sedimentary sequences, namely rock and coal. Differentiation is based on bulk density differences: rock formations (sandstone, siltstone and shale) have a noticeably higher bulk density than coal formations. The two televiwer probes provide an image of the wall of the borehole in which the probe is lowered. The optical televiwer is used in dry holes while the acoustic televiwer is used in water-filled holes. With the use of appropriate software, geophysical data (particularly from the televiwer) is manipulated and orientation data (dip and dip direction) is obtained for identified geotechnical features. The predictive methodology that follows (see Section 4) explains how this data is used to identify hazards in current and future highwalls.

### **3.5 Conclusion**

Geological, geotechnical and geophysical field investigations in differing geological and geotechnical environments indicate that it is necessary to identify and accurately describe geological discontinuities in order to assess highwall stability. It is also necessary to understand that the topography of the strata, controlled by the palaeo-floor, plays a significant role in the overall assessment of the rock mass.

Rock mass behaviour in slopes is predominantly controlled by the interactions between discontinuities and the highwall face (slope). Inherent rock mass properties, such as RQD and UCS have been shown to be of less importance (van Heerden, 2004b), although they should not be ignored completely and can be used to assist with the overall evaluation of slope behaviour.

## **4. PREDICTIVE METHODOLOGY FOR SLOPE STABILITY HAZARD RATING**

### **4.1 Introduction**

Section 2 reviewed the four common mechanisms of slope failure: circular, plane, toppling and wedge failure. Of these four mechanisms, only toppling failure was not observed during field investigations, nor was it reported on in any of the slope failure incident reports. This does not mean that toppling failure cannot, or does not, occur and it will still be considered in this methodology. Circular failure occurs predominantly in soft overburden soils and highly weathered overburden and will only be briefly discussed. The predominant failure mechanisms are the plane and wedge failure mechanisms. The methodology will thus concentrate on these modes of failure.

Although the majority of the fieldwork, including the geophysical wireline logging investigation, was conducted at New Vaal Colliery, the approach adopted here regarding slope stability hazard identification and rating is also applicable to other sites. The methodology has been developed using geological and geotechnical information gathered from a test site at New Vaal Colliery. The matrix-type rating system proposed by Stewart and Letlotla (2003) is adapted and modified for this final predictive methodology.

### **4.2 Methodology**

A basic understanding of the rock mass in which a slope exists, or is to be engineered, is the first step in any slope stability assessment programme. This information is typically available in the form of a geological model built using information from various sources, including borehole cores, surface and exposure mapping, and remotely sensed data. Analysis of the geological model will allow for the identification of major geological trends and indicate the likelihood of the occurrence of localised geotechnical features. Examination of these trends and potential features in relation to existing and proposed highwall slopes will allow for a preliminary assessment of the potential for highwall failure.

#### **4.2.1 Analysis of the geological model**

The New Vaal Colliery mine-scale geological model has been examined and was discussed in Section 3.1. The test site for further geological, geotechnical and geophysical investigations

was located in the West Pit and it is assumed that the current highwall orientation and direction of advance (Figure 3.1.7) remain constant for the purpose of subsequent interpretations. The following points were noted with regards to a preliminary assessment of slope stability in the West Pit:

- i. The palaeo-floor topography is highly undulating in the West Pit and this is expected to increase the frequency of localised geotechnical features, such as minor faulting and jointing, in the overlying rock mass (refer to Figure 3.1.1);
- ii. Dykes and faults have previously been mapped in the area, particularly in the southern portion (refer to Figure 3.1.2 and Figure 3.1.4);
- iii. Highwall orientation is sub-parallel (within  $\pm 20^\circ$ ) to the NE-SW striking joint set (refer to Figure 3.1.5 and Figure 3.1.7).

It will be appreciated that the combined effects of geology, observed geotechnical features and the highwall orientation in the West Pit indicated that slope stability in this area needed more detailed and focused attention. The test site in the West Pit covers an area of approximately 95 000 m<sup>2</sup> and has been modelled independently from the remaining mine area. Figure 4.2.1.1 is a plot of the current mining block layout within the test site area, indicating highwall advance direction and a reference highwall (crest), which will be evaluated in terms of stability. Actual mining (coal loading) thus takes place across the width of a mining block (60 m) and advances in the direction of the long axis of a mining block, either from the north-east or from the south-west. The mining block is 100 m in length.

A generalised stratigraphic column is illustrated in Figure 4.2.1.2. Existing information from the geological borehole database was used to model and contour the contacts between the major litho-stratigraphic horizons, namely surface topography and the floors of the top seam, middle seam and bottom seam coal horizons. Figures 4.2.1.3 through 4.2.1.6 are the modelled contour plots of these four surfaces respectively.

# Anglo Coal New Vaal Colliery

## West Pit Test Site

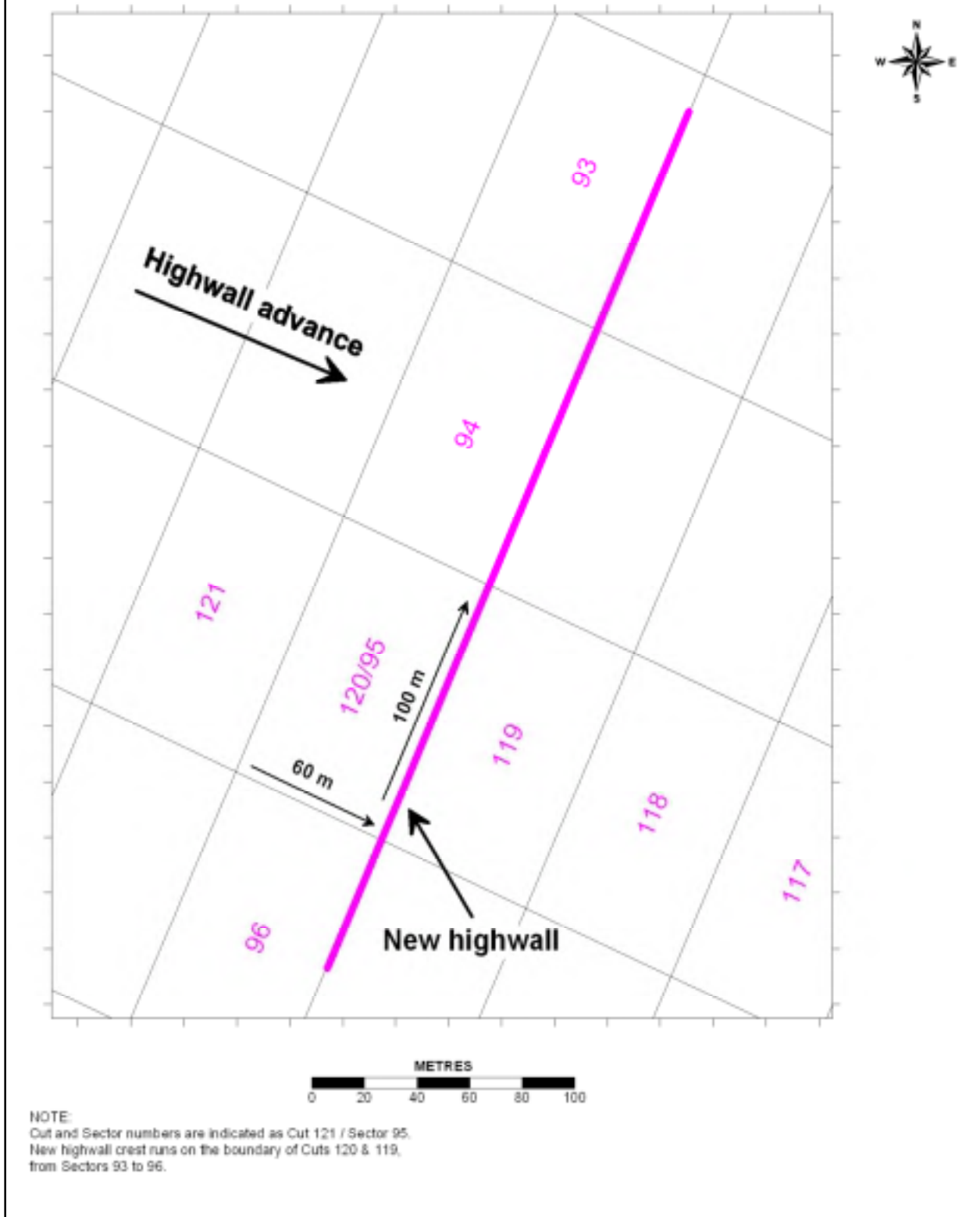
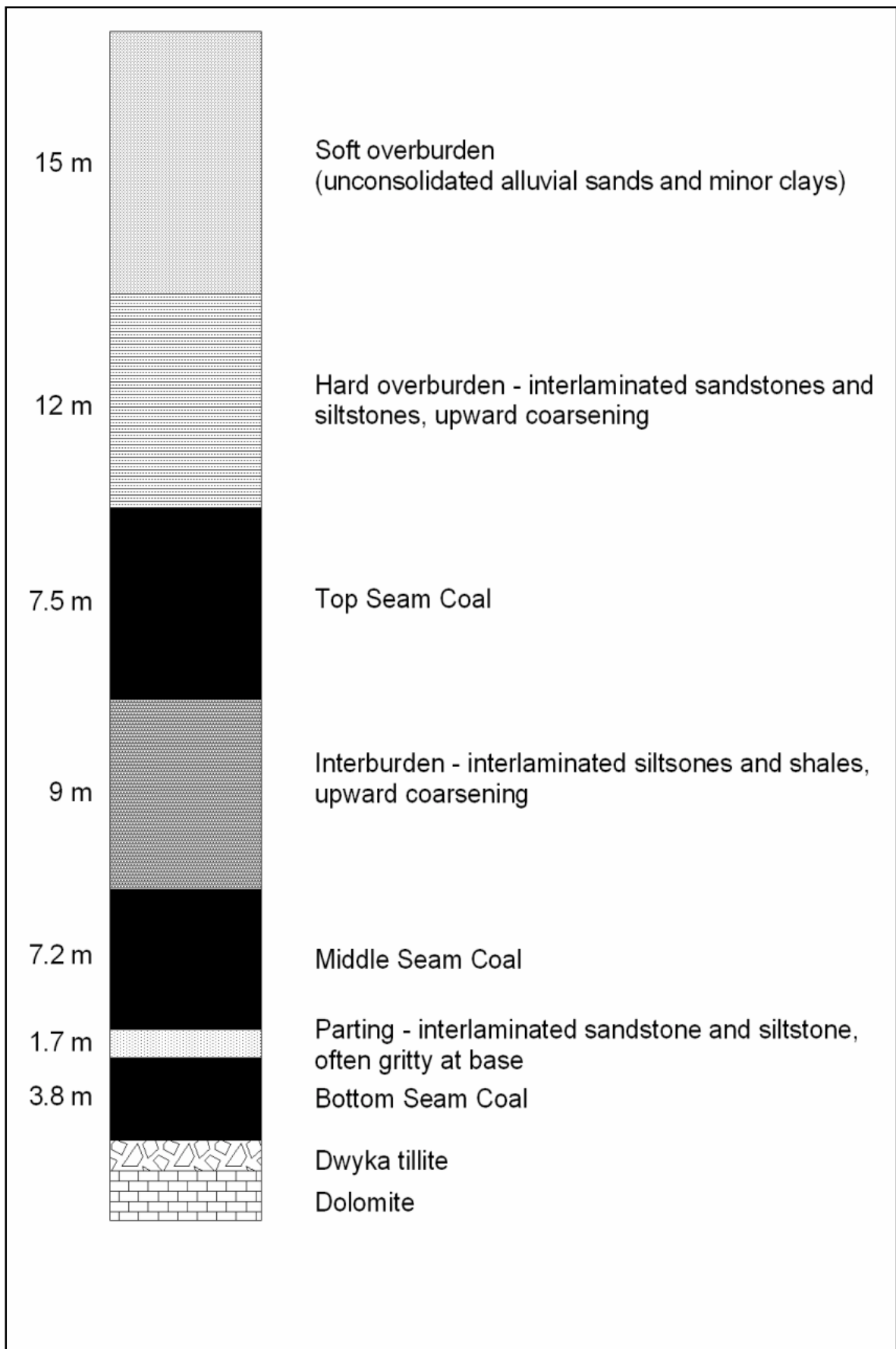


Figure 4.2.1.1: West Pit test site, New Vaal Colliery



**Figure 4.2.1.2:** Generalised stratigraphic column for New Vaal Colliery. Average thicknesses are indicated, except for the lower two lithological units – these are irrelevant since the base of all workings will be the base of the Bottom Seam Coal

# Anglo Coal New Vaal Colliery

## West Pit Test Site

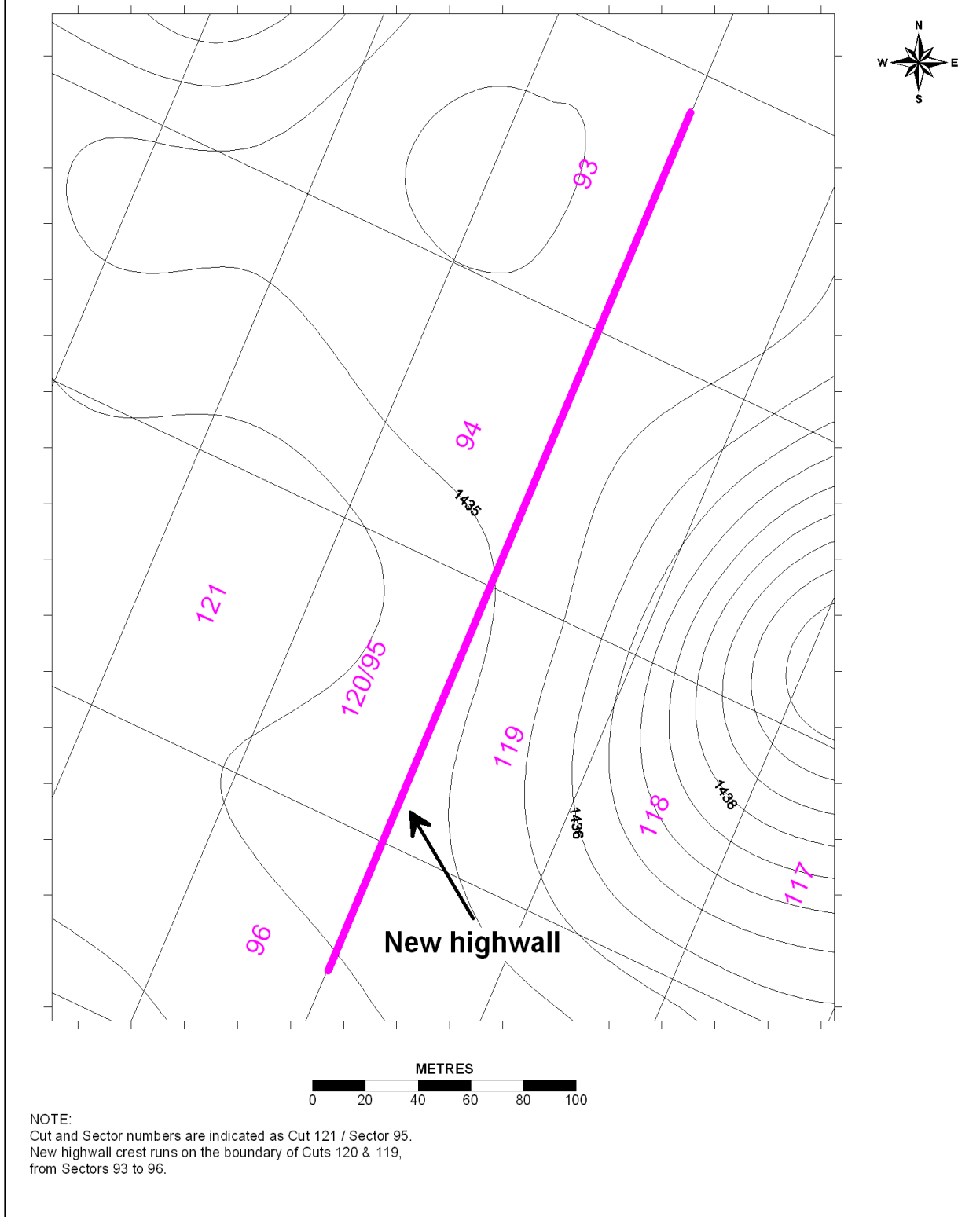
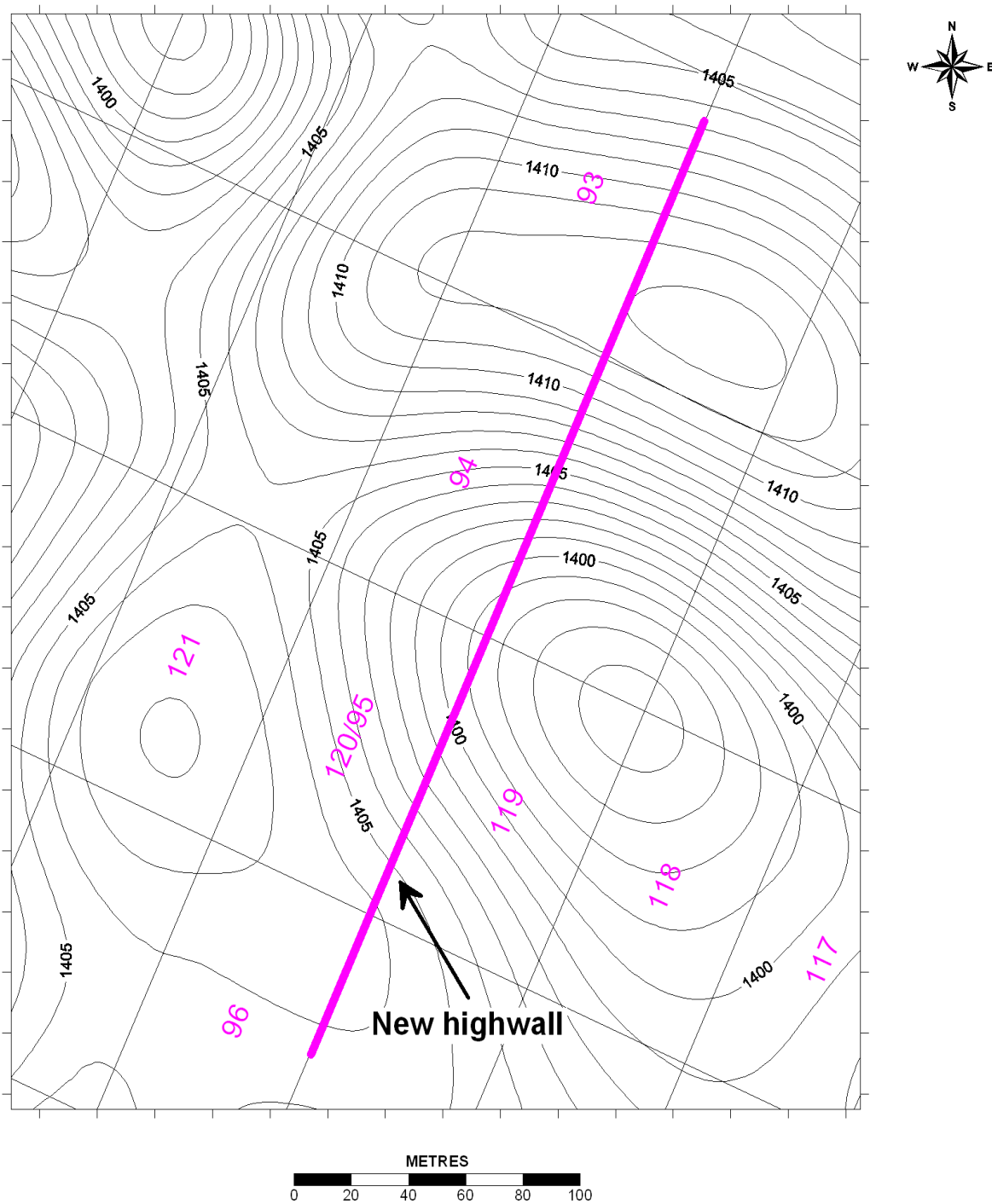


**Figure 4.2.1.3:** Surface elevation contours in metres above mean sea level (m.a.m.s.l)

# Anglo Coal New Vaal Colliery

## West Pit Test Site

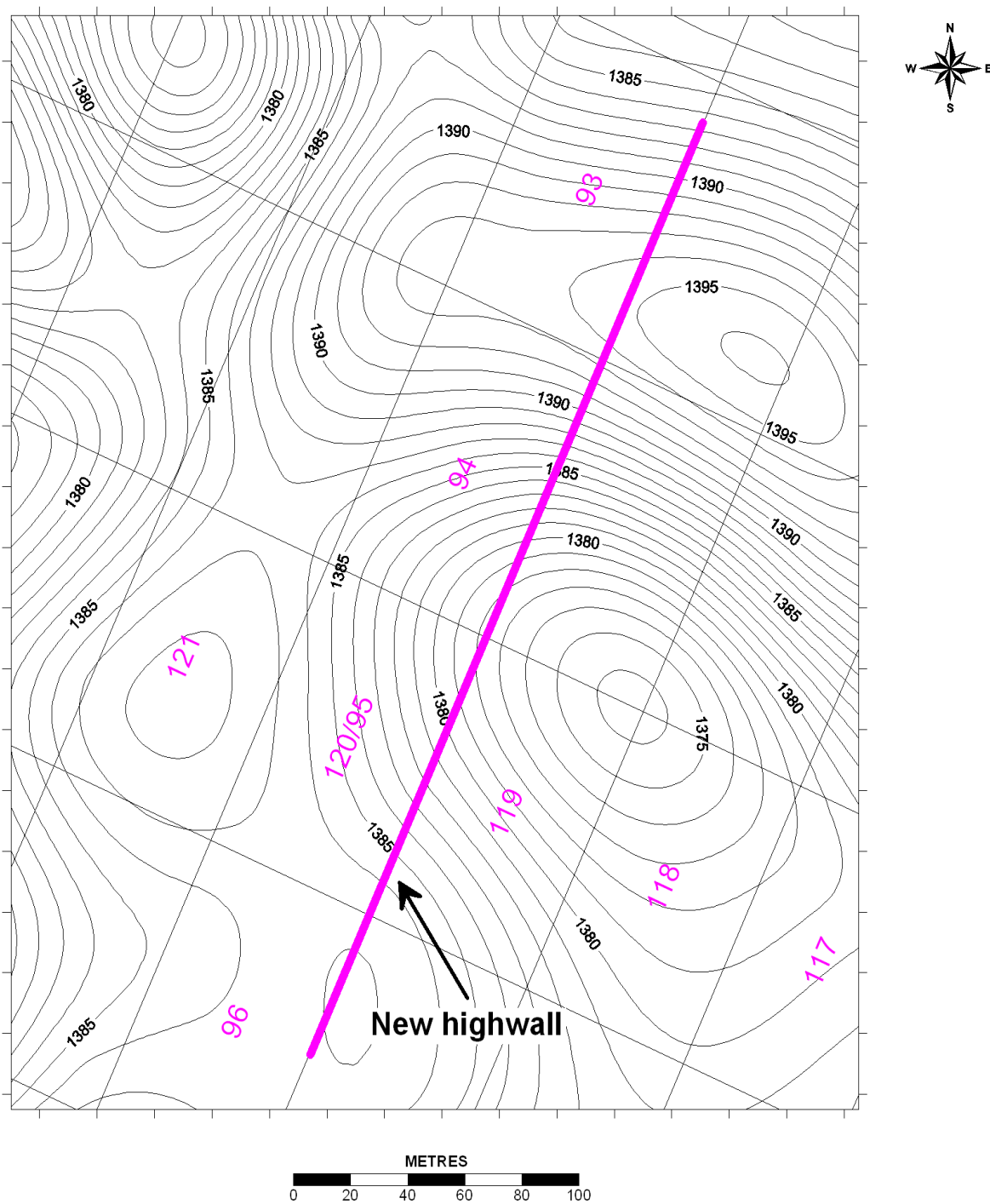


NOTE:  
Cut and Sector numbers are indicated as Cut 121 / Sector 95.  
New highwall crest runs on the boundary of Cuts 120 & 119,  
from Sectors 93 to 96.

**Figure 4.2.1.4:** Top Seam Coal floor elevation contours (m.a.m.s.l)

# Anglo Coal New Vaal Colliery

## West Pit Test Site

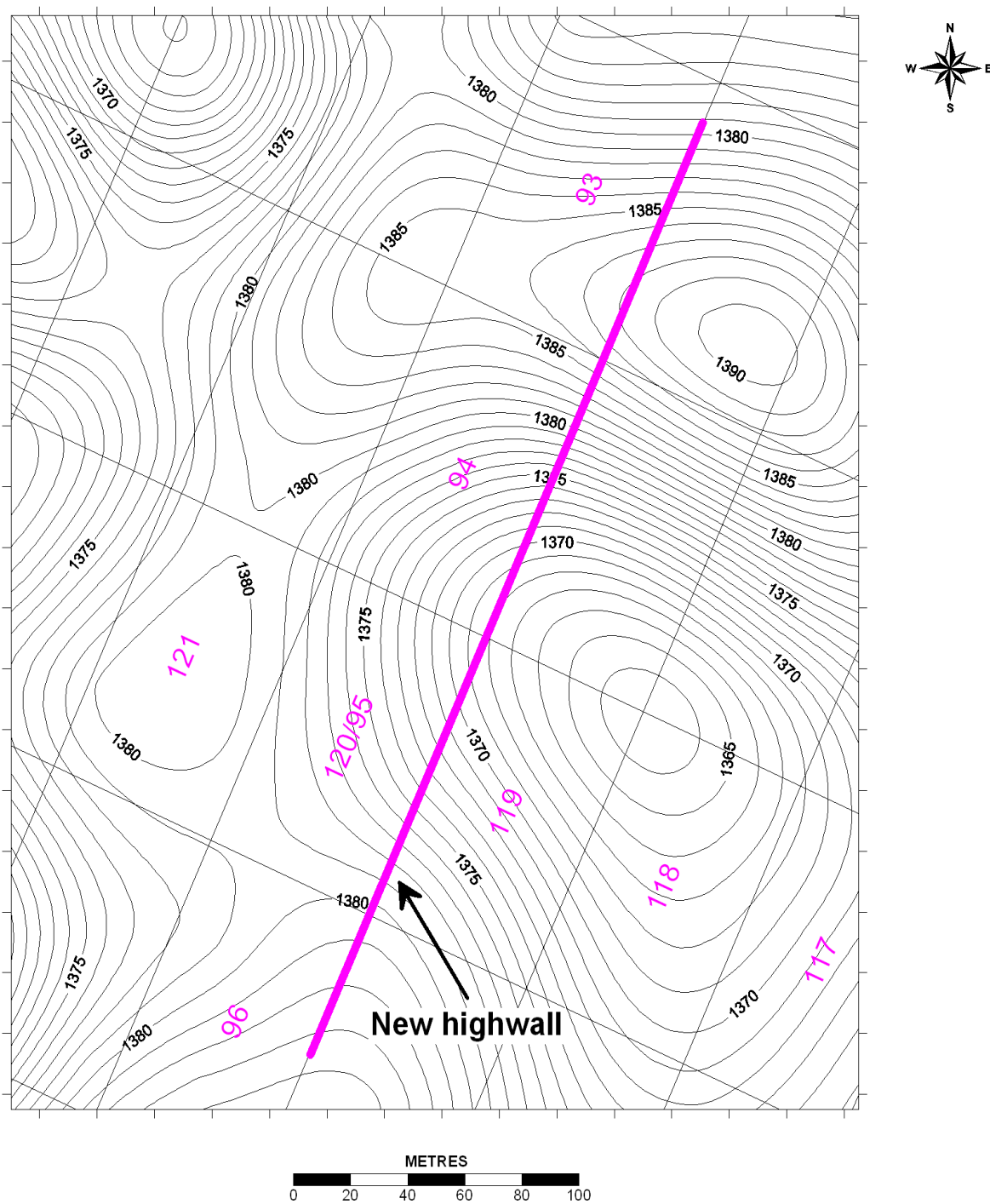


NOTE:  
Cut and Sector numbers are indicated as Cut 121 / Sector 95.  
New highwall crest runs on the boundary of Cuts 120 & 119,  
from Sectors 93 to 96.

**Figure 4.2.1.5:** Middle Seam Coal floor elevation contours (m.a.m.s.l)

# Anglo Coal New Vaal Colliery

## West Pit Test Site



NOTE:  
Cut and Sector numbers are indicated as Cut 121 / Sector 95.  
New highwall crest runs on the boundary of Cuts 120 & 119,  
from Sectors 93 to 96.

**Figure 4.2.1.6:** Bottom Seam Coal floor elevation contours (m.a.m.s.l)

It is immediately apparent from the three coal seam floor contour plots that the gradient of the strata at any given point increases progressively down the sequence. This is evidenced by the fact that the contour lines become more closely spaced from plot to plot. This is expected in a sedimentary depositional environment where deeper areas will accumulate thicker sediments and, as new sediments are deposited, the topography tends to level out and accumulated sediments attain constant thicknesses. Owing to the effects of differential compaction, it is also expected that the lower stratigraphic horizons will display an increased occurrence of localised jointing and listric faulting. This was, in fact, observed during in-pit mapping at New Vaal (Stewart and Letlotla, 2003).

Figure 4.2.1.7 is a 3-dimensional (3D) profile view of the Top Seam floor. This image clearly illustrates the topography of the strata and how the strata dip relative to the new highwall.

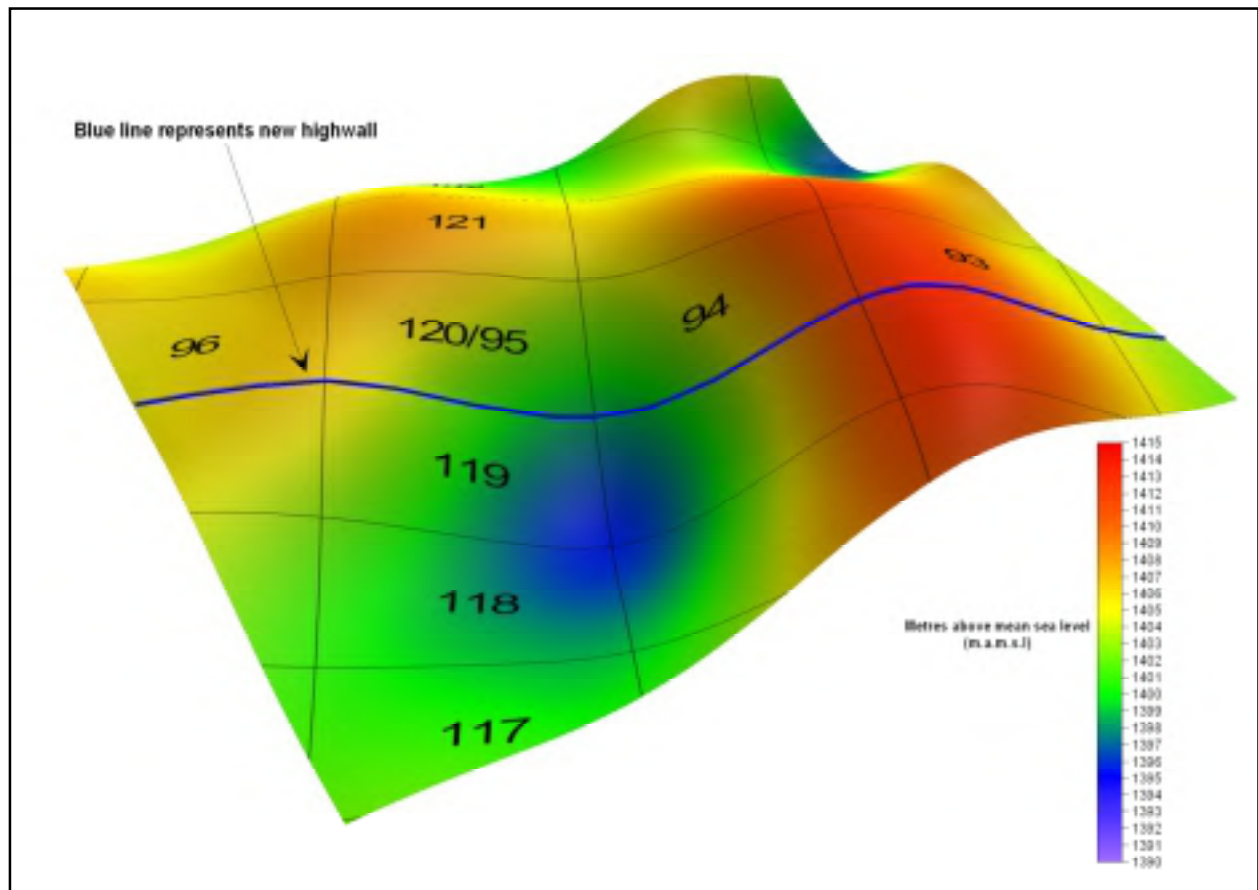


**Figure 4.2.1.7:** A 3-dimensional profile view of the Top Seam floor topography

It is not necessary to produce similar plots for the lower two seam floors. Suffice it to say that the gradients will get steeper, as indicated by the contour plots. The geological information reviewed thus far allows for a good understanding of certain rock mass geometries relative to the new highwall and these are summarised as follows:

- The surface topography is unrelated to the underlying topography – compare contour plots presented in Figures 4.2.1.3 through 4.2.1.6;
- A surface 'high' (elevated area) exists almost directly above a palaeo-low – compare contour plots presented in Figures 4.2.1.3 through 4.2.1.6;
- The strata are dipping either into or parallel to the new highwall – refer to Figure 4.2.1.7;
- An increased frequency of jointing and listric faulting is expected in areas of steeper gradient and in the lower stratigraphic units, and;
- Circular step faulting with radial jointing is expected around the palaeo-low zone (Stewart and Letlotla, 2003).

**4.2.2 Analysis of geophysical data: Stereography**

In order to further characterise the rock mass in terms of geotechnical features, a series of six boreholes was drilled along the line of the new highwall for geophysical wireline logging purposes. The exact positions of these boreholes, relative to the new highwall, are presented in Figure 4.2.2.1.

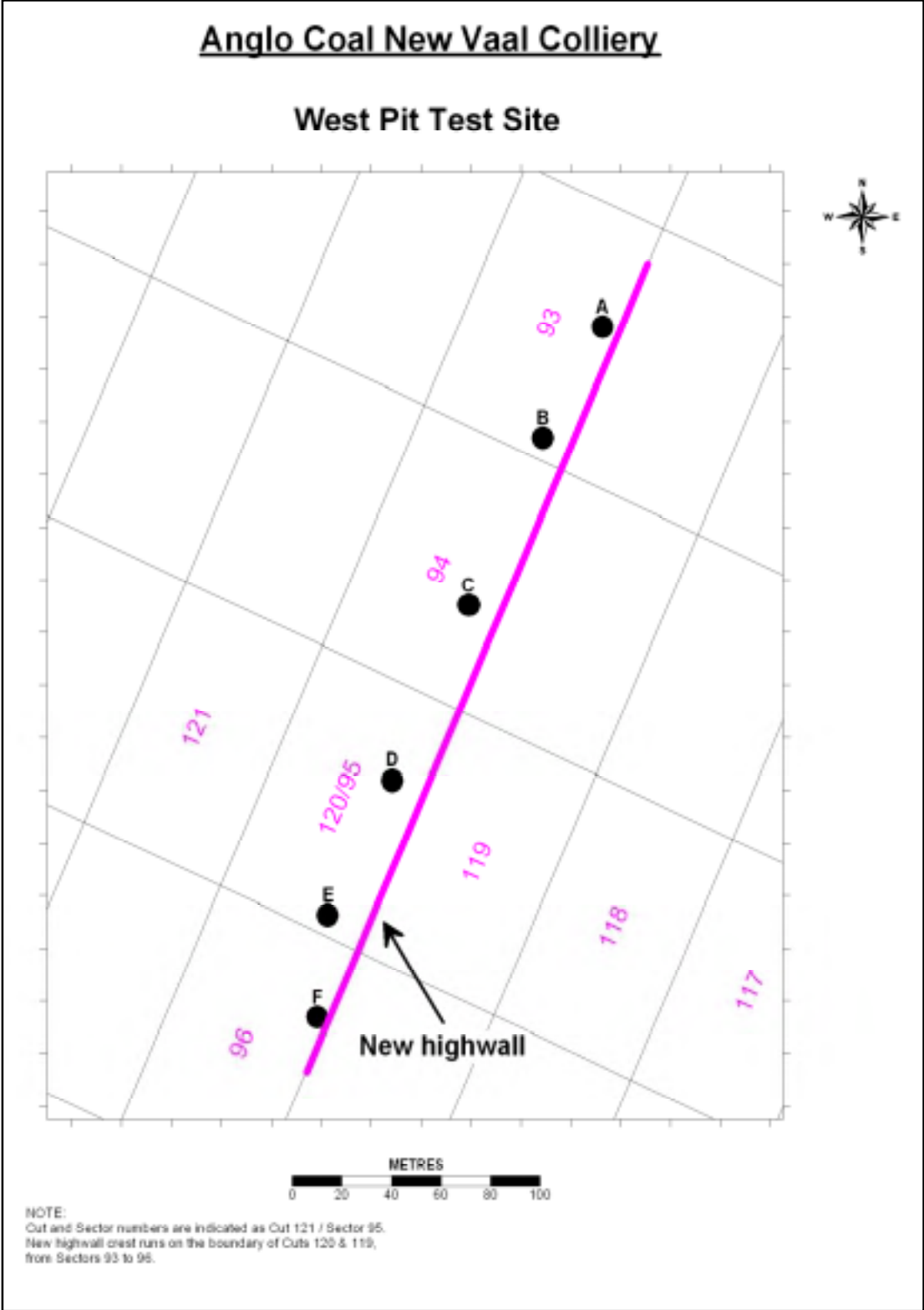


**Figure 4.2.2.1:** Positions of geophysically logged boreholes (A to F) relative to highwall

The acquired data - in particular, the optical and acoustic televiewer data - was then processed using WellCAD software. Outputs from this software are used to produce a combination geotechnical / lithological log, an example of which is given in Table 4.2.2.1.

**Table 4.2.2.1:** Combined geotechnical / lithological log

From	To	Interval	Azimuth	Dip	Fracture Description	Major Lithology
0	21.43	21.43				<b>SAND</b>
<b>Lith Unit Thickness</b>		<b>21.43</b>			<b>RQD =</b>	<b>0.0%</b>
21.43	21.63	0.50	331.91	22.97	Planar Fracture	<b>Siltstone Hard Overburden</b>
21.93	21.95	0.02	281.78	25.85	Non-Continuous Fracture	
21.95	22.17	0.22	315.58	15.12	Open fracture	
22.17	22.46	0.30	38.72	8.26	Non-Continuous Fracture	
22.46	22.61	0.15	329.57	51.91	Planar Fracture	
22.61	22.68	0.06	341.94	57.93	Planar Fracture	
22.68	22.89	0.22	14.92	19.49	Non-Continuous Fracture	
22.89	22.97	0.07	62.18	83.14	Non-Continuous Fracture	
22.97	23.22	0.25	116.68	4.47	Non-Continuous Fracture	
23.22	23.55	0.33	99.72	83.83	Non-Continuous Fracture	
23.55	23.63	0.09	32.40	9.68	Weak layer / washout	
23.63	23.68	0.05	359.30	8.25	Open fracture	
23.68	24.22	0.54	162.11	63.06	Planar Fracture	
<b>Lith Unit Thickness</b>		<b>2.79</b>			<b>RQD =</b>	<b>89.6%</b>
24.22	24.24	0.02	172.50	62.39	Open fracture	<b>Sandstone Hard Overburden</b>
24.24	24.32	0.08	165.24	47.86	Planar Fracture	
24.32	25.13	0.81	336.17	9.47	Bedding / layering	
25.13	25.46	0.34	177.58	81.84	Non-Continuous Fracture	
25.46	25.62	0.16	9.09	18.04	n/a	
<b>Lith Unit Thickness</b>		<b>1.40</b>			<b>RQD =</b>	<b>93.3%</b>
25.62	25.73	0.11	192.79	76.74	Non-Continuous Fracture	<b>Leader Seam Coal</b>
<b>Lith Unit Thickness</b>		<b>0.11</b>			<b>RQD =</b>	<b>100.0%</b>
25.73	26.86	1.13	73.02	9.47	Open fracture	<b>Leader Seam Interburden</b>
26.86	27.33	0.47	346.17	14.74	Open fracture	
<b>Lith Unit Thickness</b>		<b>1.60</b>			<b>RQD =</b>	<b>100.0%</b>
27.33	27.67	0.34	354.84	20.35	Open fracture	<b>TOP SEAM COAL</b>
27.67	28.01	0.33	316.24	16.40	Bedding / layering	
28.01	28.26	0.25	9.03	25.87	Bedding / layering	
28.26	30.26	2.00	359.40	10.01	Bedding / layering	
30.26	30.72	0.45	97.85	62.63	Non-Continuous Fracture	
30.72	31.66	0.95	45.51	6.61	Bedding / layering	
31.66	32.88	1.21	6.61	12.48	Bedding / layering	
32.88	33.20	0.33	32.61	14.94	Bedding / layering	
33.20	33.45	0.25	79.93	8.82	Bedding / layering	
33.45	34.14	0.69	153.67	74.52	Open fracture	
34.14	34.30	0.15	9.41	19.97	Bedding / layering	
34.30	34.56	0.27	320.18	19.01	Open fracture	
34.56	34.84	0.27	28.29	11.17	Bedding / layering	
34.84	34.92	0.09	38.48	20.63	Bedding / layering	
34.92	35.21	0.28	22.87	23.02	Bedding / layering	
35.21	35.75	0.54	9.84	17.00	Bedding / layering	
35.75	35.82	0.07	358.62	24.97	Weak layer / washout	
35.82	36.04	0.22	12.93	16.63	Open fracture	
36.04	36.07	0.03	13.69	20.12	Open fracture	
36.07	36.22	0.15	8.40	15.98	Open fracture	
36.22	36.33	0.11	44.06	12.40	Planar Fracture	
36.33	36.56	0.23	32.38	18.74	Bedding / layering	
<b>Lith Unit Thickness</b>		<b>9.23</b>			<b>RQD =</b>	<b>97.9%</b>
36.56	36.90	0.34	336.35	16.64	Non-Planar Fracture	<b>Sandstone Interburden</b>
36.90	38.41	1.52	0.63	12.85	Planar Fracture	
38.41	38.72	0.31	13.15	18.27	Bedding / layering	
38.72	39.22	0.50	348.13	0.07	Bedding / layering	
39.22	39.22	0.42	2.29	18.75	Bedding / layering	
<b>Lith Unit Thickness</b>		<b>2.66</b>			<b>RQD =</b>	
39.22	40.28	1.07	11.87	14.52	Open fracture	<b>Siltstone Interburden</b>
40.28	40.49	0.20	167.30	31.54	Open fracture	
40.49	40.53	0.04	11.92	11.01	Open fracture	
40.53	40.67	0.13	329.43	3.58	Open fracture	
40.67	41.53	0.86	3.13	5.02	Non-Continuous Fracture	
41.53	42.16	0.64	267.77	28.54	Open fracture	
42.16	43.27	1.11	206.27	39.40	Planar Fracture	
43.27	44.05	0.78	17.08	20.23	Open fracture	
44.05	44.38	0.33	0.34	18.25	Planar Fracture	
44.38	45.08	0.70	163.80	46.33	Open fracture	
45.08	45.20	0.12	152.57	42.67	Non-Continuous Fracture	
45.20	45.28	0.08	165.41	55.87	Open fracture	
45.28	45.45	0.17	1.81	25.43	Non-Continuous Fracture	
45.45	45.78	0.32	351.88	11.85	Weak layer / washout	
45.78	46.83	1.06	141.35	51.51	Non-Continuous Fracture	
46.83	47.23	0.39	15.97	16.60	Planar Fracture	
47.23	47.29	0.06	52.11	24.65	Open fracture	
47.29	47.36	0.08	35.92	25.00	Open fracture	
47.36	47.45	0.09	12.99	18.51	Planar Fracture	
47.45	47.50	0.04	351.77	26.72	Non-Planar Fracture	
<b>Lith Unit Thickness</b>		<b>8.28</b>			<b>RQD =</b>	<b>95.3%</b>
47.50	47.87	0.37	18.26	18.60	Bedding / layering	<b>MIDDLE SEAM COAL</b>
47.87	48.08	0.21	45.58	24.20	Bedding / layering	
48.08	48.47	0.39	354.06	28.78	Vein	
48.47	49.13	0.67	191.17	44.78	Open fracture	
49.13	49.31	0.18	198.18	64.34	Non-Continuous Fracture	
49.31	49.35	0.04	12.43	83.90	Non-Continuous Fracture	
49.35	49.66	0.31	356.70	27.86	Bedding / layering	
49.66	50.22	0.56	28.41	21.36	Bedding / layering	
50.22	51.06	0.84	168.91	51.63	Open fracture	
51.06	51.15	0.09	184.64	65.77	Non-Continuous Fracture	
51.15	52.31	1.16	353.12	15.28	Weak layer / washout	
52.31	53.36	1.06	354.54	23.72	Bedding / layering	
53.36	53.56	0.20	30.63	17.32	Bedding / layering	
53.56	53.82	0.26	3.08	18.58	Open fracture	
53.82	54.11	0.28	52.98	31.06	Non-Continuous Fracture	
54.11	54.65	0.54	19.89	21.64	Bedding / layering	
54.65	54.99	0.34	359.63	66.25	Non-Planar Fracture	
54.99	55.33	0.34	3.87	12.48	Non-Continuous Fracture	
<b>Lith Unit Thickness</b>		<b>7.84</b>			<b>RQD =</b>	<b>98.4%</b>
55.33	55.44	0.10	323.40	25.99	Open fracture	<b>Parting</b>
55.44	56.16	0.72	335.38	53.29	Non-Continuous Fracture	
<b>Lith Unit Thickness</b>		<b>0.82</b>			<b>RQD =</b>	<b>100.0%</b>
56.16	56.34	0.19	352.22	48.39	Non-Continuous Fracture	<b>BOTTOM SEAM COAL</b>
56.34	56.40	0.05	355.72	26.53	Non-Continuous Fracture	
56.40	57.37	0.98	328.59	29.79	Planar Fracture	
57.37	57.77	0.39	33.50	56.80	Non-Continuous Fracture	
57.77	57.83	0.06	349.02	45.23	Non-Continuous Fracture	
57.83	58.32	0.50	23.21	31.16	Non-Continuous Fracture	
<b>Lith Unit Thickness</b>		<b>2.17</b>			<b>RQD =</b>	
58.32	58.43	0.10	15.15	30.95	Bedding / layering	<b>FLOOR ROCK</b>
58.43	58.48	0.06	209.29	53.24	Open fracture	
58.48	58.61	0.13	9.48	52.23	Open fracture	
58.61	58.75	0.14	356.17	61.13	Open fracture	
58.75	58.82	0.07	0.80	66.14	Open fracture	
58.82	58.93	0.11	18.22	74.50	Non-Continuous Fracture	
58.93	58.99	0.05	328.55	39.51	Non-Continuous Fracture	
58.99	59.05	0.07	348.50	57.42	Open fracture	
59.05	59.14	0.09	106.70	39.63	Non-Continuous Fracture	
<b>Lith Unit Thickness</b>		<b>0.82</b>			<b>RQD =</b>	

The next stage of interpretation involves the use of stereographic projections. Stereographic projections allow for the plotting and visualisation, in two dimensions only, of the relationships and potential interactions between discontinuities themselves with the highwall. All stereoplots are based on the Schmidt Equal Area stereonet.

Orientation and dip data for the various types of discontinuities were obtained through geophysical wireline logging and processing in WellCAD (Table 4.2.2.2). The data for each type of discontinuity within each lithological unit were then plotted on a series of stereonet, along with orientation and dip data for the new highwall, allowing for inferences to be made regarding individual bench and overall highwall stability. The points that are plotted represent the mid-points along the great circles of the various planes (geological discontinuities) and not the poles. A line drawn from the centre of the stereonet through the point to intersect the outer circle defines the plane's dip direction or azimuth. An arc, centred in the middle of the plot with a radius extending to the point, drawn to intersect the internal radius line defines the plane's dip angle.

In order to illustrate the use of stereographic projections for structural analysis, a series of stereonet was plotted for the hard overburden and top seam coal horizons using the orientation data presented in Table 4.2.2.1. Only the open fracture, planar fracture and bedding / layering data are used. Orientation data for these geotechnical features has been reorganised and is presented in Table 4.2.2.2. In these examples, it has been assumed that the highwall strikes 24° east of north and dips at 85° to the north-west (commonly represented as 024/85)

**Table 4.2.2.2:** *Geotechnical orientation data for overburden and Top Seam coal units*

Depth (m)	Lithological Unit	Geotechnical Feature	Azimuth (°)	Dip (°)
21.93	Overburden	Planar Fracture	332	23
22.61	Overburden	Planar Fracture	330	52
22.68	Overburden	Planar Fracture	342	58
24.22	Overburden	Planar Fracture	162	63
24.32	Overburden	Planar Fracture	165	48
22.17	Overburden	Open Fracture	316	15
23.68	Overburden	Open Fracture	359	8
24.24	Overburden	Open Fracture	173	62
26.86	Overburden	Open Fracture	73	10
27.33	Overburden	Open Fracture	346	15
36.33	Top Seam Coal	Planar Fracture	44	12
27.67	Top Seam Coal	Open Fracture	355	20
34.14	Top Seam Coal	Open Fracture	154	75
34.56	Top Seam Coal	Open Fracture	320	19
36.04	Top Seam Coal	Open Fracture	13	17
36.07	Top Seam Coal	Open Fracture	14	20
36.22	Top Seam Coal	Open Fracture	8	16
28.01	Top Seam Coal	Bedding	316	16
28.26	Top Seam Coal	Bedding	9	26
30.26	Top Seam Coal	Bedding	359	10
31.66	Top Seam Coal	Bedding	46	7
32.88	Top Seam Coal	Bedding	7	12
33.20	Top Seam Coal	Bedding	33	15
33.45	Top Seam Coal	Bedding	80	9
34.30	Top Seam Coal	Bedding	9	20
34.84	Top Seam Coal	Bedding	28	11
34.92	Top Seam Coal	Bedding	38	21
35.21	Top Seam Coal	Bedding	23	23
35.75	Top Seam Coal	Bedding	10	17
36.56	Top Seam Coal	Bedding	32	19

Figure 4.2.2.2 is the resultant stereoplot for the planar fractures identified in the overburden unit. Included on the plot is the 30° friction angle represented as a circle. A friction angle of 30° is commonly assumed for Karoo sediments, particularly the sandstones, siltstones and shales. The highwall great circle is also plotted to assist with interpretation.

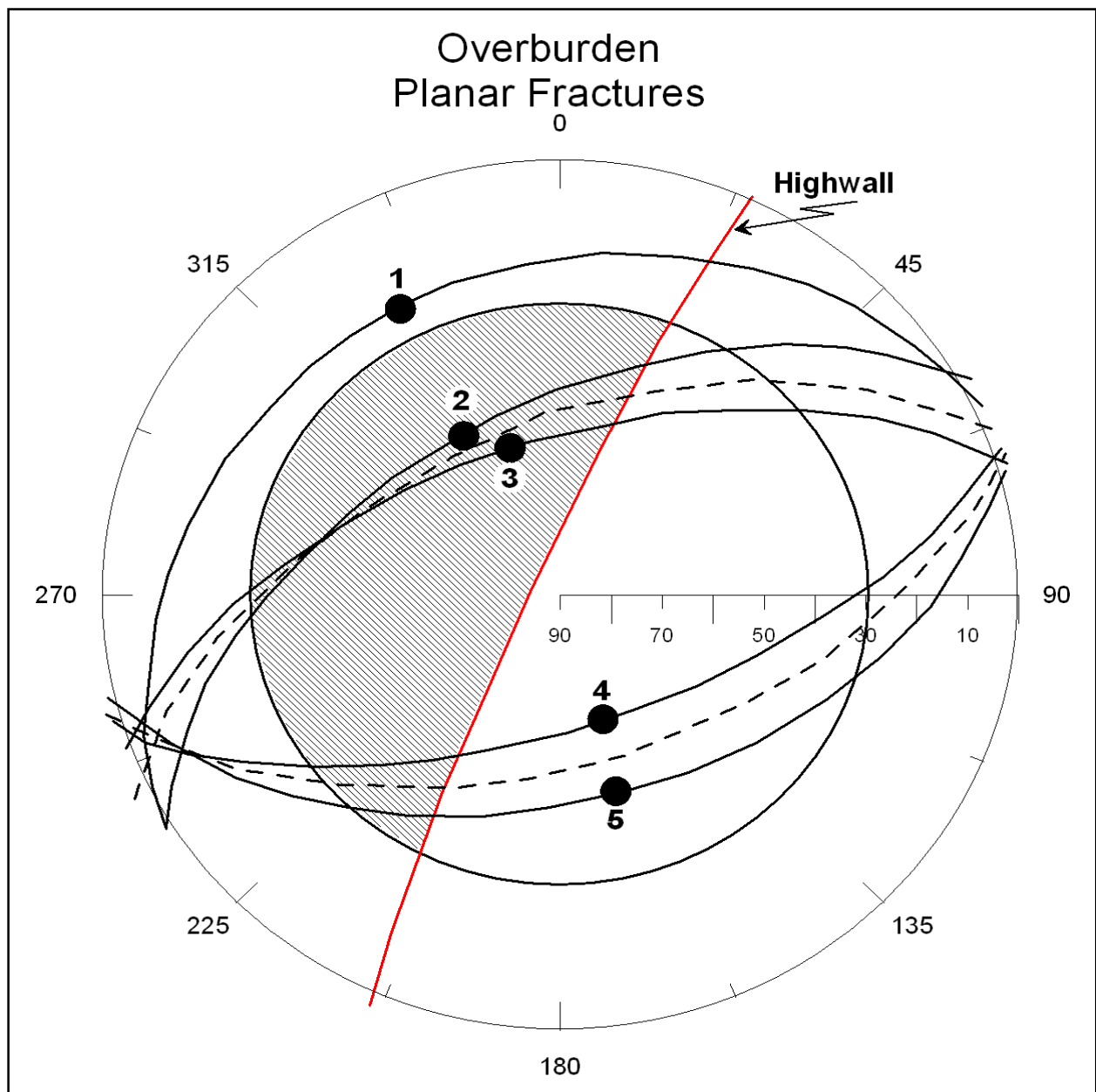


**Figure 4.2.2.2:** Stereoplot of Planar Fractures in Overburden (digitized from hand-drawn stereoplot)

The shaded area in the stereoplot is the 'daylight' window; i.e. planes or wedges occurring in this area are considered unstable unless other factors promote stability. This is explained in the following interpretation of the stereoplot in Figure 4.2.2.2.

Interpretation of overburden planar fracture stereoplot (Figure 4.2.2.2):

- Planar Fracture 1 (PF<sub>1</sub>) is dipping out of the highwall shallower than the friction angle (does not plot in shaded area). Strike angle of intersection with highwall is 38°, therefore not sub-parallel. Both of these conditions negate planar failure.
- PF<sub>1</sub> forms wedges with PF<sub>4</sub> and PF<sub>5</sub>, however, lines of intersection are very shallow (do not intersect in shaded area) and therefore wedge failure is not possible.

- $PF_2$  and  $PF_3$  occur within 7 cm of each other (vertically) and are therefore considered to be members of the same discontinuity set. The dotted great circle between their respective great circles represents their average dip direction and dip. Although this fracture plane daylights in the highwall face (plots in shaded area), the strike angle of intersection with the highwall is  $42^\circ$  and planar failure is therefore unlikely.
- $PF_4$  and  $PF_5$  occur within 10 cm of each other (vertically) and are therefore considered to be members of the same discontinuity set. The dotted great circle between their respective great circles represents their average dip direction and dip. This fracture plane dips into the highwall and thus no movement is expected on this plane.
- The wedge that is formed by the intersection of  $PF_{2/3}$  and  $PF_{4/5}$  dips out of the highwall at an angle shallower than the friction angle and is therefore considered to be stable.

Figure 4.2.2.3 is the stereoplot for the open fractures and the interpretation follows.

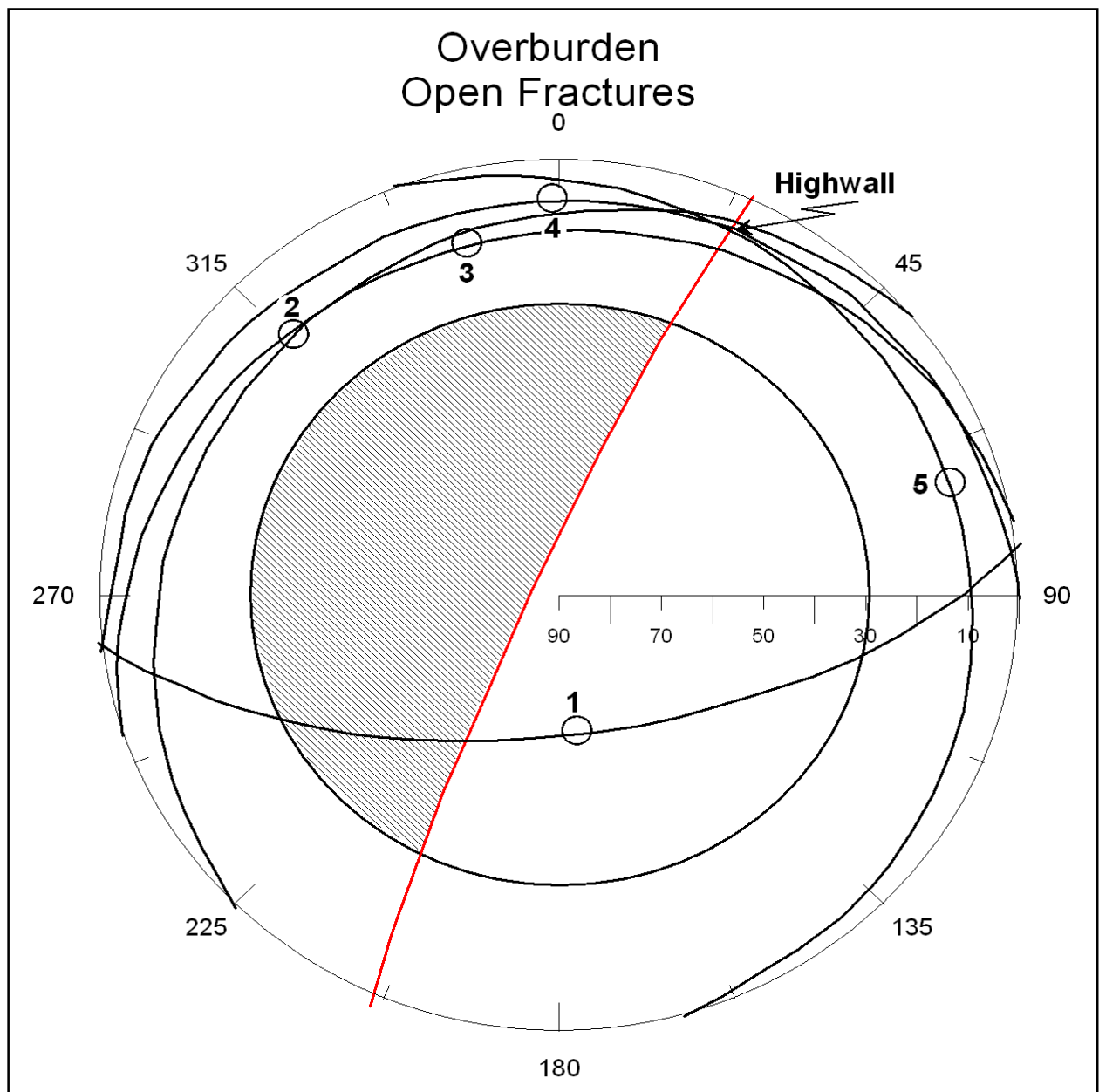


**Figure 4.2.2.3:** Stereoplot of open fractures in overburden (digitized from hand-drawn stereoplot)

#### Interpretation of overburden open fracture stereoplot (Figure 4.2.2.3):

- Open fracture 1 (OF<sub>1</sub>) dips steeply (62°) into the highwall and no movement is expected on this discontinuity.
- OF<sub>2</sub>, OF<sub>3</sub> and OF<sub>4</sub> all dip gently (< 30°) out of the highwall and therefore no planar failures are to be expected.
- OF<sub>5</sub> dips gently (< 30°) into the highwall and thus no movement on this discontinuity is expected.

Since only one bedding plane was identified in the overburden unit, no plot is generated, since a single bedding plane may not be fully representative of the entire lithological unit. However, strata azimuth and dip can be obtained from the geological model.

Interpretation of both planar and open fractures for the overburden indicates that the highwall will be stable *at this point of observation*. It must be stressed that the discontinuity data was obtained from a single borehole drilled in close proximity to the highwall and the interpretations are subject to a number of assumptions. It is assumed that the discontinuities are persistent (10's of metres) along strike and dip. In the absence of information relating to discontinuity persistence, this assumption has to be made. Thus, all discontinuities identified in a borehole are considered to have potential destabilising effects on the highwall and the resulting interpretations will therefore be worst-case scenarios. Information regarding discontinuity condition in terms of roughness and in-fill material is also not considered, since these cannot be determined from the wireline televiewer data. Field observations will need to be considered to assist an interpretation. Groundwater and highwall loading conditions are also not considered in the stereoplot interpretation and this data, along with the aforementioned, will be introduced in the final hazard rating matrix.

For the top seam coal horizon, only stereoplots for the open fractures (Figure 4.2.2.4) and bedding planes (Figure 4.2.2.5) were generated. Only one planar fracture was identified in this horizon and, thus, a plot is not warranted. The orientation and dip of this discontinuity indicate that there is no potential for planar failure as it dips gently into the highwall (044/12).

#### Interpretation of top seam coal open fracture stereoplot (Figure 4.2.2.4):

NOTE: not all great circles are plotted. Those for OF<sub>4</sub>, OF<sub>5</sub> and OF<sub>6</sub> plot close together and thus only OF<sub>4</sub> is plotted.

- Open fracture 1 (OF<sub>1</sub>) dips steeply (75°) into the highwall and therefore no potential for planar failure exists.
- All remaining fractures dip out of the highwall but at less than 30° and, therefore, no failures are expected on these discontinuities.
- The wedge formed by the intersection of OF<sub>1</sub> and OF<sub>2</sub> dips very gently to the south-west and no wedge failure is expected.

#### Interpretation of top seam coal bedding plane stereoplot (Figure 4.2.2.5):

NOTE: no great circles are plotted. This large data set will result in a busy stereoplot and the interpreter needs to visualise the great circles.

- Bedding Planes 1 and 2 are outliers to the majority of the data. They have potentially been misinterpreted as bedding planes. Since they are all very gently dipping there is little cause for concern.
- The two concentrated groups (A and B) indicate that the bedding dips gently north to north-east *i.e.* the strata strike is almost perpendicular to the highwall and is relatively flat lying.

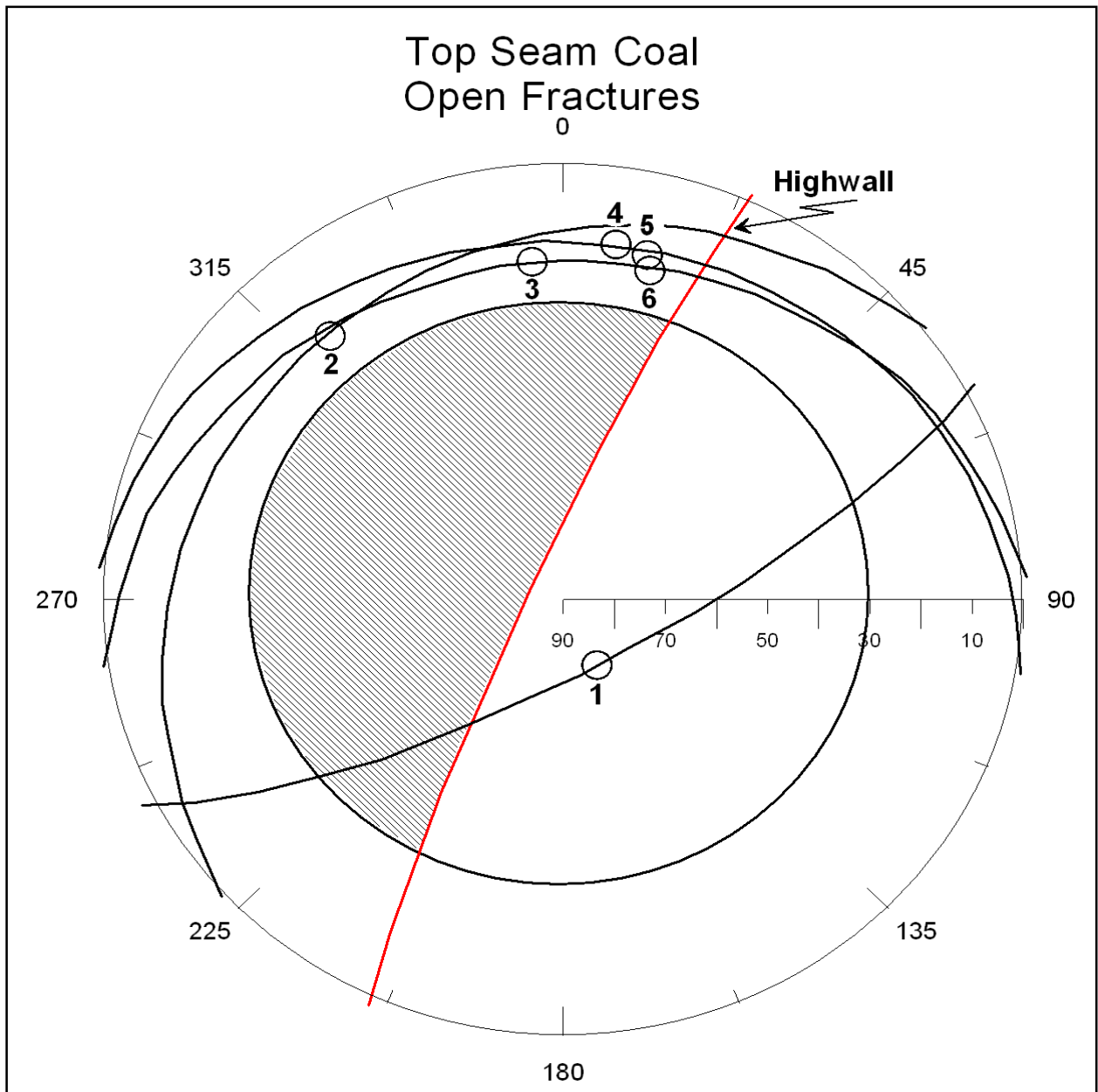


**Figure 4.2.2.4:** Stereoplot of open fractures in top seam coal (digitized from hand-drawn stereoplot)

With the background to interpreting stereoplots in terms of structural analysis regarding highwall stability, the data acquired from the geophysical wireline logging of the six boreholes drilled along an actual highwall (Figure 4.2.2.1) is plotted and interpreted. Only discontinuity data has been interpreted from televiewer data, since bedding plane data can be obtained from the geological model. In a previous report (van Heerden, 2004b) it was noted that manipulation of televiewer data in WellCAD requires an experienced interpreter. The data from the six boreholes in this case has been interpreted by the author who has limited exposure to data interpretation of televiewer data in WellCAD. However, since the purpose of this exercise is to develop a methodology regarding highwall stability hazard rating, the author's lack of experience in this particular area is not considered to be a limiting factor. The concept of applying stereography to structural analysis is well known and is applicable to this highwall hazard rating methodology.

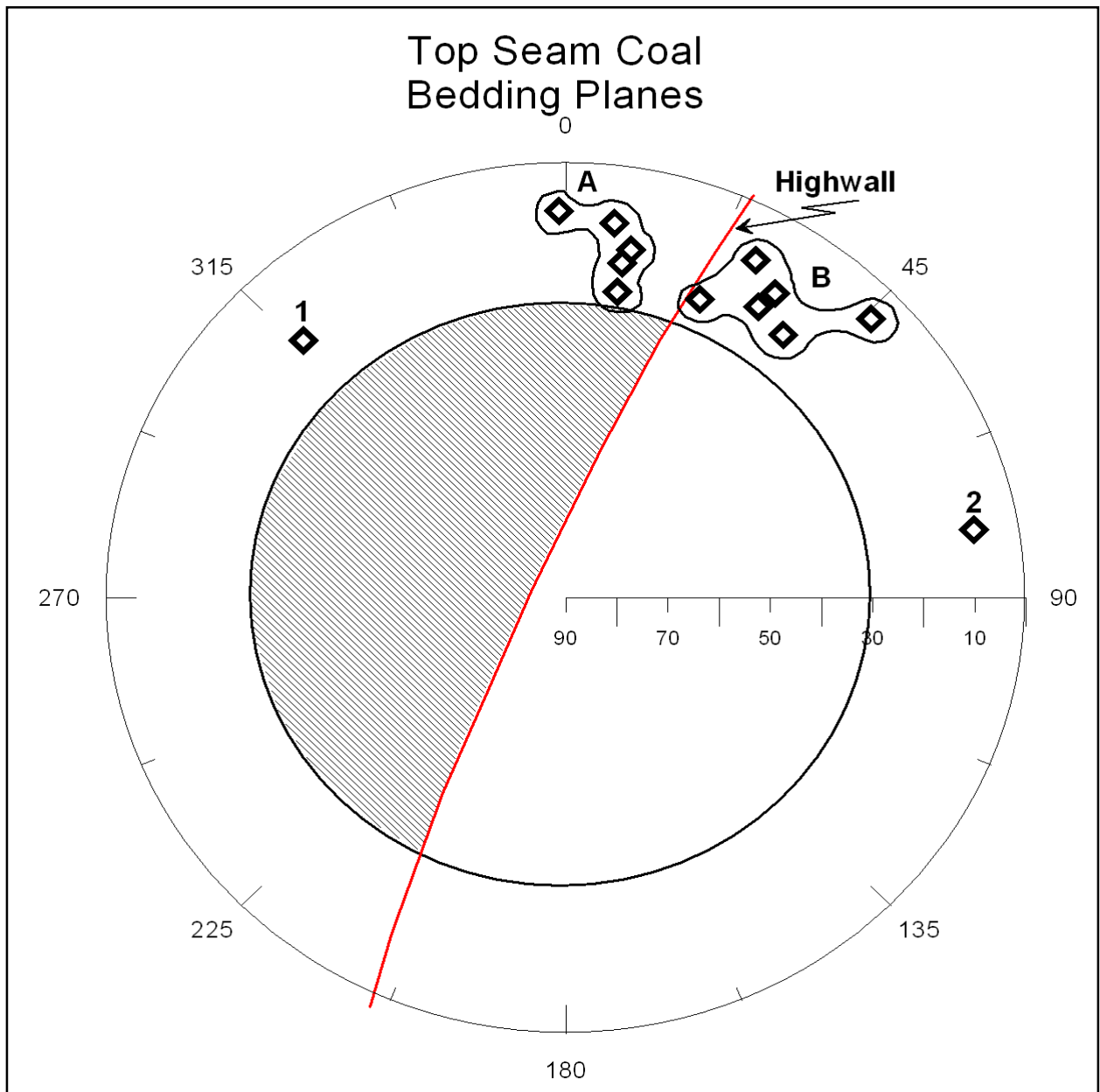


**Figure 4.2.2.5:** Stereoplot of bedding planes in top seam coal (digitized from hand-drawn stereoplot)

### 4.3 Application of the Methodology in a Real Case Scenario

The methodology outlined in Section 4.2 involves two main steps: i) analysis of the geological model, and ii) stereography. The preceding stereographic projections and interpretations are not related to any of the six boreholes but were used to explain their use in the overall methodology.

However, in this section, discontinuity data obtained from selected boreholes is used in applying a hazard rating to the new highwall in the West Pit Test Site at New Vaal Colliery (Figure 4.2.1.1). Owing to the erratic spread and density of the data, highwall sectors 119/93 and 119/94 are evaluated for a highwall consisting of the overburden, top seam coal and interburden lithological units; while highwall sector 119/95 will be evaluated for a highwall consisting of the middle seam coal, parting and bottom seam coal lithological units. The first step involving the analysis of the geological model has already been carried out and discussed under Section 4.2.1. Sector-specific geological information and stereography are discussed here for each highwall section defined above.

#### 4.3.1 Hazard Rating for Highwall Sectors 119/93 and 119/94

Analysis of the geological model for these two sectors reveals the following:

- The surface elevation (Figure 4.2.1.3) is constant in Sector 93 while it dips towards the highwall in Sector 94 due to an increased elevation towards Cuts 118 and 117 in the same sector range. This implies additional loading in Sector 94 relative to Sector 93.
- The Top Seam Coal floor elevation contour plan (Figure 4.2.1.4) shows the seam rising from the start of Sector 93 to reach a maximum towards the end of the sector and then it dips more steeply to a minimum elevation at the end of Sector 94. The contours also indicate a change in dip azimuth from parallel to the highwall at the start of Sector 93 to perpendicular to the highwall at the end of Sector 94.
- Judging by the contour pattern of the floor of the Middle Seam Coal (Figure 4.2.1.5), which is very similar to the Top Seam Coal floor contour pattern, the floor of the interburden can be assumed to show a similar pattern, although the dips will be slightly steeper.
- Although the regional jointing pattern has been described (Section 3.1 and Figure 3.1.5), cognisance must be given to potential localised discontinuities. These are illustrated in Figure 4.3.1.1.

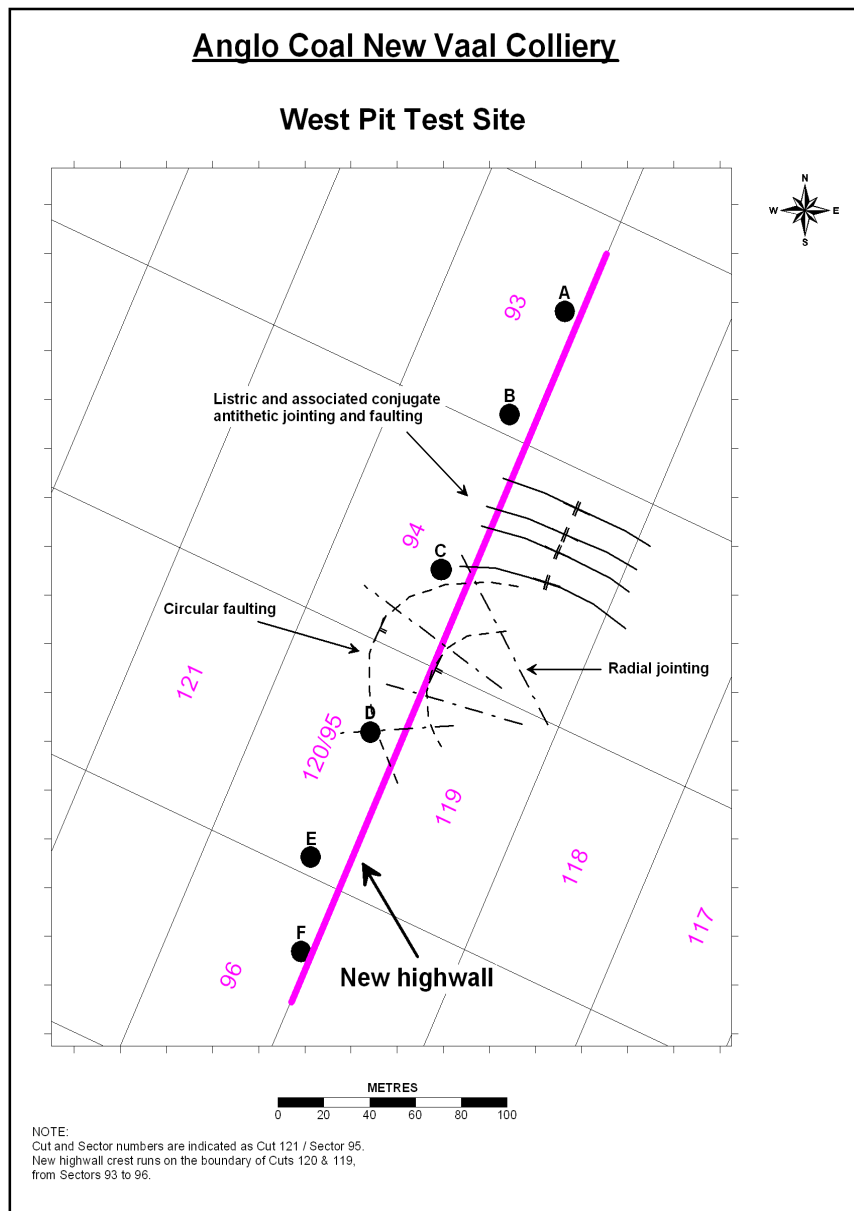


**Figure 4.3.1.1:** Potential discontinuity pattern (faults and joints) in overburden and top seam coal units inferred from contour data

From the above points, the following can be inferred regarding highwall stability:

- Strata dip direction favours highwall stability (it dips either parallel to or into the highwall).
- There is potential for planar failure on the NE-SW trending regional joint set, if it is persistent in this area. This is due to the additional loading in the Sector 94 area, and the potential for release planes to be formed by the NW-SE jointing that may be present.
- Potential wedges formed by the intersection of both regional joint sets, if persistent in this area, may also be affected by the additional loading in the Sector 94 area.

The above inferences are now assessed against stereography based on interpreted geophysical wireline data obtained from Boreholes A and C.

The stereoplot for discontinuities identified in the upper lithological units in Borehole A is given in Figure 4.3.1.2. As can be seen from this plot, all identified discontinuities dip in a SSE direction at angles of greater than  $30^\circ$ . Although steeper than the friction angle, the strike angle of intersection with the highwall is far greater than  $20^\circ$  and no movement is expected on these discontinuities. In addition, these discontinuities are dipping towards the upslope direction of the strata and possibly represent localised tensional fracturing of the strata.

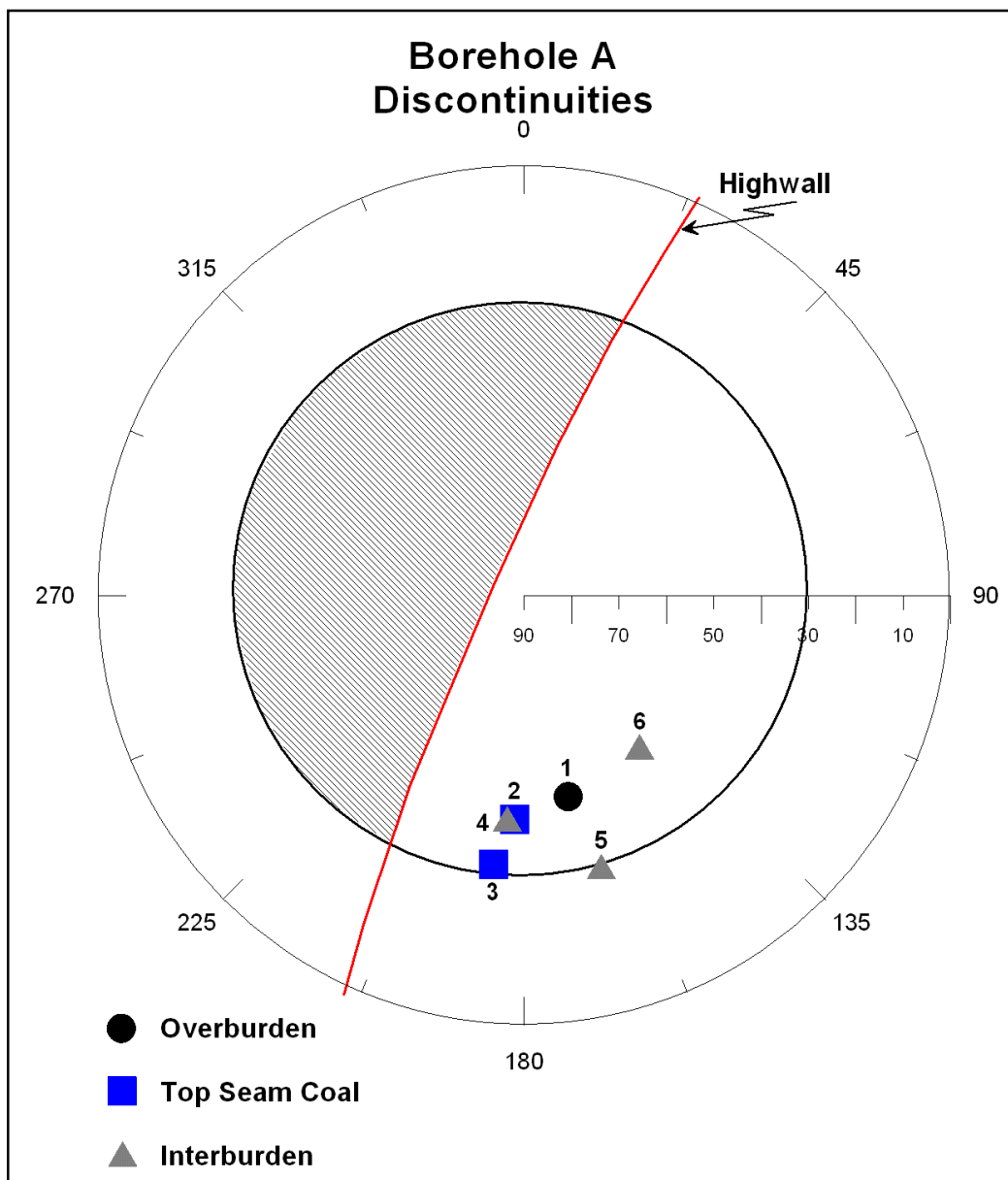


**Figure 4.3.1.2:** Stereoplot of discontinuities identified in Borehole A for overburden, Top Seam Coal and interburden

No information regarding discontinuity condition (roughness), in-fill material and groundwater condition is obtainable from wireline televiewer data. However, field observations and previous work (Stewart and Letlotla, 2003; Sonneveldt and Enserink, 1997) indicate that small-scale discontinuity roughness is variable and typically no in-fill material is present. Groundwater conditions are also variable, depending on the season and slope dewatering practices. These aspects are included in the hazard-rating matrix.

Figure 4.3.1.3 is the hazard matrix for the discontinuities identified in the upper lithological units of Borehole A. Each joint set represents the average discontinuity dip direction (azimuth) and dip for the discontinuities identified in each lithological unit.

Highwall Azimuth		294	Relative Orientations		HAZARD ?
Strata Azimuth		359	Relative to Highwall	65	N
Strata Dip		10	Dip	10	N
					<b>NONE</b>
<b>Plane Formation:</b>					
<b>Joint Set 1 Overburden</b>	Azimuth	168	Relative to Highwall	126	N
	Dip	47	Dip	47	Y
	In-fill	N			N
	Water	N			N
<b>Joint Set 1 Total Hazard</b>					<b>NONE</b>
<b>Joint Set 2 Overburden</b>	Azimuth	185	Relative to Highwall	109	N
	Dip	38	Dip	38	Y
	In-fill	N			N
	Water	N			N
<b>Joint Set 2 Total Hazard</b>					<b>NONE</b>
<b>Joint Set 3</b>	Azimuth	164	Relative to Highwall	130	N
	Dip	41	Dip	41	N
	In-fill	N			N
	Water	N			N
<b>Joint Set 3 Total Hazard</b>					<b>NONE</b>
<b>Wedge Formation:</b>					
<b>J1 &amp; J2</b>	Dir. of Sliding		Relative to Highwall		
	Dip		Dip		
	In-fill				
	Water				
<b>J1 &amp; J2 Total Hazard</b>					
<b>J2 &amp; J3</b>	Dir. of Sliding		Relative to Highwall		
	Dip		Dip		
	In-fill				
	Water				
<b>J2 &amp; J3 Total Hazard</b>					
<b>J1 &amp; J3</b>	Dir. of Sliding		Relative to Highwall		
	Dip		Dip		
	In-fill				
	Water				
<b>J1 &amp; J3 Total Hazard</b>					
<b>Bedding Plane Sliding Hazards:</b>		<b>NONE</b>			
<b>Planar Failure Hazards:</b>			<div style="border: 1px solid black; padding: 5px;"> <p>Relative Orientation is the difference, in degrees, between the Highwall azimuth and the discontinuity, or line of intersection, azimuth.</p> <p>A Relative Orientation Angle of 25° or less is considered to be highly hazardous since the planes are striking sub-parallel to parallel. Angles greater than 25° are not considered hazardous.</p> <p>The presence of in-fill material and / or water on discontinuities is considered hazardous.</p> </div>		
J1	<b>NONE</b>				
J2	<b>NONE</b>				
J3	<b>NONE</b>				
<b>Wedge Failure Hazards:</b>					
J1 & J2					
J2 & J3					
J1 & J3					
<b>OVERALL SLOPE STABILITY HAZARD RATING:</b>					<b>NONE</b>

Figure 4.3.1.3: Slope stability hazard rating matrix for Borehole A

The hazard matrix is qualitative rather than quantitative and is therefore subjective. This does not detract from the value of the system, since rock mass behaviour in differing geological and geotechnical settings is not consistent, although the basic mechanics of rock mass behaviour are. Each joint set and wedge hazard rating is based on a combination of “yes” and “no” hazards. This implies that the user requires a certain level of experience in order to assign the overall hazard for each discontinuity and, ultimately, the overall slope stability hazard rating. The range of hazards include: none, low, moderate, and high. The final rating is intended to be indicative of the potential for instability.

The stereoplot for discontinuities identified in the upper lithological units in Borehole C is given in Figure 4.3.1.4. Noticeably more discontinuities for the same lithological units have been identified in this borehole than in Borehole A. The borehole is positioned in an area where the strata are dipping more steeply than the strata in the vicinity of Borehole A. As previously mentioned, a relative increase in the strata dip has been observed to have an impact on the localised discontinuity frequency throughout the strata.

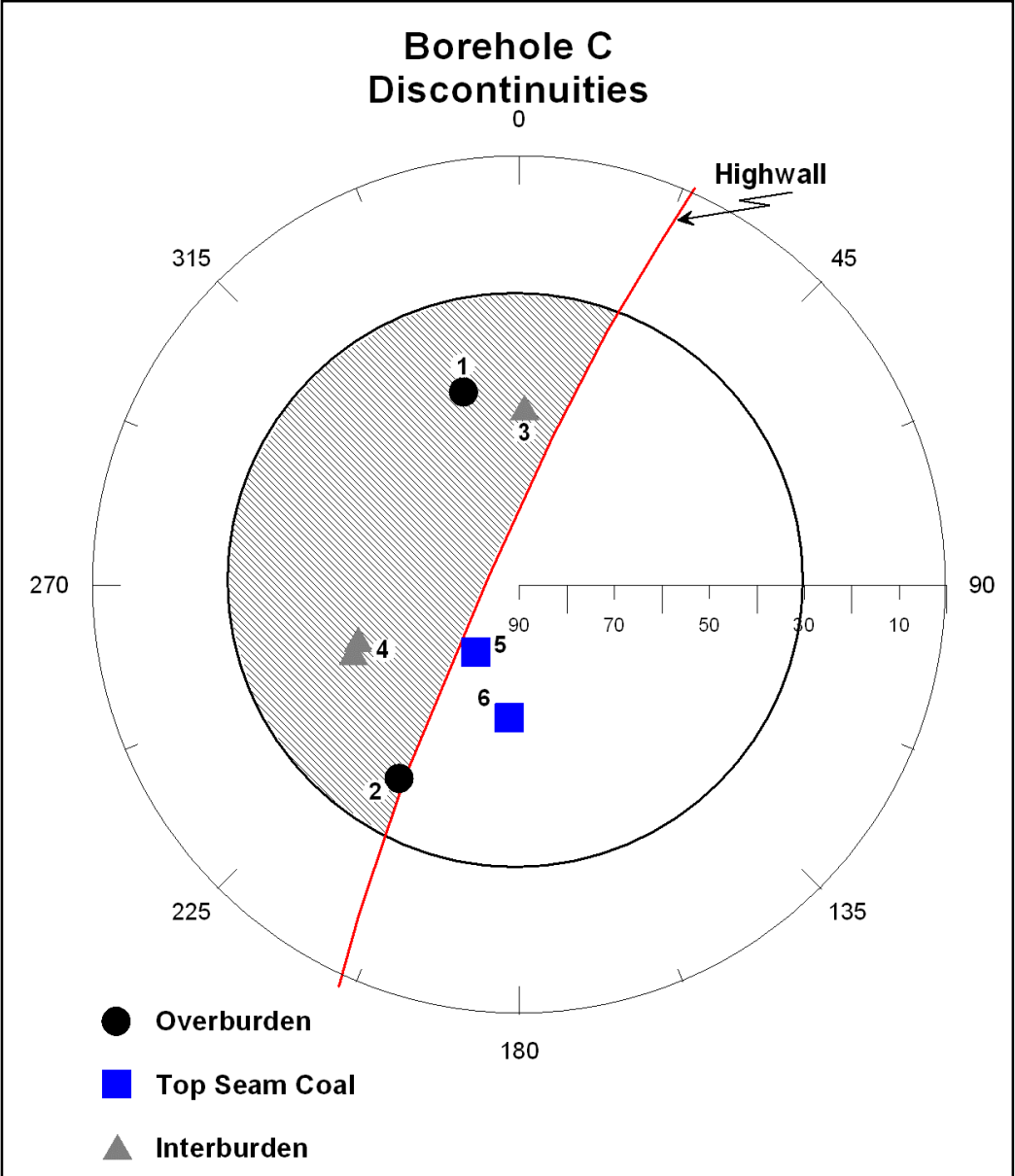


**Figure 4.3.1.4:** Stereoplot of discontinuities identified in Borehole C for overburden, Top Seam Coal and interburden

The majority of the discontinuities dip in a general SW direction. This is consistent with the anticipated localised discontinuity pattern (Figure 4.3.1.1). In addition, there is a split in the discontinuity dip direction, specifically in the overburden and interburden lithological units, indicating the presence of conjugate discontinuity sets. Stewart and Letlotla (2003) observed that in areas of relatively steep dip, antithetic jointing and faulting is not uncommon. The impact of conjugates is the potential for unstable wedges to be formed. It is therefore necessary to further interpret the stereoplot by plotting the great circles for the discontinuities. This will allow for potentially unstable wedges to be identified.

Figure 4.3.1.5 presents a series of stereoplots for the Borehole C discontinuities at each stage of wedge analysis, starting with the plots of all the great circles.

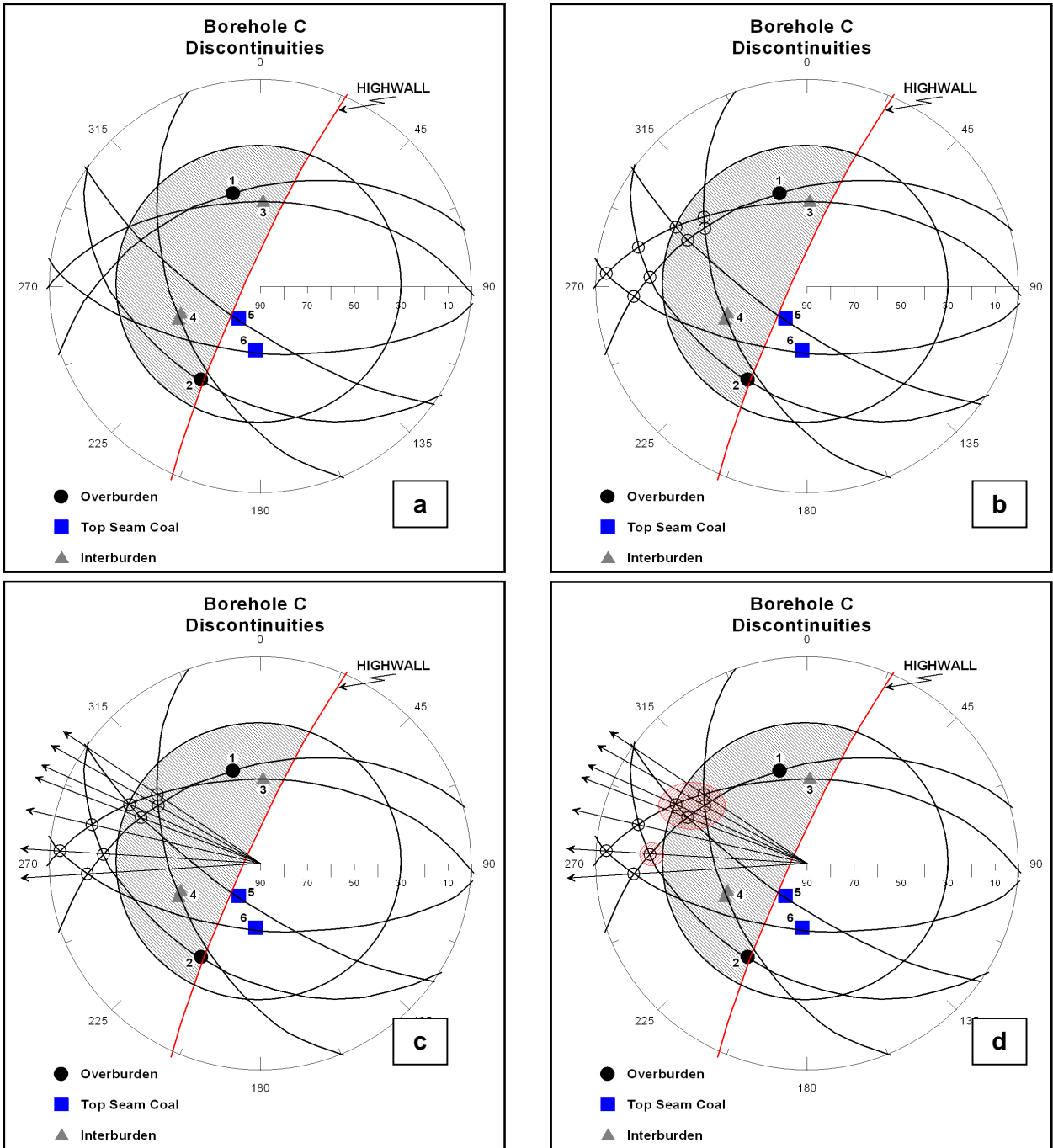


**Figure 4.3.1.5:** a) Great circles for discontinuities D1 to D6; b) Intersections (circled) between conjugate pairs forming wedges; c) Lines drawn through intersections indicating direction of potential sliding; d) Danger zones (red hatched) where a conjugate pair's line of intersection is greater than 30°

Figure 4.3.1.5 indicates that the discontinuity pairs that form potentially unstable wedges are: D1/D2; D1/D4; D1/D5; D3/D4; and D3/D5. With the exception of the D1/D2 wedge, all the others fall within the 30° friction angle circle, indicating that their individual lines of intersection are greater than 30° and, therefore, sliding is possible. The D1/D2 wedge is included, since its line of intersection is only a few degrees less than the critical angle and movement (sliding) may be induced by other factors such as additional highwall loading. In this instance, additional loading can be induced by the elevated surface topography to the SE of Borehole C (Figure 4.2.1.3). Such features need to be taken into account when the stability of highwall slopes is assessed.

For the purposes of this interpretation, only the wedge analysis section of the hazard matrix will be completed. It is evident from the stereoplots that none of the individual discontinuities have potential plane failures associated with them, since none of them strike sub-parallel or parallel to the highwall. In addition, only those discontinuity combinations that have been identified to be potentially unstable will be used. The modified hazard matrix for Borehole C is presented in Figure 4.3.1.6.

Highwall Azimuth		294	Relative Orientations		HAZARD ?
Strata Azimuth		165	Relative to Highwall	129	N
Strata Dip		7.5	Dip	7.5	N
					<b>NONE</b>
<b>Wedge Formation:</b>					
<b>D1 / D2</b>	Dir. of Sliding	273	Relative to Highwall	21	Y
	Dip	25	Dip	25	Y
	In-fill	N			N
	Water	N			N
	<b>D1 / D2 Total Hazard</b>				<b>MODERATE</b>
<b>D1 / D4</b>	Dir. of Sliding	301	Relative to Highwall	7	Y
	Dip	42	Dip	42	Y
	In-fill	N			N
	Water	N			N
	<b>D1 / D4 Total Hazard</b>				<b>HIGH</b>
<b>D1 / D5</b>	Dir. of Sliding	292	Relative to Highwall	2	Y
	Dip	38	Dip	38	Y
	In-fill	N			N
	Water	N			N
	<b>D1 / D5 Total Hazard</b>				<b>HIGH</b>
<b>D3 / D4</b>	Dir. of Sliding	304	Relative to Highwall	10	Y
	Dip	40	Dip	40	Y
	In-fill	N			N
	Water	N			N
	<b>D3 / D4 Total Hazard</b>				<b>HIGH</b>
<b>D3 / D5</b>	Dir. of Sliding	295	Relative to Highwall	1	Y
	Dip	30	Dip	30	Y
	In-fill	N			N
	Water	N			N
	<b>D3 / D5 Total Hazard</b>				<b>HIGH</b>
<b>Bedding Plane Sliding Hazards:</b>		<b>NONE</b>	<div style="border: 1px solid black; padding: 5px;"> <p>Relative Orientation is the difference, in degrees, between the Highwall azimuth and the discontinuity, or line of intersection, azimuth.</p> <p>A Relative Orientation Angle of 25° or less is considered to be highly hazardous since the planes are striking sub-parallel to parallel. Angles greater than 25° are not considered hazardous.</p> <p>The presence of in-fill material and / or water on discontinuities is considered hazardous.</p> </div>		
<b>Planar Failure Hazards:</b>		<b>NONE</b>			
<b>Wedge Failure Hazards:</b>					
<b>D1 / D2</b>	<b>MODERATE</b>				
<b>D1 / D4</b>	<b>HIGH</b>				
<b>D1 / D5</b>	<b>HIGH</b>				
<b>D3 / D4</b>	<b>HIGH</b>				
<b>D3 / D5</b>	<b>HIGH</b>				
<b>OVERALL SLOPE STABILITY HAZARD RATING:</b>		<b>HIGH</b>			

Figure 4.3.1.6: Hazard matrix for Borehole C – modified for wedge failure hazards only

The hazard matrix, for the wedges identified in Borehole C as potentially unstable (Figure 4.3.1.6), indicates that the highwall in that region (refer to borehole position in Figure 4.3.1.1) has a high probability for instability. However, further fieldwork is necessary to confirm this assessment. It has previously been mentioned that no information regarding discontinuity persistence (along dip and strike) is gathered from geophysical wireline televiwer data and, thus, in-pit highwall and surface mapping will have to be carried out on a continuous basis as the current highwall advances to the new position. Only through detailed mapping will valuable data, such as discontinuity persistence and the presence or development of surface tension cracks, be obtained. It is possible, however, to flag this area of the pit (Cut 119, Sector 93) as a potentially hazardous area, requiring follow-up work as mining advances into this area.

#### **4.3.2 Hazard Rating for Highwall Sector 119/95**

Analysis of the geological model in the 119/95 zone reveals the following:

- The surface elevation contours (Figure 4.2.1.3) indicate a rising topography in an easterly direction.
- The floor elevation contours of both the Middle and Bottom Seam (Figures 4.2.1.5 and 4.2.1.6 respectively), however, dip in a NE direction. This implies a thickening of both burdens and seams in this direction.
- The potential for localised discontinuities is high owing to differential compaction. The pattern is expected to be similar to that illustrated in Figure 4.3.1.1.

The inferences regarding highwall stability in this sector will be very similar to those made for the previous two sectors. However, this particular highwall only comprises the Middle Seam Coal to the floor of the Bottom Seam Coal. Geophysical wireline televiwer data obtained from Boreholes D and E was used with stereography to determine the potential impacts that identified discontinuities may have on the stability of the highwall in this sector.

Figure 4.3.2.1 is a stereoplot of discontinuities identified in Borehole D. The majority of the discontinuities dip in a general SW direction, with one exception dipping to the NE. The discontinuities dipping to the SW, although relatively steep, strike at too high an angle to the highwall to result in plane failure. However, there is a potential for unstable wedges to be formed between the SW-dipping discontinuities and the NE-dipping discontinuity. A wedge analysis is performed, similar to that for Borehole C, and the series of stereoplots is presented in Figure 4.3.2.2.

As can be seen from this series of stereoplots, discontinuity D6 forms wedges with all the other discontinuities, and all the lines of intersection dip close to perpendicular out of the highwall. However, only the pairs D1/D6 and D3/D6 dip more steeply than 30° (Figure 4.3.2.2.d). The pairs D2/D6 and D4/D6 have been highlighted as being potentially unstable because even though their lines of intersection dip less than 30°, additional highwall loading (Figure 4.2.1.3) may influence the stability of these wedges. The line of intersection for the D5/D6 pair dips at approximately 10° and is thus considered to be stable. All the discontinuity pairs are entered into the hazard matrix (Figure 4.3.2.3) to establish the overall hazard rating for the section of the highwall in the vicinity of Borehole D.

As can be seen from the hazard matrix, the overall rating is “moderate to high”. Although the strata dip close to 10° into the highwall, and therefore have a stabilising effect on the highwall, the two wedges dipping steeply out of the highwall are cause for concern. This area will require more detailed highwall and surface mapping as mining progresses into the area. Borehole E has been drilled in the same sector (119/95) as Borehole D and the discontinuity data for Borehole E will be analysed in the same fashion as for the previous boreholes. Since two holes are used for this sector, the results from the two hazard matrices can either be averaged or used independently.

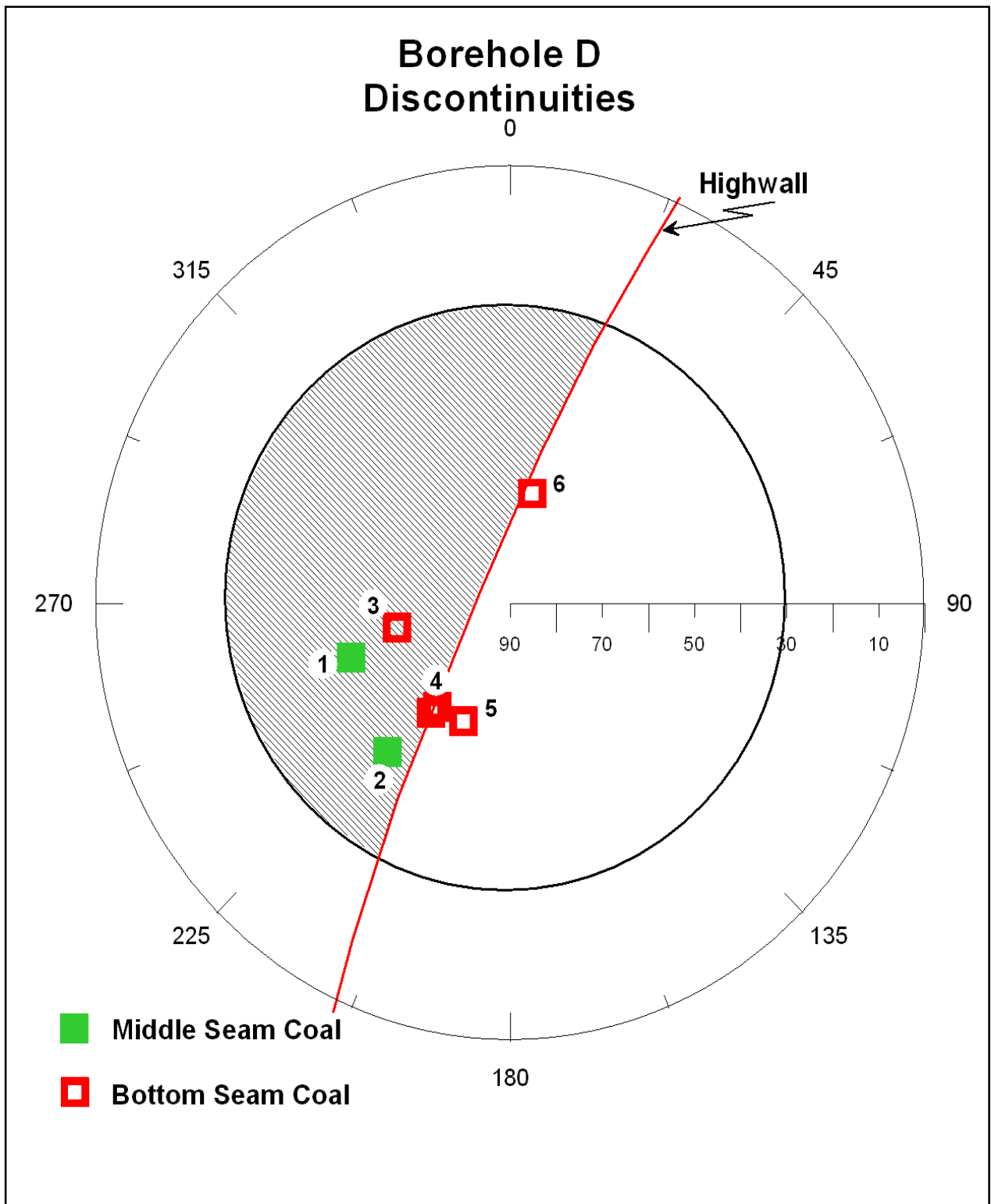


**Figure 4.3.2.1:** Stereoplot of discontinuities identified in Borehole D for Middle and Bottom Seam Coal units

It is important not to simply average all hazard ratings in a given sector, since the geology and geotechnical factors can change dramatically over very short distances, as is the case at New Vaal Colliery. Where the geology and geotechnical environment is reasonably consistent, as at Wonderwater, the averaging of hazard ratings becomes more viable.

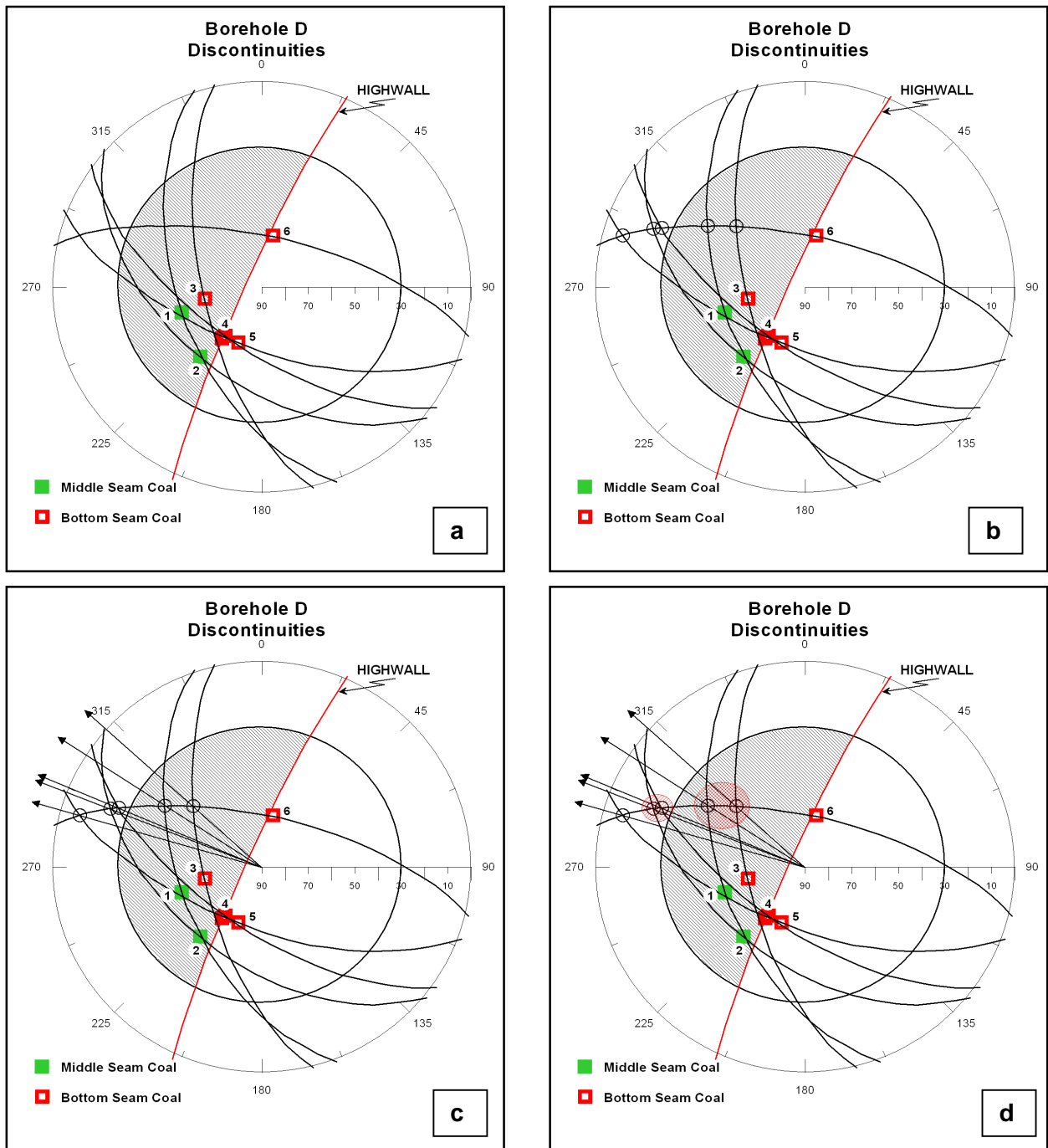


**Figure 4.3.2.2:** a) Great circles for discontinuities D1 to D6; b) Intersections (circled) between conjugate pairs forming wedges; c) Lines drawn through intersections indicating direction of potential sliding; d) Danger zones (red hatched) where a conjugate pair's line of intersection is greater than  $30^\circ$

The stereoplot of the discontinuities identified in Borehole E is presented in Figure 4.3.2.4. There is a wide range of discontinuity dip directions although all dip steeply ( $>60^\circ$ ). The basement topography, as indicated by the Bottom Seam Coal floor contours (Figure 4.2.1.6), in this area appears to be locally gently dipping. To the south of the borehole, the Bottom Seam rises gently, while to the north-east it dips relatively steeply. This increase in the dip around Borehole E may influence the localised jointing and fracturing pattern. What is apparent from the stereoplot (Figure 4.3.2.4) is that more discontinuities dip sub-parallel to the highwall than in Borehole D, indicating the possibility of plane failure. There is also the potential for unstable wedges to form.

Highwall Azimuth		294	Relative Orientations		HAZARD ?
Strata Azimuth		80	Relative to Highwall	146	N
Strata Dip		9.8	Dip	9.8	N
					<b>NONE</b>
<b>Wedge Formation:</b>					
D1 / D6	Dir. of Sliding	303	Relative to Highwall	9	Y
	Dip	40	Dip	40	Y
In-fill		N			N
Water		N			N
					<b>D1 / D2 Total Hazard</b>
					<b>MODERATE</b>
D3 / D6	Dir. of Sliding	312	Relative to Highwall	18	Y
	Dip	50	Dip	50	Y
In-fill		N			N
Water		N			N
					<b>D1 / D4 Total Hazard</b>
					<b>HIGH</b>
D2 / D6	Dir. of Sliding	291	Relative to Highwall	3	Y
	Dip	22	Dip	22	N
In-fill		N			N
Water		N			N
					<b>D1 / D5 Total Hazard</b>
					<b>MODERATE</b>
D4 / D6	Dir. of Sliding	293	Relative to Highwall	1	Y
	Dip	24	Dip	24	N
In-fill		N			N
Water		N			N
					<b>D3 / D4 Total Hazard</b>
					<b>MODERATE</b>
D5 / D6	Dir. of Sliding	286	Relative to Highwall	8	Y
	Dip	8	Dip	8	N
In-fill		N			N
Water		N			N
					<b>D3 / D5 Total Hazard</b>
					<b>NONE</b>
<b>Bedding Plane Sliding Hazards:</b>		<b>NONE</b>			
<b>Planar Failure Hazards:</b>		<b>NONE</b>			
<b>Wedge Failure Hazards:</b>					
D1 / D2		<b>HIGH</b>			
D1 / D4		<b>HIGH</b>			
D1 / D5		<b>MODERATE</b>			
D3 / D4		<b>MODERATE</b>			
D3 / D5		<b>NONE</b>			
<p>Relative Orientation is the difference, in degrees, between the Highwall azimuth and the discontinuity, or line of intersection, azimuth.</p> <p>A Relative Orientation Angle of 25° or less is considered to be highly hazardous since the planes are striking sub-parallel to parallel. Angles greater than 25° are not considered hazardous.</p> <p>The presence of in-fill material and / or water on discontinuities is considered hazardous.</p>					
<b>OVERALL SLOPE STABILITY HAZARD RATING:</b>			<b>MODERATE to HIGH</b>		

**Figure 4.3.2.3:** Hazard matrix for Borehole D – modified for wedge failure hazards only

The discontinuities D1, D2, D6 and D7 all dip sub-parallel and steeply out of the highwall, indicating that plane failures are a distinct possibility. The great circles for these discontinuities are plotted on the stereoplot in Figure 4.3.2.5 and the directions of potential sliding for each discontinuity are also shown.

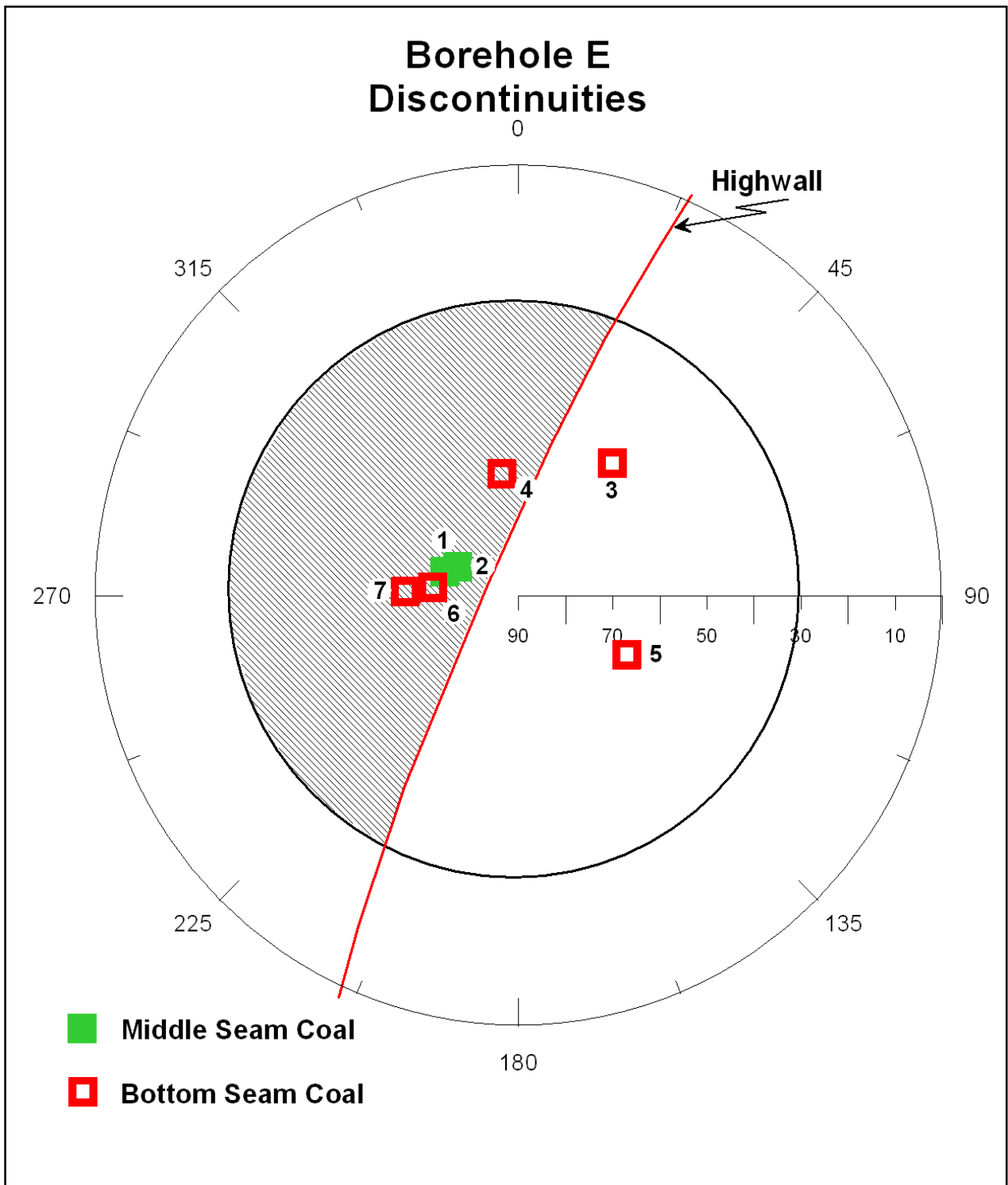


**Figure 4.3.2.4:** Stereoplot of discontinuities identified in Borehole E for Middle and Bottom Seam Coal units

Before the information regarding the potential plane failures is entered into the hazard matrix, the potential for unstable wedges to form must be assessed. The wedge failure analysis is again performed by way of the series of stereoplots, as shown in Figure 4.3.2.6. As can be seen, up to eight potentially unstable wedges can be formed. All are dipping out of the highwall and all the lines of intersection are steeper than  $30^\circ$ . The only exception is the wedge formed by the discontinuity pair D3/D5, which is dipping into the highwall and is therefore stable. Although the intersections between the discontinuities D1, D2, D6 and D7 do not form wedges, the area is highlighted as being hazardous, since the numerous intersecting discontinuities may have a destabilising effect on the rock mass.

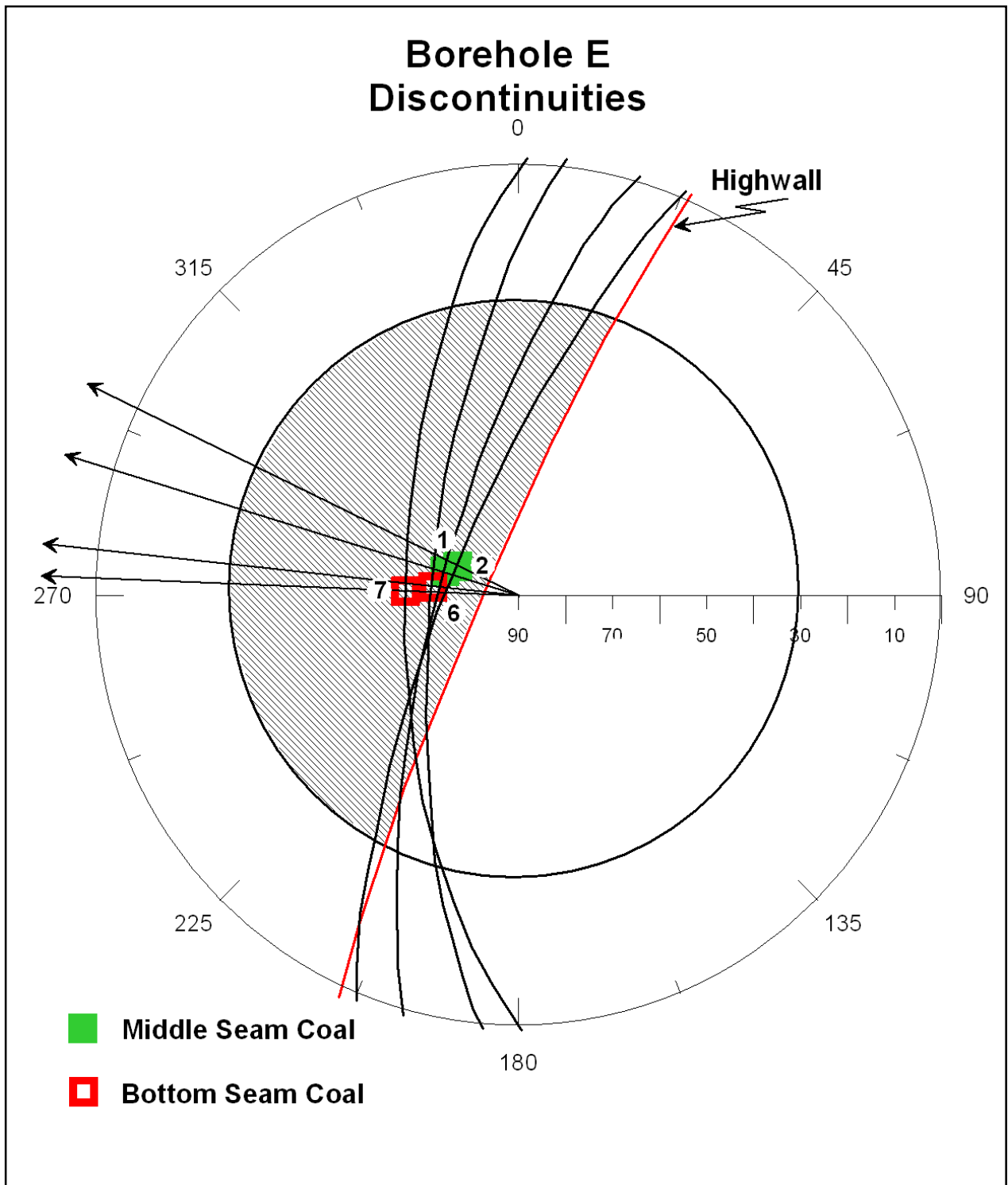


**Figure 4.3.2.5:** Great circles for discontinuities that may result in plane failure. Also indicated are the individual directions of potential sliding for each discontinuity

The hazard matrix for plane failures is presented in Figure 4.3.2.7 and the hazard matrix for the wedge failures is presented in Figure 4.3.2.8. These are presented separately so as not to clutter the matrix, and the final hazard rating for Borehole E takes into account both hazard matrices. As indicated by the plane failure hazard matrix (Figure 4.3.2.7), plane failure in the vicinity of Borehole E is very likely. Considering the geometries necessary for plane failure to occur (Section 2.3), it is necessary to follow up with detailed surface and highwall mapping as mining approaches this area.

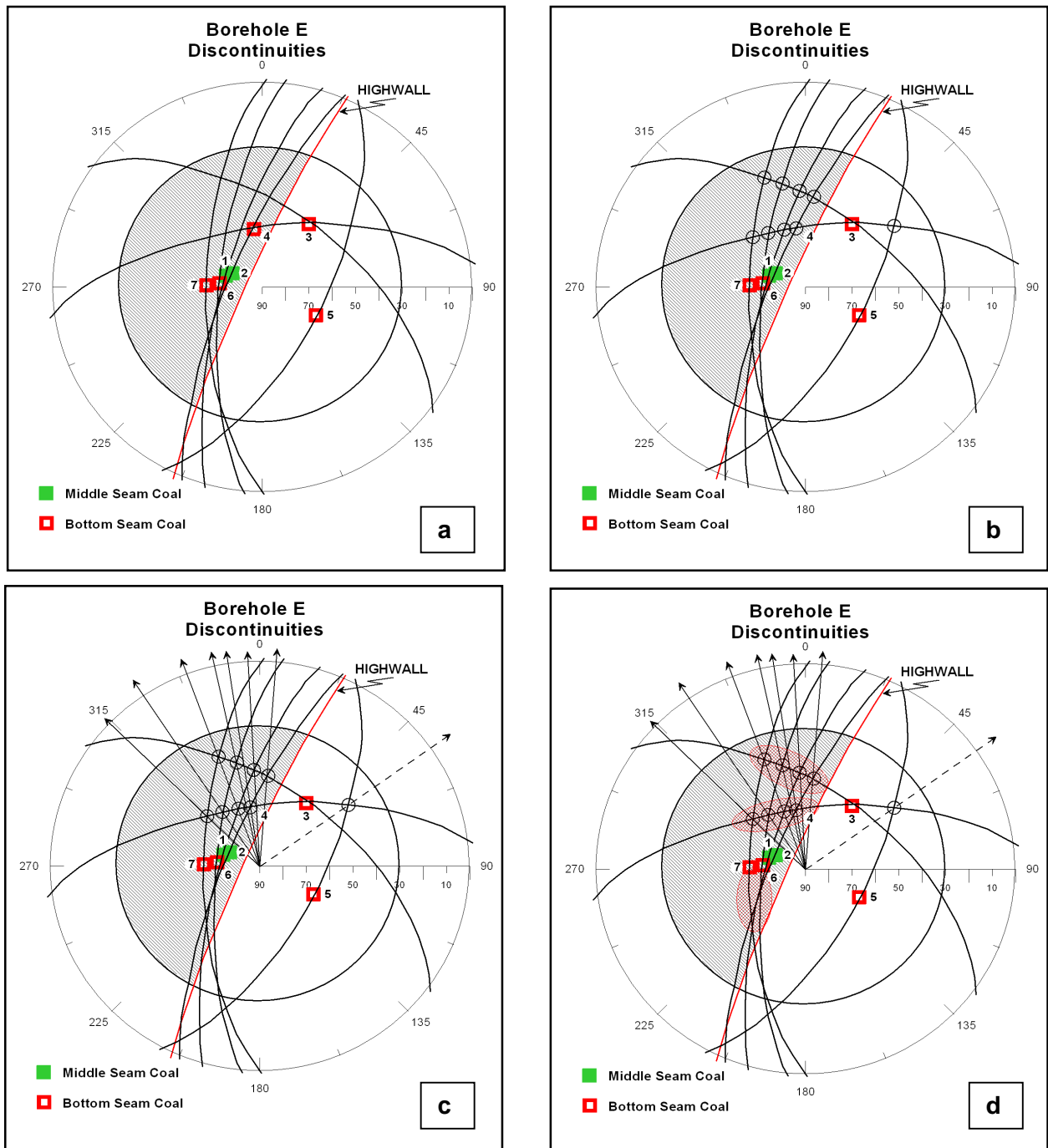


**Figure 4.3.2.6:** a) Great circles for discontinuities D1 to D7; b) Intersections (circled) between conjugate pairs forming wedges; c) Lines drawn through intersections indicating direction of potential sliding; d) Danger zones (red hatched) where a conjugate pair's line of intersection is greater than 30°

The potential for wedge failure is also high as indicated in the wedge failure hazard matrix (Figure 4.3.2.8). The wedge formed by the discontinuity pair D3/D5 is omitted from the hazard matrix since it is clear that this wedge does not pose any stability problems as it dips into the highwall. All the other wedges are considered to pose stability problems, and it is thus necessary to follow up with detailed in-pit mapping as mining enters this area.

Highwall Azimuth		294	Relative Orientations		HAZARD ?
Strata Azimuth		24	Relative to Highwall	90	N
Strata Dip		6.9	Dip	6.9	N
					<b>NONE</b>
<b>Plane Formation:</b>					
<b>D1</b>	Azimuth	287	Relative to Highwall	7	Y
	Dip	74	Dip	74	Y
	In-fill	N			N
	Water	N			N
<b>D1 Total Hazard</b>					<b>HIGH</b>
<b>D2</b>	Azimuth	291	Relative to Highwall	3	Y
	Dip	76	Dip	76	Y
	In-fill	N			N
	Water	N			N
<b>D2 Total Hazard</b>					<b>HIGH</b>
<b>D6</b>	Azimuth	276	Relative to Highwall	18	Y
	Dip	72	Dip	72	Y
	In-fill	N			N
	Water	N			N
<b>D6 Total Hazard</b>					<b>HIGH</b>
<b>D7</b>	Azimuth	273	Relative to Highwall	21	Y
	Dip	66	Dip	66	Y
	In-fill	N			N
	Water	N			N
<b>D7 Total Hazard</b>					<b>HIGH</b>
<b>Bedding Plane Sliding Hazards:</b>		<b>NONE</b>	<div style="border: 1px solid black; padding: 5px;"> <p>Relative Orientation is the difference, in degrees, between the Highwall azimuth and the discontinuity, or line of intersection, azimuth.</p> <p>A Relative Orientation Angle of 25° or less is considered to be highly hazardous since the planes are striking sub-parallel to parallel. Angles greater than 25° are not considered hazardous.</p> <p>The presence of in-fill material and / or water on discontinuities is considered hazardous.</p> </div>		
<b>Planar Failure Hazards:</b>					
<b>D1</b>	<b>HIGH</b>				
<b>D2</b>	<b>HIGH</b>				
<b>D6</b>	<b>HIGH</b>				
<b>D7</b>	<b>HIGH</b>				
<b>Wedge Failure Hazards:</b>		<b>NONE</b>			
<b>OVERALL SLOPE STABILITY HAZARD RATING:</b>					<b>HIGH</b>

**Figure 4.3.2.7:** Hazard matrix for Borehole E – modified for plane failure hazards only

Both the plane failure hazard matrix and the wedge failure hazard matrix indicate that the highwall in the vicinity of Borehole E has a high probability of being unstable. Considering the hazard matrices for both Borehole D and Borehole E, it can be concluded that the overall slope stability hazard rating for the middle and bottom seam coal highwall is high. The entire sector (119/95) appears prone to both wedge and plane failures and, therefore, it is critical that detailed in-pit highwall and surface mapping be conducted to further qualify the current interpretation.

Highwall Azimuth	294	Relative Orientations	HAZARD ?
<b>Strata Azimuth</b>	24	<b>Relative to Highwall</b>	<b>90</b>
<b>Strata Dip</b>	6.9	<b>Dip</b>	<b>6.9</b>
			N
			N
			<b>NONE</b>
<b>Wedge Formation:</b>			
<b>D1 / D4</b>	Dir. of Sliding	340	<b>Relative to Highwall</b>
	Dip	63	<b>Dip</b>
	In-fill	N	
	Water	N	
			Y
			Y
			N
			N
		<b>D1 / D4 Total Hazard</b>	<b>HIGH</b>
<b>D2 / D4</b>	Dir. of Sliding	351	<b>Relative to Highwall</b>
	Dip	63	<b>Dip</b>
	In-fill	N	
	Water	N	
			Y
			Y
			N
			N
		<b>D2 / D4 Total Hazard</b>	<b>HIGH</b>
<b>D6 / D4</b>	Dir. of Sliding	326	<b>Relative to Highwall</b>
	Dip	61	<b>Dip</b>
	In-fill	N	
	Water	N	
			Y
			Y
			N
			N
		<b>D6 / D4 Total Hazard</b>	<b>HIGH</b>
<b>D7 / D4</b>	Dir. of Sliding	314	<b>Relative to Highwall</b>
	Dip	58	<b>Dip</b>
	In-fill	N	
	Water	N	
			Y
			Y
			N
			N
		<b>D7 / D4 Total Hazard</b>	<b>HIGH</b>
<b>D1 / D3</b>	Dir. of Sliding	357	<b>Relative to Highwall</b>
	Dip	47	<b>Dip</b>
	In-fill	N	
	Water	N	
			Y
			Y
			N
			N
		<b>D1 / D3 Total Hazard</b>	<b>HIGH</b>
<b>D2 / D3</b>	Dir. of Sliding	5	<b>Relative to Highwall</b>
	Dip	50	<b>Dip</b>
	In-fill	N	
	Water	N	
			Y
			Y
			N
			N
		<b>D2 / D3 Total Hazard</b>	<b>HIGH</b>
<b>D6 / D3</b>	Dir. of Sliding	347	<b>Relative to Highwall</b>
	Dip	43	<b>Dip</b>
	In-fill	N	
	Water	N	
			Y
			Y
			N
			N
		<b>D6 / D3 Total Hazard</b>	<b>HIGH</b>
<b>D7 / D3</b>	Dir. of Sliding	340	<b>Relative to Highwall</b>
	Dip	39	<b>Dip</b>
	In-fill	N	
	Water	N	
			Y
			Y
			N
			N
		<b>D7 / D3 Total Hazard</b>	<b>HIGH</b>
<b>Bedding Plane Sliding Hazards:</b>		<b>NONE</b>	
<b>Planar Failure Hazards:</b>		<b>NONE</b>	
<b>Wedge Failure Hazards:</b>			
	<b>D1 / D4</b>	<b>HIGH</b>	
	<b>D2 / D4</b>	<b>HIGH</b>	
	<b>D6 / D4</b>	<b>HIGH</b>	
	<b>D7 / D4</b>	<b>HIGH</b>	
	<b>D1 / D3</b>	<b>HIGH</b>	
	<b>D2 / D3</b>	<b>HIGH</b>	
	<b>D6 / D3</b>	<b>HIGH</b>	
	<b>D7 / D3</b>	<b>HIGH</b>	
<b>OVERALL SLOPE STABILITY HAZARD RATING:</b>			<b>HIGH</b>

Relative Orientation is the difference, in degrees, between the Highwall azimuth and the discontinuity, or line of intersection, azimuth.

A Relative Orientation Angle of 25° or less is considered to be highly hazardous since the planes are striking sub-parallel to parallel. Angles greater than 25° are not considered hazardous.

The presence of in-fill material and / or water on discontinuities is considered hazardous.

**Figure 4.3.2.8:** Hazard matrix for Borehole E – modified for wedge failure hazards only

### 4.3.3 Overall test site highwall slope stability

The overburden - Top Seam Coal - interburden highwall stability appears to progressively deteriorate from sector 119/93 towards sector 119/94. The middle and bottom seam highwall in sector 119/95 appears to be highly unstable. These conclusions are based on two main areas of investigation: geological model analysis and stereography based on geophysical wireline data. It is satisfying to note that these conclusions are not inconsistent with practical experience gained through actual mining operations at New Vaal Colliery. Poor highwall conditions at New Vaal are commonly associated with highly undulating floor topography that results in higher than normal joint intensity and variability, as predicted for the new highwall in the test site area.

### 4.4 Conclusion

The methodology outlined in Section 4.2 and applied in Section 4.3 allows the mine geologist to predict potentially hazardous highwalls ahead of mining. The methodology is primarily based on the principles of stereography and is qualitative rather than quantitative. The actual hazard ratings assigned in the test site matrices are subjective and are based on the author's experience. The subjectivity in the assigning of hazard ratings for observed and interpreted geotechnical and geological features implies that a relatively high level of understanding of the specific mine's rock mass characteristics and behaviour in different circumstances is needed before hazard ratings can be confidently assigned.

Several issues are not taken directly into account in this methodology:

- RQD;
- UCS;
- Effects of water and in-fill material;
- Nature of discontinuities:
  - Persistence along dip and strike
  - Roughness
- Overall slope height and dip;
- Assumed homogeneity of lithological units.

The primary reason for this is the lack of sufficient data regarding these issues. A large database of rock mass related information is needed before these aspects can be incorporated in a more quantitative manner into the methodology. In addition, a lack of detailed in-pit mapping data necessitates that assumptions are made regarding the interpretation of geophysical wireline televiewer data. Detailed geotechnical models typically do not exist for many mine sites.

Since there is no rationale for the making safe of coal opencast highwalls (Butcher *et al.*, 2001), it would be premature to expect that this predictive methodology, in its current format, could significantly impact on current mine design practices. However, the ability to predict potentially unstable areas ahead of mining will go a long way towards ensuring safer and more productive opencast mining operations.

## 5. RECOMMENDATIONS

This research has clearly shown that there is a need to develop a much better understanding of the geotechnical environments in current and future opencast mining areas. Limited research has been conducted to date regarding rock mass characteristics and behaviour in traditional opencast mining areas. Mining personnel appear to have had very little exposure to rock mass-related issues and concepts, specifically those dealing with slope stability probability classification systems.

This methodology can be developed further only by actively applying it in current mining operations and conducting detailed structural and geotechnical investigations. There is also the need to build significant databases of the various rock mass-related characteristics and behaviour patterns in the opencast mining areas.

## 6. REFERENCES

- Bieniawski, Z.T. (1989). Engineering Rock Mass Classifications. publ. Wiley, New York. 251p.
- Butcher, R.J., Walker, D.J., Joughin, W.C, Birtles, A.N. (2001). Methodology for the safe cleaning and making safe of various height highwalls. SIMRAC Draft Final Report: GEN 703.
- Hack, R. (1998). Slope stability probability classification, SSPC. 2<sup>nd</sup> Edition. publ. ITC, Enschede, The Netherlands. ISBN 90 6164 154 3. 258p.
- Hack, R. (2002). An evaluation of slope stability classification. In: Keynote Lecture. Proc. ISRM EUROCK'2002, Portugal, Madiera, Funchal, 25-28 November 2002. Editors: C. Dinis da Gama & L. Ribeira e Sousa, Publ. Sociedade Portuguesa de Geotecnia, Av. Do Brasil, 101, 1700-066 Lisboa, Portugal. pp 3-32.
- Haines, A. and Terbrugge, P.J. (1991). Preliminary estimation of rock slope stability using rock mass classification systems. Proc. 7<sup>th</sup> Cong. On Rock Mechanics. ISRM. Aachen, Germany. 2<sup>nd</sup> Ed. Wittke W publ. Balkema, Rotterdam. pp 887-892.
- Hoek, E. and Bray, J. (Eds.) (1981). Rock Slope Engineering. Revised 3<sup>rd</sup> Edition. Stephen Austin and Sons Limited, Hemford, England. 358p.
- Lindsay, P., Campbell, R.N., Fergusson, D.A., Gillard, G.R., Moore, T.A. (2000). Predicting slope stability in open pit gold and coal mines. Proc. 2000 New Zealand Minerals and Mining Conference, 29-31 October 2000.
- Romana, M. (1991). SMR Classification. Proc. 7<sup>th</sup> Cong. On Rock Mechanics. ISRM. Aachen, Germany. 2<sup>nd</sup> Ed. Wittke W publ. Balkema, Rotterdam. pp 955-960.
- Sonneveldt, S. and Enserink, W. (1997). Joint survey at New Vaal Colliery. New Vaal Colliery Internal Report. 51p.
- Stewart, R.S. and Letlotla, S. (2003). The impact of geotechnical factors on high- and low-wall stability. COALTECH 2020 Task 1.4, Sub-task 1, Report Number: 2003-0190. CSIR Miningtek, Johannesburg. 43p.
- van Heerden, G. (2004a). Investigate other possible causes for sloughing. COALTECH 2020 Task 1.4, Sub-task 3a, Report Number: 2004-0174. CSIR Miningtek, Johannesburg. 14p.
- van Heerden, G. (2004b). Wireline logging applicability for the identification of geotechnical features. COALTECH 2020 Task 1.4, Sub-task 3b, Report Number: 2004-0175. CSIR Miningtek, Johannesburg. 16p.